HIGHWAY RESEARCH BOARD

Bulletin 279

Bridge Design Studies and Piling Tests

1960

National Academy of Sciences—
National Research Council

publication 819

HIGHWAY RESEARCH BOARD

Officers and Members of the Executive Committee

1960

OFFICERS

PYKE JOHNSON, *Chairman* — W. A. BUGGE, *First Vice Chairman*

R. R. BARTELSMEYER, *Second Vice Chairman*

FRED BURGGRAF, *Director* — ELMER M. WARD, *Assistant Director*

Executive Committee

BERTRAM D. TALLAMY, *Federal Highway Administrator, Bureau of Public Roads* (ex officio)

A. E. JOHNSON, *Executive Secretary, American Association of State Highway Officials* (ex officio)

LOUIS JORDAN, *Executive Secretary, Division of Engineering and Industrial Research, National Research Council* (ex officio)

C. H. SCHOLER, *Applied Mechanics Department, Kansas State College* (ex officio, Past Chairman 1958)

HARMER E. DAVIS, *Director, Institute of Transportation and Traffic Engineering, University of California* (ex officio, Past Chairman 1959)

R. R. BARTELSMEYER, *Chief Highway Engineer, Illinois Division of Highways*

J. E. BUCHANAN, *President, The Asphalt Institute*

W. A. BUGGE, *Director of Highways, Washington State Highway Commission*

MASON A. BUTCHER, *County Manager, Montgomery County, Md.*

A. B. CORNTHWAITE, *Testing Engineer, Virginia Department of Highways*

C. D. CURTISS, *Special Assistant to the Executive Vice President, American Road Builders' Association*

DUKE W. DUNBAR, *Attorney General of Colorado*

H. S. FAIRBANK, *Consultant, Baltimore, Md.*

PYKE JOHNSON, *Consultant, Automotive Safety Foundation*

G. DONALD KENNEDY, *President, Portland Cement Association*

BURTON W. MARSH, *Director, Traffic Engineering and Safety Department, American Automobile Association*

GLENN C. RICHARDS, *Commissioner, Detroit Department of Public Works*

WILBUR S. SMITH, *Wilbur Smith and Associates, New Haven, Conn.*

REX M. WHITTON, *Chief Engineer, Missouri State Highway Department*

K. B. WOODS, *Head, School of Civil Engineering, and Director, Joint Highway Research Project, Purdue University*

Editorial Staff

FRED BURGGRAF — ELMER M. WARD — HERBERT P. ORLAND

2101 Constitution Avenue — Washington 25, D. C.

HIGHWAY RESEARCH BOARD

Bulletin 279

Bridge Design Studies and Piling Tests

1960

Presented at the
39th ANNUAL MEETING
January 11-15, 1960

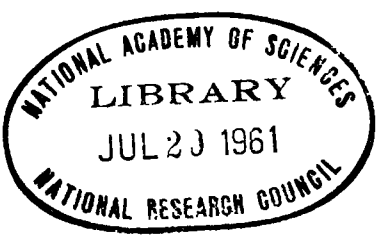

1961
Washington, D.C.

Department of Design

T.E. Shelburne, Chairman
Director of Research, Virginia Department of Highways
University of Virginia, Charlottesville

COMMITTEE ON BRIDGES

G.S. Paxson, Chairman
Assistant State Highway Engineer
Oregon State Highway Commission, Salem

Raymond Archibald, Chief Bridge Engineer, Division of Highways, Juneau, Alaska

J.N. Clary, Engineer of Bridges, Virginia Department of Highways, Richmond

E.M. Cummings, Manager of Sales, Bethlehem Steel Company, Bethlehem, Pennsylvania

Frederick H. Dill, Assistant to Vice President of Engineering, American Bridge Division, United States Steel Corporation, Pittsburgh, Pennsylvania

E.L. Erickson, Chief, Bridge Division, Office of Engineering, Bureau of Public Roads, Washington, D.C.

R.S. Fountain, Bridge Engineer, Portland Cement Association, Chicago, Illinois

F.M. Fuller, Raymond Concrete Pile Company, New York, New York

H. deR. Gibbons, The Union Metal Manufacturing Company, Canton, Ohio

John J. Hogan, Consulting Structural Engineer, Portland Cement Association, New York, New York

W.T. Lankford, Applied Research Laboratory, United States Steel Corporation, Monroeville, Pennsylvania

Adrian Pauw, Professor of Civil Engineering, University of Missouri, Columbia

M.N. Quade, Consulting Engineer, Parsons, Brinckerhoff, Hall and MacDonald, New York, New York

William H. Rabe, Ohio Department of Highways, Columbus

C.P. Siess, Professor, Department of Civil Engineering, University of Illinois, Urbana

Charles B. Trueblood, Armco Drainage and Metal Products, Inc., Middletown, Ohio

J.A. Williams, Missouri State Highway Commission, Jefferson City

Contents

Transfer of Load Between Precast Bridge Slabs

ADRIAN PAUW and JOHN E. BREEN, respectively, Professor and Assistant Professor of Civil Engineering, University of Missouri, Columbia

● THIS PAPER presents the procedures used and the results obtained in a series of static load tests designed to study the mechanism of load transfer between adjacent precast bridge-slab sections. These tests were undertaken as one phase of a general structural and economic study of precast bridge units under the sponsorship of the Missouri State Highway Commission and the Bureau of Public Roads. Because little or no information was available on the nature of the mechanism of load transfer between precast slab sections, this test program was necessarily of an exploratory nature and was therefore designed to give specific information for the standard channel sections presently used by the Missouri State Highway Department.

THE MISSOURI STANDARD CHANNEL SECTION

The precast channel section used by the Missouri State Highway Department has a standard width of 3 ft 2 in., and a depth of 18 in. Sections of the same depth may be used for either H-10 or H-15 loading by providing different amounts of longitudinal reinforcement. The standard lengths range from 21.5 to 34 ft in modular increments of 6.25 ft. Typical details are shown in Figure 1. Seven parallel units are used for a 20-ft roadway and an additional special 2-ft wide unit, for a 22-ft roadway. Stiffening diaphragms are provided at 6 ft 3 in. on centers and the units are bolted together at points midway between the diaphragms using 1-in.-diameter bolts with beveled washers at each end.

Three holes are provided in the channel legs at each bolt location to permit use of the units in skewed structures. The design provides for shear transfer between units by the 1-in.-diameter tie bolts and by a $\frac{3}{4}$-in.-wide keyway filled with a dry-packed cement mortar to within 1 in. of the top surface. After the units are erected an asphalt wearing surface is placed to provide a smooth riding surface.

DETAILS OF TEST ARRANGEMENT

The sections were too large to permit full-scale testing for all length and load combinations. In the static-load test program for the individual units, half-scale models were therefore selected to simplify handling. The results of the model tests were correlated by one set of full-scale tests, using the 21.5-ft span. The results obtained from tests of the half-scale model were found to be in excellent agreement with test results for the full-size sections. Similarly full-scale testing for the load transfer series was not feasible because of laboratory space limitations and it was therefore decided to limit the test to a study of the behavior of three half-scale models of the standard 27.75-ft section for H-10 loading. Dimensions of the model section are also shown in Figure 1.

The shear keys provided in the model section were scaled down to be representative of the keys used in the prototype. Figure 2 shows an over-all view of the test frame and the test arrangement. Load cells were provided at the reaction points under each channel leg and the load was applied through a calibrated load cell by means of a hydraulic jack. Other instrumentation was provided to measure deflections, slip between units, and strains in the reinforcement and in the concrete.

To separate the effect of the tie bolts from that of the shear keys, the units were loaded in a preliminary series of tests in which shear transfer was provided by the tie bolts alone. Care was taken in this series not to overload the units and thereby damage the sections before the final tests. On completion of this test series the tie bolts were

loosened and the keys packed with a dry cement-mortar grout consisting of one part portland cement and two parts sand. The tie bolts were then retightened. A close-up of the key detail is shown in Figure 3.

TESTING PROGRAM

To permit comparison with the test results for the individual sections the three half-scale model sections used in the load transfer series were made as nearly identical as possible with the sections used in the flexural capacity series. To obtain the maximum amount of information possible with a single set of specimens, a special loading sequence was followed. This sequence can best be explained by referring to Figure 4.

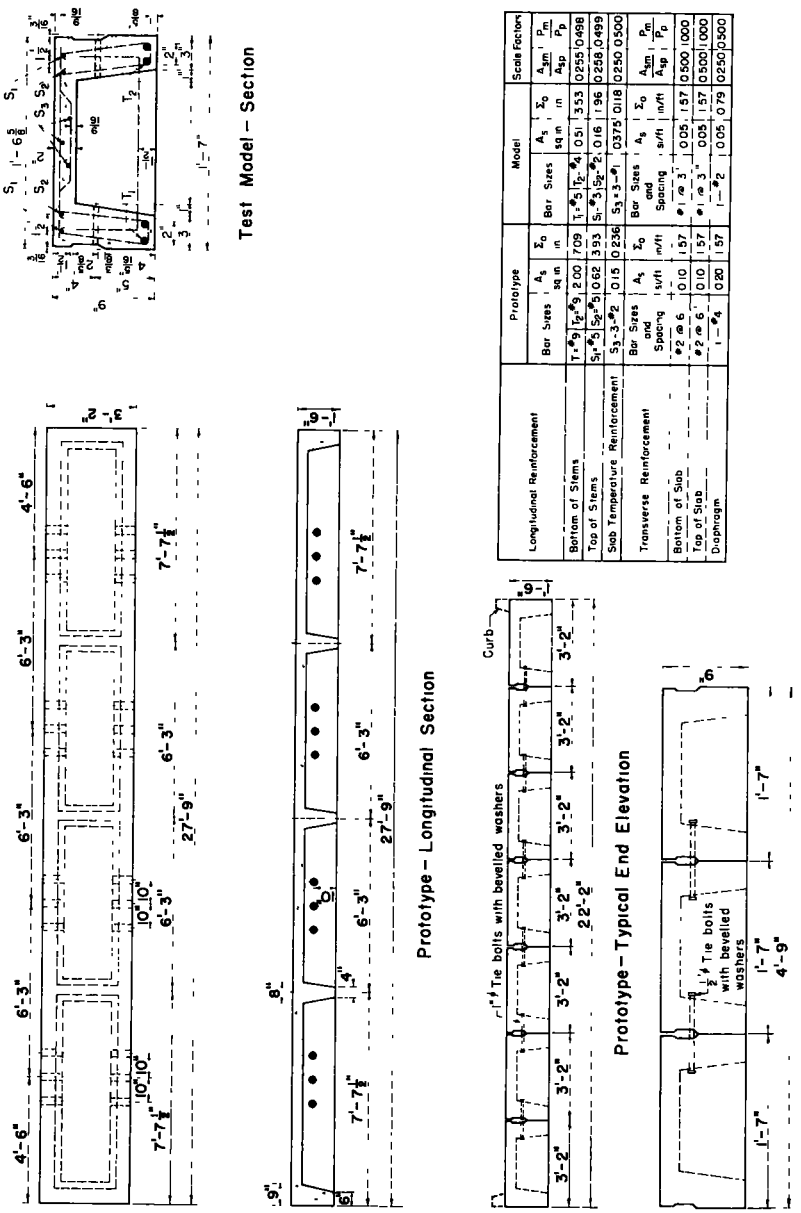

Longitudinal Reinforcement	Prototype				Model				Scale Factors	
	Bar Sizes	A_s sq in	Σ_0 in		Bar Sizes	A_s sq in	Σ_0 in		$\frac{A_{sm}}{A_{sp}}$	$\frac{P_m}{P_p}$
Bottom of Stems	T_1-#9, T_2-#9	2.00	.709		T_1-#5, T_2-#4	.051	.353		.0255	.0498
Top of Stems	S_1-#5, S_2-#5	.062	.393		S_1-#3, S_2-#2	.016	.196		.0258	.0499
Slab Temperature Reinforcement	S_3-3-#2	.015	.0236		S_3-3-#1	.0375	.0118		.0250	.0500
Transverse Reinforcement	Bar Sizes and Spacing	A_s sq in/ft	Σ_0 in/ft		Bar Sizes and Spacing	A_s sq in/ft	Σ_0 in/ft		$\frac{A_{sm}}{A_{sp}}$	$\frac{P_m}{P_p}$
Bottom of Slab	#2 @ 6	.010	.157		#1 @ 3	.005	.157		.0500	.1000
Top of Slab	#2 @ 6	.010	.157		#1 @ 3	.005	.157		.0500	.1000
Diaphragm	1 – #4	.020	.157		1 – #2	.005	.079		.0250	.0500

Figure 1. Details of standard channel test sections.

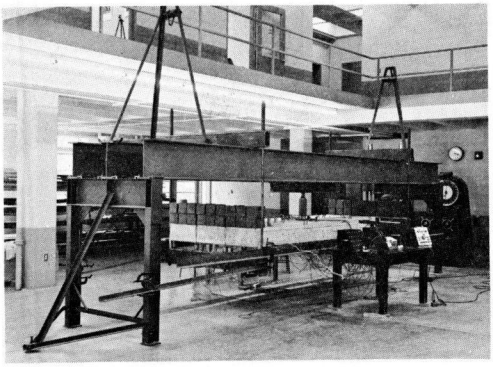

Figure 2. Test arrangement.

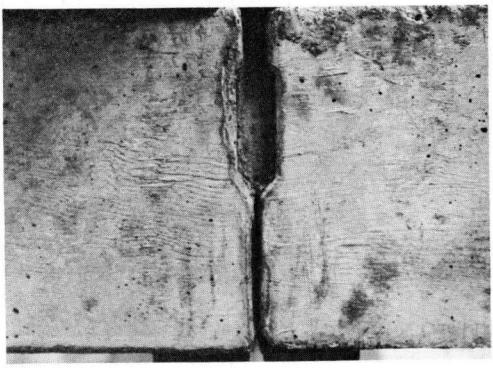

Figure 3. Closeup of key detail.

Seven methods of load application were used. In series I, II, and III, the load was applied at the midpoint of the center, the west, and the east channel, respectively. In series IV and V the load was applied at the north quarter-point of the center and of the west channel, respectively. Finally, in series VI and VII the load was split and applied to the outside channels at the center, and at the north quarter-point, respectively.

The test series with the joints grouted were designated by subscripts, where the subscript letter defined the maximum load applied in the particular series. While this loading sequence permitted obtaining the maximum amount of information, it did complicate interpretation of the measurements, especially for the load ranges for which the loading sequence resulted in cumulative increments of permanent distortion. The sequence of loading, showing the loading limits, is summarized in Table 1.

INSTRUMENTATION

The disposition of the instrumentation used in the test is shown in Figure 5. The instruments used and their points of application were as follows:

1. One pancake-type load cell, 60,000-lb capacity, used to measure the applied load.
2. Twelve spool-type load cells, 10,000-lb capacity, under the channel stems to measure the reactions.
3. Twelve deflectometers, one 1.0-in. range deflectometer under each channel stem at the center of the span, and one 0.5-in. range deflectometer at the center of the diaphragm at the one-quarter and at the three-quarter points of each channel.
4. Eighteen SR-4 strain gages to measure the longitudinal steel strains in each stem; six each, at the one-quarter, the center, and the three-quarter points.
5. Six SR-4 strain gages to measure the transverse stell strains in the diaphragms of the center and west channels at the one-quarter, the center, and the three-quarter points.
6. Nine extensometers to measure the concrete strains in each of the interior diaphragms.
7. Six extensometers mounted directly above the center of each stem, to measure the concrete strains at the center of the span.
8. Two pairs of slip gages, mounted between channels at the center of the span, to measure slip and rotation of the channel sections.
9. Twelve bench marks for auxiliary large deflection measurements with a height gage.

Figure 6 shows a bank of reaction cells in place. The precast sections were carefully grouted on the reaction-cell bearing plates, to equalize the initial dead-load reactions. Some difficulty was encountered with the use of these cells in that their accuracy at very low loads was impaired by mechanical hysteresis and zero drift.

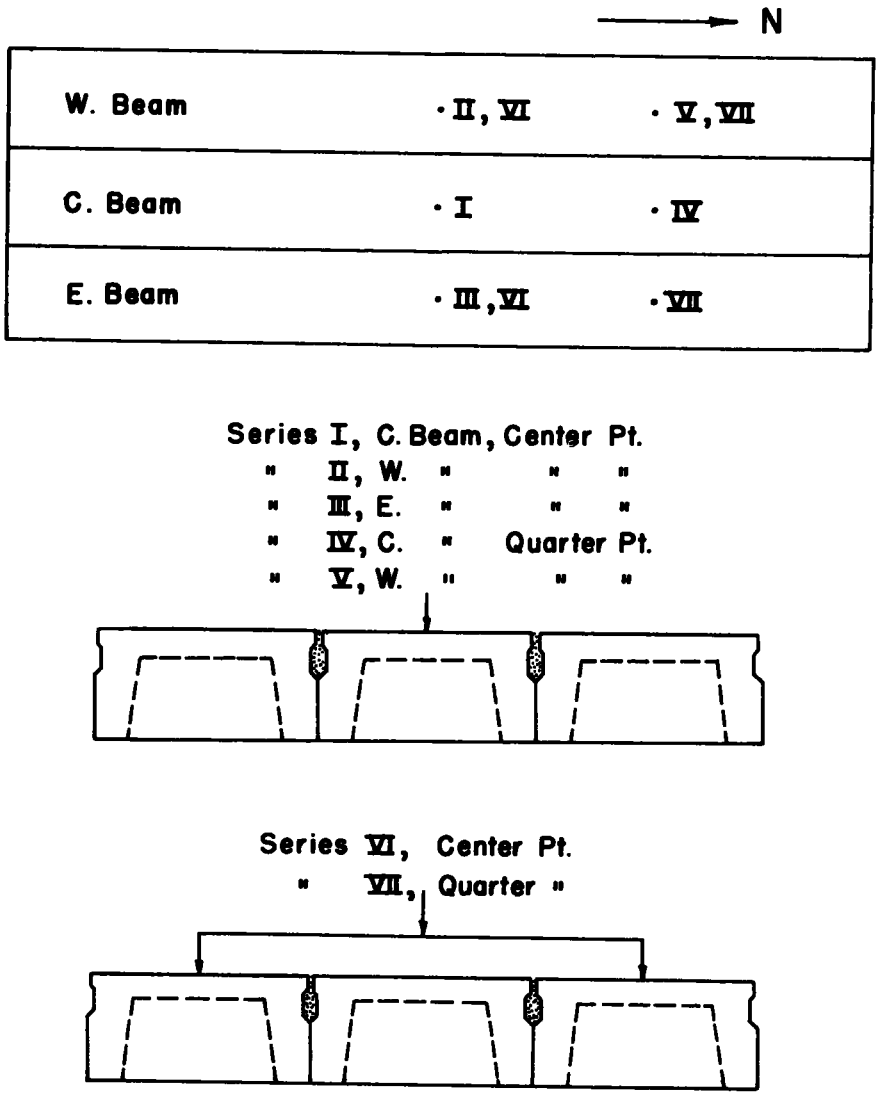

Figure 4. Loading sequence.

This difficulty was overcome by preloading the cells by placing six 50-lb weights on the end of each section.

The plunger-type deflectometers used are shown in Figure 7. These deflectometers were used in place of dial gages because of the inaccessibility of the deflection stations and because their use permitted measurements to be made from a central location. The deflectometers were supported by a steel framework resting on the reaction supports of the testing frame as shown in Figure 6. When the deflections became large, the deflectometers were removed and deflections measured with the height gage shown in Figure 8 using tensioned wires attached to the testing frame as reference base lines. The height gage was provided when a vibrating reed the vibration of which was damped when the reed came in contact with the base-line wire thus giving a sensitive

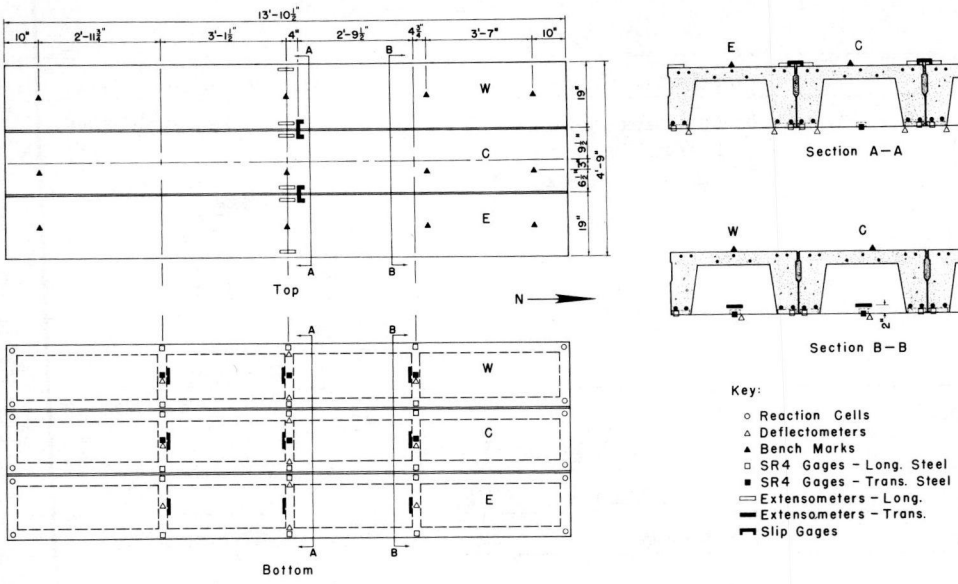

Figure 5. Instrumentation.

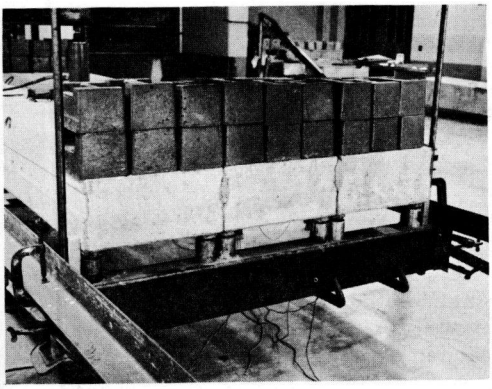

Figure 6. Bank of reaction cells.

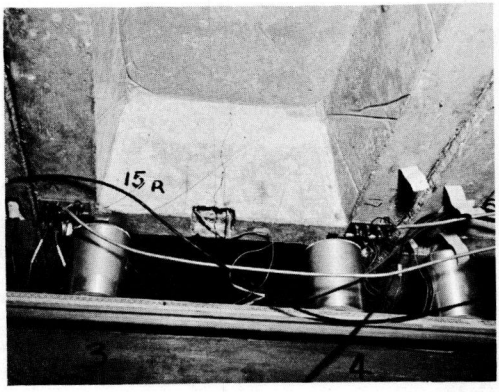

Figure 7. Deflectometers.

indication of position. The micrometer adjustment on the height gage permitted the determination of deflections to an accuracy of about 0.002 in.

Figure 7 also shows the areas of concrete blocked out to permit attachment of SR-4 gages. Reinforcement was prepared for gage installation before casting the channels and small sections of concrete were blocked out with pieces of styrofoam. After hardening of the concrete, the pieces of styrofoam were easily removed and the gages installed. By this technique the need for waterproofing the gages was avoided and all gages were found to operate satisfactorily.

Figure 9 is a close-up view of the clip-on type extensometer used to measure concrete strains. The extensometer (a detailed description of this instrument as well as of the deflectometer and the load cell is given in "Technical Report No. 1, Structural and Economic Study of Precast Bridge Units - Instrumentation," University of Missouri Engineering Experiment Station, 1957) is essentially a three-hinged arch with two SR-4 gages on the center hinge acting as the strain transducer. Inasmuch as two gages are used, one in tension and one in compression, the meter is automatically

TABLE 1A

LOADING

Subletter	Method of Connection	Maximum Applied Load, lb
None	Lateral bolts only	3750
a	Lateral bolts and grouted shear key	3750
b	"	7500
c	"	11250
d	"	15000
e	"	18000
f	"	25000
g	"	30000
h	"	Complete failure

TABLE 1B

LOADING SEQUENCE

Series	Bolts Only	Bolts and Grouted Key							
		a	b	c	d	e	f	g	h
I	1	6	13	20	27	30	31	32	33
II	2	7	14	21	28				34
III	3	8	15	22					35
IV	4	9	16	23					
V	5	10	17	24					
VI		11	18	25	29				
VII		12	19	26					

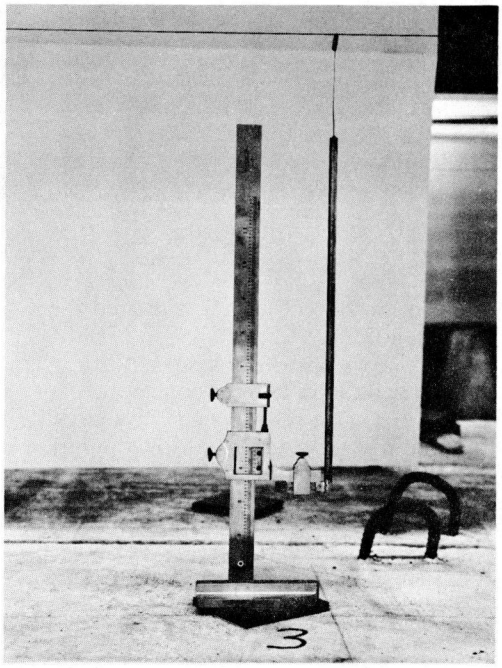

Figure 8. Height gage.

temperature-compensated. A pretensioning screw is provided to permit zero adjustment and to allow application of pretension when the meter is used to measure compressive strains. The meter has a gage length of 4 in. and is attached by cementing the binding posts to the concrete. Figure 10 shows the

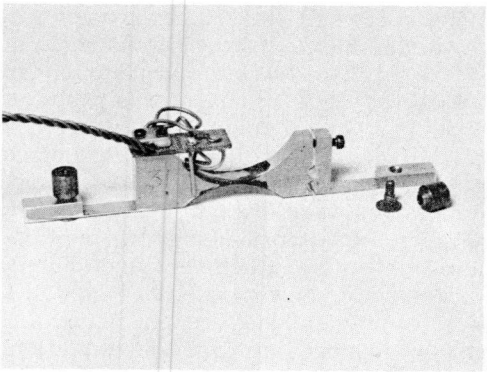

Figure 9. Extensometer.

extensometers installed on the three channel sections. Also shown in this figure are two slip gages and the pancake-type load cell directly under the loading jack.

The details of the slip gage are shown in Figure 11. These gages were patterned after similar instruments used at Lehigh University and were found to perform quite satisfactorily. Both slip and rotation can be determined from the dial readings; relative slip being determined from the difference of the dial increments, and relative rotation, from the sum.

TEST OBJECTIVES

Before discussing the actual test results it is desirable to consider precisely what is to be determined. A single channel unit can carry at most one line of wheel loads acting along the longitudinal centerline of the section. After the units have been joined together by tie bolts and grouted keyways to form an integral bridge slab it is reasonable to expect that part of the load applied to a particular unit will be transferred through shear to the adjacent sections. It is required then to obtain a load transfer coefficient by which the wheel loads may be multiplied to give the effective equivalent design load for a single unit. The present design policy of the Missouri State Highway Department is to consider that the precast units act as a solid slab. The load distribution is then computed by the formula (AASHO, Standard Specifications for Highway Bridges, 7th Edition, p. 25)

$$E = \frac{10N + W}{4N}$$

in which

E = width of slab over which a wheel load is distributed,
N = number of lanes of traffic on the bridge,
W = width of roadway between curbs of the bridge.

Thus for a 20-ft roadway, E = 5 ft giving a load reduction coefficient of 0.63 for a 3-ft 2-in. wide channel section.

The purpose of the load transfer tests, therefore, was to determine load reduction coefficients which can safely be applied in the design of the individual sections. In interpreting the test results for selection of suitable load reduction coefficients the applicability of the tests to actual conditions should be considered carefully. Applicability of any particular test series depends on such factors as (a) the position of the section in the bridge (that is, whether the section is an interior or an edge unit); (b) the length-to-width ratio of the section; and (c) the location of the load.

Some other considerations in selecting a suitable reduction coefficient include (a)

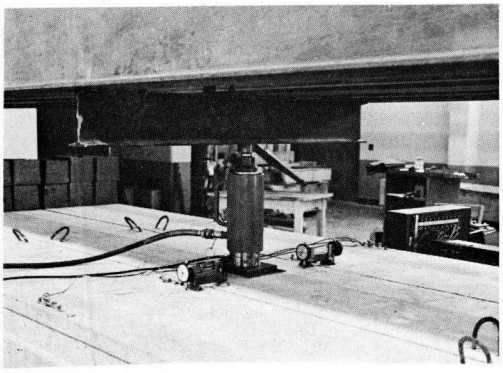

Figure 10. Instrumentation details.

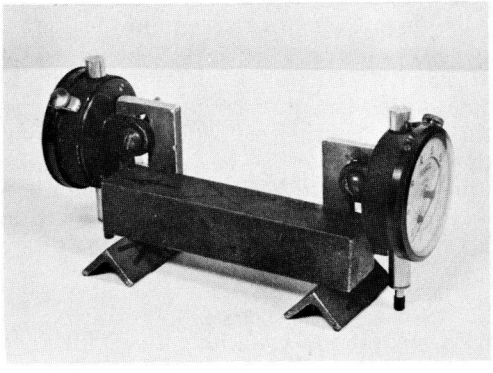

Figure 11. Slip gage.

economic design factors such as the need for interchangeability of precast sections, (b) spacing of the stiffening diaphragms, and (c) the basic design philosophy used (that is, whether the design is to be based on working load stresses or on ultimate load capacity).

The test program completed was not sufficiently extensive to answer all the questions raised by the foregoing considerations. The limited results obtained, however, do indicate very definite behavior patterns and suggest design concepts which should prove useful in planning more extensive investigations.

LIMITATIONS OF MODEL STUDIES

In using structural models it is generally impracticable to preserve a constant model ratio for the effect of both dead and live loads. Because failure of both the single channel sections and of the joined units was primarily due to flexure, the equivalent applied loads used in interpreting the test results were based on equivalent moments; that is, the moments in the model which would result in the same maximum stress levels in the steel and in the concrete in both model and prototype. Thus the equivalent single concentrated load for one line of wheels applied at the midspan of the model was found to be about 3,500 lb based on DL + LL + I for H-10 loading. For two or more working loads the equivalent applied load would have to be increased by increments of 4,100 lb to correct for the dead load of the slab.

SLIP TESTS

The observed maximum slip values in the Series I tests (tie bolts only) are compared with the values obtained in the Series Ia tests (tie bolts and grouted keyways) in Figure 12. Two significant results should be noted:

1. The magnitude of the slip in the Series I tests at an equivalent maximum normal working load was about two-thirds the deflection of a single unit at the same load (see also Fig. 16).
2. The grouting of the keyway reduced the slip in the Series Ia-Ig tests to insignificance. This reduction was further evidenced by the fact that the slip with grouted keyways at ultimate load was considerably less than the slip with tie bolts alone at working load.

From the first result it may be concluded that, although some load transfer may be developed by tie bolts alone at low stress levels, even at normal maximum working load the load transfer ratio has been reduced to insignificance. Furthermore, the relatively large slips at normal working load would tend to cause rapid deterioration of the bituminous wearing surface. On the other hand the grouted keyways were extremely effective in preventing excessive slip up to the ultimate load capacity of the combined sections. The important role of the tie bolts in developing the shearing resistance of the keys should be noted. Their principal function is to prevent lateral separation or spreading of the precast sections and their effectiveness in this respect was demonstrated by the development of stress in the stiffening diaphragms as discussed in a subsequent section.

Figure 13 shows the observed slip values for Series Ia-Ig. The test results have been plotted for the successive load increments of this series so as to give slip as a continuous function of load. The apparent discontinuities are the result of permanent slip displacement due to the cyclic load application used in the tests and the interspacing of the Series II to VI loadings. In spite of these discrepancies it may be noted that the maximum slip just before complete failure of the sections was only about one-third the slip value at working load when tie bolts alone were used.

REACTIONS

The maximum reaction values for each of the Series Ia-Ig tests are shown in Figure The end reactions were averaged for each channel stem. It is of interest that the corner reactions reached a maximum absolute value and then actually decreased as

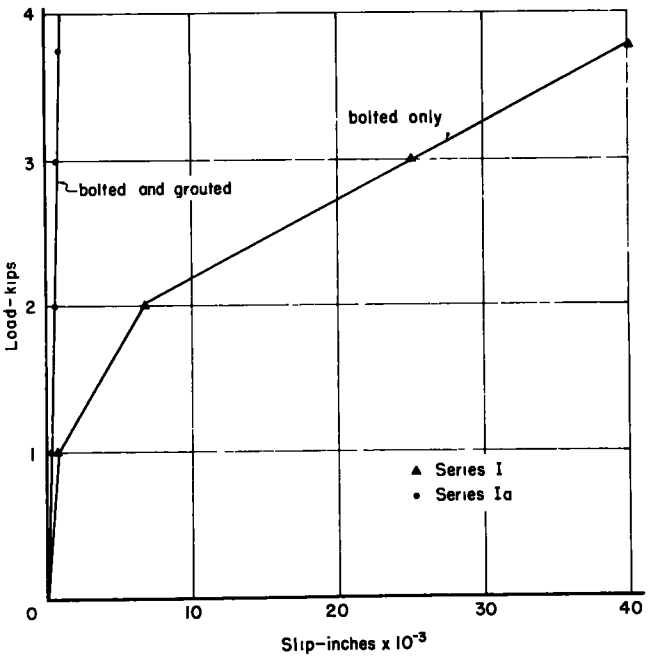

Figure 12. Relative slip.

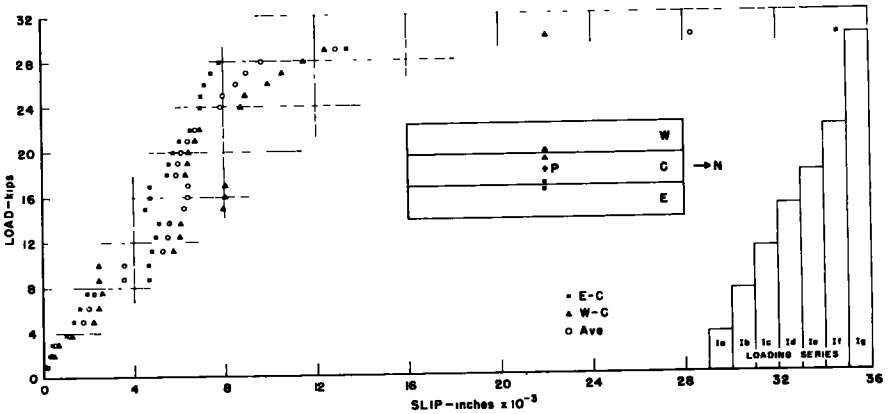

Figure 13. Slip observations—series Ia-Iq.

additional load increments were applied. This phenomenon can be explained by consideration of the redistributuion of the load which resulted from a relatively early yielding of the reinforcement in the stiffening diaphragm of the center channel (see also Fig. 20). This redistribution of load was accompanied by a marked tilting of the exterior channel sections resulting in a sharp increase in the reactions for the interior stems of these sections. These results are perhaps even more graphically demonstrated by Figure 15. Here the reactions are shown as a percentage of the total load applied. It may be noted that the center channel reactions remain relatively constant at a value of about 37 percent of the total load whereas the percentage of the load transmitted to the exterior stems of the unloaded channels decreases and that for the interior stems increases with each additional load increment. While these results cannot be used directly

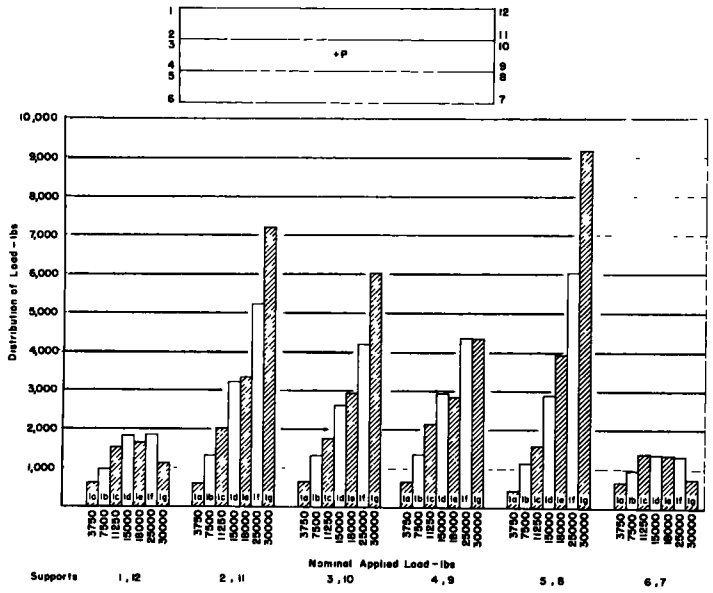

Figure 14. Reactions—series Ia-Ig.

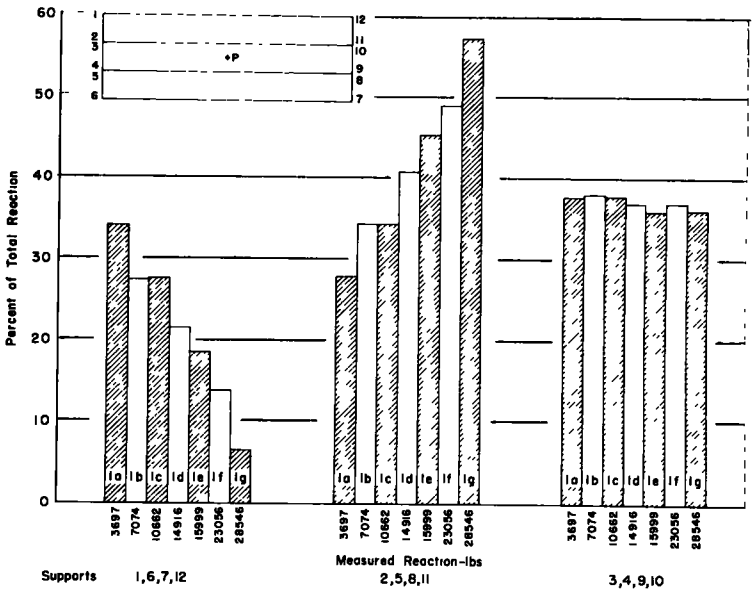

Figure 15. Reaction distribution.

to determine load reduction coefficients, they are useful in obtaining a better understanding of composite action and in providing a measure of the shear distribution between adjoining sections.

DEFLECTIONS

In addition to being an important design criterion in itself, the deflection serves as

an excellent indicator of the strain distribution. Figure 16 compares the center deflections for the connected units with the deflections for a single channel section. With tie bolts alone the deflections of the loaded channel were not significantly reduced, whereas with the keyways grouted and in the elastic range the deflections of the center unit were reduced to about one-third that for a single section.

It may be noted that for the single channel section there was a significant change in slope in the load-deflection curve at an applied load of about 11 kips. This change in slope was caused by yielding of the longitudinal reinforcement. As a result the load-deflection curve is similar in appearance to a typical stress-strain curve for the reinforcement, with the exception that the deflection curve does not become horizontal at the point of initial yield. Following initial yield of the longitudinal reinforcement, the single channel sections were able to sustain some additional load due to shifting of the neutral axis and stressing of the steel into the strain-hardening region.

The change in slope of the load-deflection curve in Figure 16 for the connected units (series Ia-Ig) is more gradual because the main reinforcement did not yield simultaneously in all units resulting in a load redistribution. The deflection of the connected units at failure was only a little over one-third the maximum deflection for the single units because failure was the result of punching of the slab rather than complete collapse of the entire section.

In Figure 17 the deflections of the channel stems at midspan are shown as a percentage of the loaded channel deflection. This figure clearly illustrates the non-linear increase in the tilting of the outside channels as additional load increments were applied. As the ultimate load was approached, the deflections of the outside stems decreased to about 70 percent. The decrease in deflection of the interior stems of the outside channels was in part due to relative slip between the sections. As a consequence of the tilting of the outside channel sections, the longitudinal steel in the adjoining stems started to yield before the yield point of the steel in the outside stem was reached. This initial yielding occurred at about twice the yield load for the single channel section and was followed by a redistribution of the load. At the load level for which the steel strains in the outside stems have reached the yield point, the load-deflection curve (Fig. 16) becomes essentially flat.

Where deflections are the limiting factor in design of relatively shallow slab sections, the load ratio for equivalent deflection at the first yield of the single section would be applicable as a basis for establishing a load reduction coefficient. From Figure 16 it may be seen that for the conditions represented by this test the coefficient would be approximately 11/26 or 0.42. This ratio was found to be consistent with observed strain patterns, because large yields of the longitudinal steel in the outside stems occurred after initial load redistribution and at a load of approximately 26 kips.

LONGITUDINAL STEEL STRAINS

The mechanism of load redistribution due to yielding of the reinforcement is further clairified by the load-strain curves shown in Figure 18. It may be noted that the steel in the center unit yielded at an applied load of about 22 kips followed by yielding of the steel in the interior stems of the outside units at about 25 kips and in the outside stems at 26 kips. The consistent behavior of the reinforcement in corresponding stems should also be noted. A comparison of the initial slopes of these strain curves provides an excellent measure of the load distribution for loads less than the load causing initial yield of the reinforcement in the center channel. Using average slope values the load reduction coefficient determined on this basis was found to be 0.41 for the mid-section.

Unfortunately, no actual data of the steel strains in the vicinity of the yield load were obtained in the tests of the corresponding individual sections, and the comparative strains shown in Figure 19 are therefore based on the known stress-strain characteristics of the reinforcement used in the tests. However the yield load of 11 kips determined on this basis is consistent with the value determined from the load-deflection curve shown in Figure 16. Using these values the load reduction coefficient at yield, following load redistribution, would be 11/26 or 0.42. This value is in excellent agreement with the reduction coefficient determined from the slopes of the strain curves in Figure

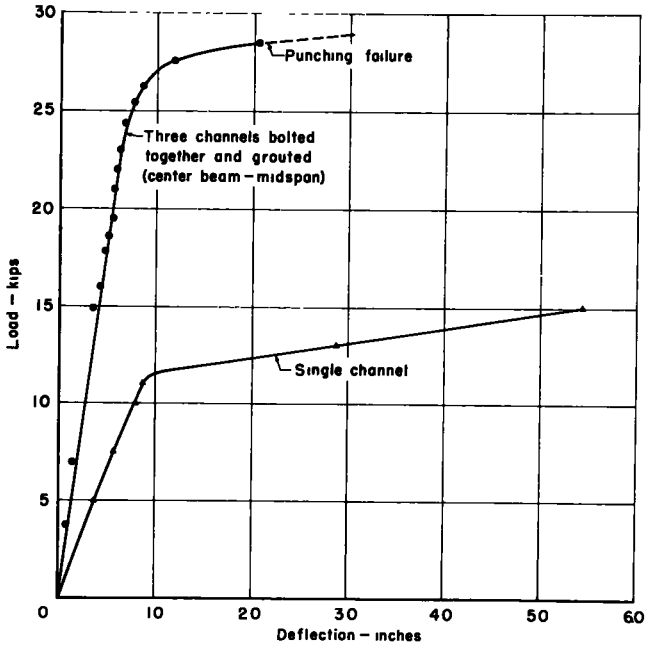

Figure 16. Comparison of channel deflections.

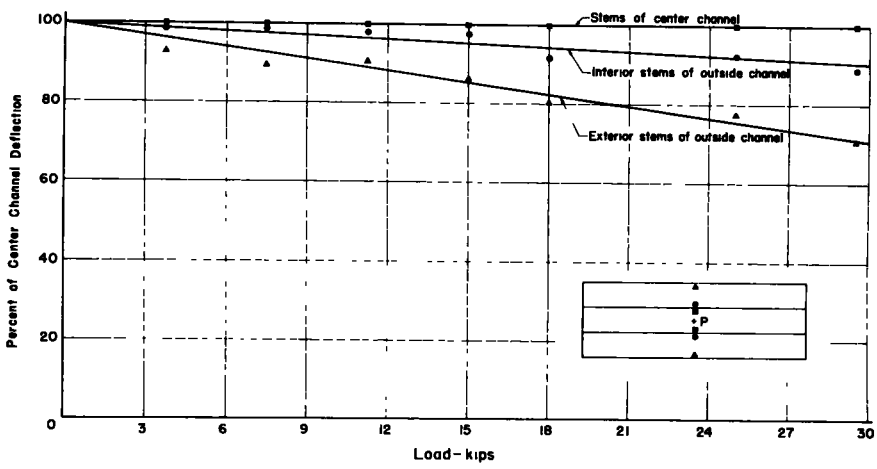

Figure 17. Relative deflection of channel stems.

18. The load reduction coefficient based on behavior at working-stress levels for this case may also be determined by comparing the average slope for the elastic range of the load-strain curves for the center channel with the slope for the single channel. The reduction coefficient determined on this basis is approximately 0.38 for this loading series.

The similarity shown in Figure 18 between the strain curves for the reinforcement in the adjoining channel stems should be noted. While the strains for the stems of the outside channels were somewhat smaller due to rotation and slip, these strains became more nearly equal as the load was distributed. It was also noted that the crack patterns developed in the adjoining stems at these loads were very similar, furth testifying to the effectiveness of the shear keys in distributing the load.

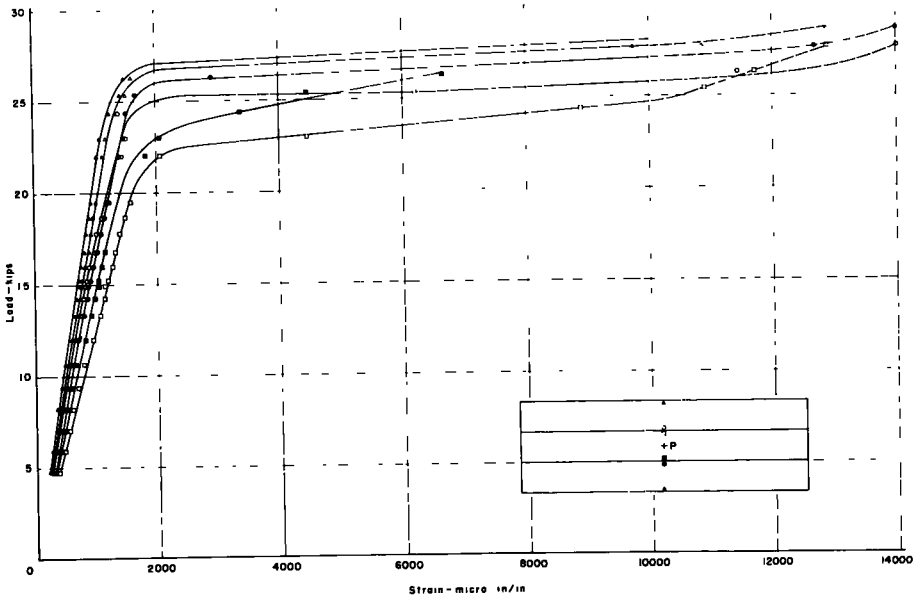

Figure 18. Longitudinal steel strains—series Ia-Ig.

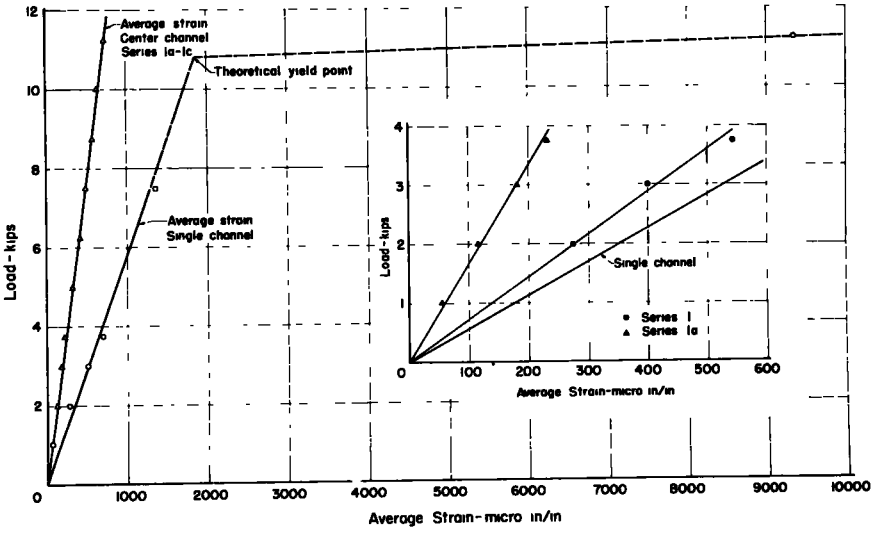

Figure 19. Comparative longitudinal steel strains.

The longitudinal steel strains for the series I test (tie bolts only) are shown in the insert in Figure 19. This plot again confirms the relative ineffectiveness of the use of tie bolts alone in distributing the load.

CONCRETE COMPRESSION STRAINS

The observed strains in the top fibers of the slab above each channel stem are plotted in Figure 20 as a function of applied load. The redistribution of the load to the outside sections is again apparent. The change in slope of the load-strain curves for

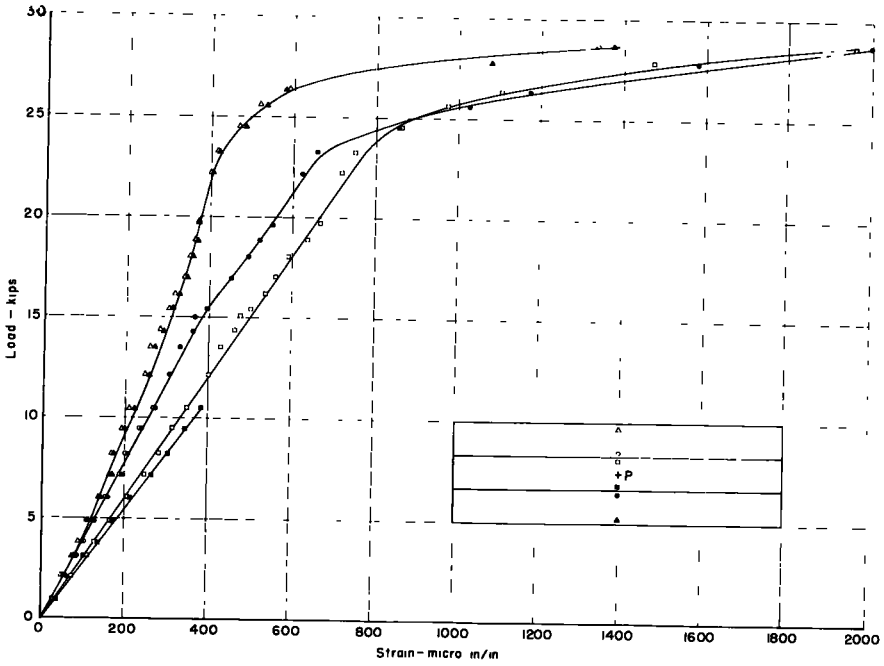

Figure 20. Longitudinal concrete compressive strains—series Ia-Ig.

the outside channels, starting at a load of approximately 15 kips, is apparently due to twisting of these sections. Figure 21 is a plot of the compression-zone depth ratio as a function of load for the center channel section. The depth ratios were computed on the basis of an assumed linear strain distribution between the observed steel strains and the maximum concrete compressive strains in the top fiber of the section. Zone A represents the loads for which the concrete had not cracked and was taking some tension. For the loads in zone B the concrete in the tension zone cracked and hence the value of k was steadily reduced until it reached a constant value in zone C. Zone D is the yield zone. In this zone the total steel stress was essentially constant and the increase in moment capacity was the result of an increase in the internal moment arm. As the yield zone was passed, the depth ratio again began to increase slightly in zone E due to strain hardening of the steel. The minimum observed k-value was found to be in excellent agreement with the value predicted by ultimate strength theory.

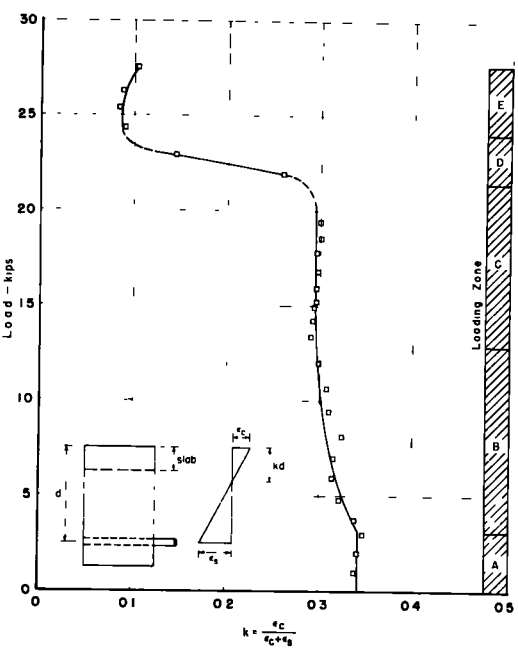

Figure 21. Compression zone depth ratio—series Ia-Ig.

TRANSVERSE STEEL STRAINS

The observed strains in the center - diaphragm reinforcement of the loaded

channel section for loading series Ia-Ie is shown in Figure 22. The significant change in slope at about 11 kips should be noted. This change indicates yielding of the reinforcement and the initiation of load redistribution. It is interesting to note that this load level coincides with the loading at which the corner reaction ceased to increase (Fig. 14). The behavior of the diaphragm was somewhat unexpected in that the observed strains in the tests of the individual sections were relatively small up to loads which resulted in yielding of the longitudinal reinforcement. On the basis of these tests it would appear that load redistribution could be delayed by increasing the diaphragm reinforcement. Assuming an initial yield load of 22 kips for the longitudinal reinforcement, doubling the amount of steel provided in the diaphragms would result in a better balance between longitudinal and transverse reinforcement.

QUALITATIVE RESULTS

Determination of the load reduction coefficient on the basis of ultimate load capacity would be irrelevant for this case because failure in the series Ig test was the result of punching of the slab as shown in Figure 23, whereas the individual sections failed due to excessive yielding of the longitudinal reinforcement followed by a secondary compression failure. The cracking pattern at ultimate load is shown in Figure 24. It should be noted that cracking was confined to the region between intermediate diaphragms at the quarter points. Figure 25 shows the failure of the center diaphragm and the spalling of the slab resulting from the punching failure. This failure occurred at an applied load of 28.7 kips. It is apparent that, even at this load, slip and separation of adjoining channel stems was negligible. After the punching of the center channel, loading was continued by applying load to the outside channels. The final failure due to secondary compression is shown in Figure 26.

SUMMARY AND CONCLUSIONS

The applicable load reduction coefficients (that is, the factors by which the wheel loads should be multiplied to give the reduced equivalent design load for a single section) for the test series discussed are summarized in Table 2. The load reduction coefficients based on yield strains and deflections after load redistribution are slightly more conservative than the coefficients based on working-load strains. This result may have been influenced somewhat by the premature yielding of the diaphragm reinforcement. As has previously been noted, the failure modes at ultimate load were incompatible and therefore ultimate load capacity should not be used as a method of

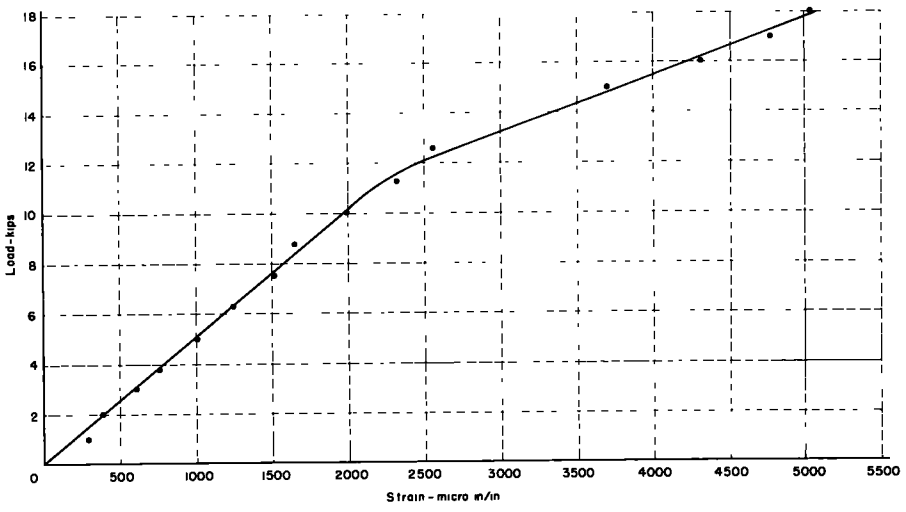

Figure 22. Diaphragm steel strains at midspan.

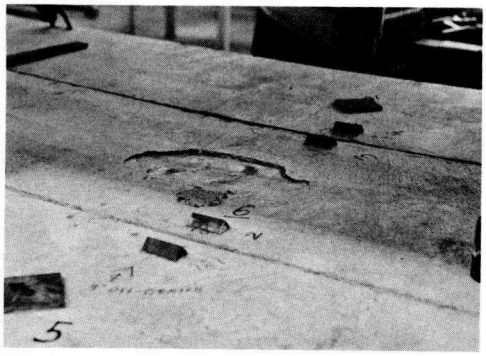

Figure 23. Punching failure.

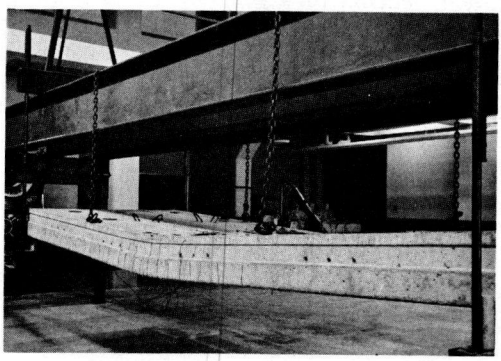

Figure 24. Crack pattern at ultimate load.

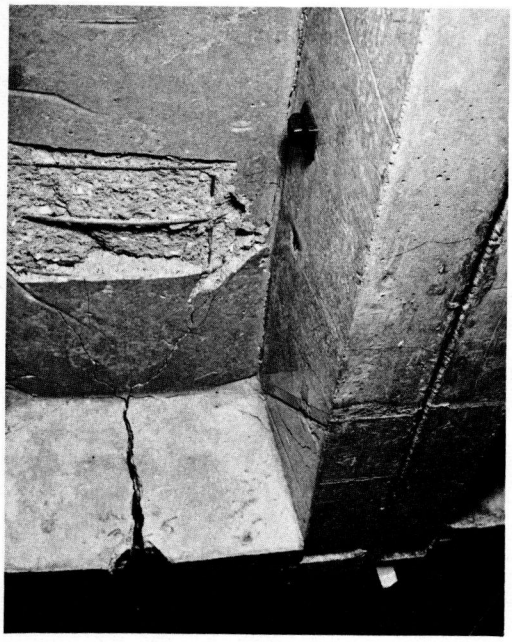

Figure 25. Diaphragm failure.

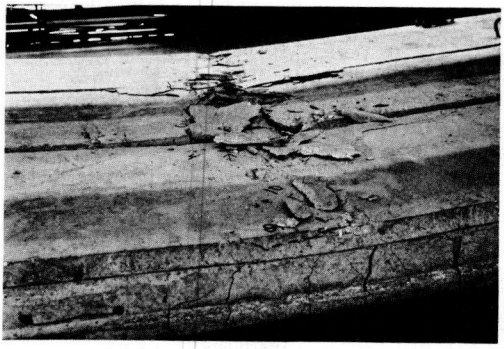

Figure 26. Secondary compression failure.

comparison in this case. Because of the reserve capacity developed by load redistribution, either the equivalent yield-load deflection or the secondary yielding of the principal reinforcement appears to offer the most rational basis for the determination of a suitable load reduction coefficient.

It should be noted that only the principal

TABLE 2

LOAD-REDUCTION COEFFICIENTS

Basis of Determination	Coef.	Comments
Slope of strain curve	0.41	Based on average initial slope (Fig. 18)
Equivalent-yield deflection	0.42	Allowance for load redistribution
Initial-yield strain	0.50	No allowance for load redistribution
Secondary-yield strain	0.42	Allowance for load redistribution
Working-load strain	0.38	
Ultimate load	0.54	Incompatible failure
End reactions	0.37	

test series has been discussed and that the results reported should therefore only be used under conditions which are sufficiently similar to make them applicable. However, the results obtained are believed to be sufficiently encouraging to warrant additional study and experimentation to make more economical designs possible.

ACKNOWLEDGMENTS

The work reported herein was supported by the Missouri State Highway Commission and by the Bureau of Public Roads under a cooperative research agreement. The assistance of Ravi R. Kohli, graduate research assistant, in the performance of the testing and in the reduction of the data is gratefully acknowledged.

Dynamic Tests of a Three-Span Continuous I-Beam Highway Bridge

C. L. HULSBOS and D. A. LINGER, respectively, Professor and Instructor of Civil Engineering, Iowa Engineering Experiment Station, Iowa State University, Ames

This paper presents the results of the static and dynamic testing of a three-span continous I-beam highway bridge. Live load stress frequency curves for selected points are shown, and the static and dynamic load distribution to the longitudinal composite beam members are given.

The bridge has four traffic lanes with a roadway width of 48 ft. Six longitudinal continous WF beams act compositely with the reinforced concrete slab to carry the live load. The beams have partial length cover plates at the piers.

Previous research has indicated that beams with partial length cover plates have a very low fatigue strength. It was found in this research that the magnitude of the stresses due to actual highway loads were very much smaller than those computed from specification loading. Also, the larger stresses which were measured occurred a relatively small number of times. These data indicate that some requirements for reduced allowable stresses at the ends of cover plates are too conservative.

The load distribution to the longitudinal beams was determined for static and moving loads and includes the effect of impact on the distribution. The effective composite section was found at various locations to evaluate the load distribution data. The composite action was in negative as well as positive moment regions. The load distribution data indicate that the lateral distribution of live load is consistent with the specifications but that there is longitudinal distribution, and therefore the specifications are to conservative.

●IN 1944 the first specifications for the design of composite highway bridges were published as a part of the American Association of State Highway Officials "Standard Specifications." The acceptance of this type of construction is shown by the increased use of composite steel and concrete in highway bridges. The resulting bridge structure is lighter and has a larger span depth ratio than ever before.

In the composite steel stringer bridge with a reinforced concrete slab, the roadway slab is used not only to transfer the load laterally, but also to form a composite section in conjunction with the longitudinal steel stringers. Therefore the slab adds not only lateral stiffness but also considerably to the basic longitudinal load-carrying capacity of the stringers. Thus, the steel stringer can be reduced considerably in size with a saving in both dead load and the cost of the structure. In addition, the reduction in dead load allows the basic superstructure to be decreased in size, resulting in a much lighter bridge.

Additional reduction in the size of the steel stringers can be obtained if the structure is made continuous over a number of supports. This continuity tends to increase the ultimate load-carrying capacity of the bridge structure. This is an aspect which should be considered because of loading at some future time, which might produce an extreme overload on the bridge.

However, some problems arise when the stringer is made continuous. The most significant is that the "Standard Specifications" do not permit the use of composite action in the area of negative moments. Inasmuch as composite action is not accepted, cover plates must be added to the longitudinal stringers along some portion of this negative moment region.

Recent results of fatigue tests of rolled beams with cover plates indicate that fatigue might be critical in the life of this type of structure (1). Fatigue life depends on the magnitude of the static stress and on the amplitude of the superimposed dynamic stresses. It can be shown that with specification loading, stress reversals at the ends of the cover plates are large enough to cause fatigue failure after the required number of reversals. However, these computed stresses may be erroneous, because many assumptions, mainly those of load distribution and impact, are made in their calculations.

The problem of fatigue is acute because of the dynamic behavior of a continuous type of bridge. This behavior, usually vibration, is a result of the large span depth ratio. Its consequence is not only increased stress, which is usually within the impact factor, but also the repetition of this stress resulting from prolonged vibration.

A recent survey (2) shows that over one-half the state highway departments in this country are using rolled beams with partial length cover plates. These state highway commissions use various types of cover plate termination details. These end details have an important effect on the fatigue strength of rolled sections with partial length cover plates.

The Iowa State Highway Commission is now using a cover plate termination detail with a rectangular end which is tapered and welded along its entire end. However, a type of cover plate termination detail previously used in Iowa (Fig. 4a) was investigated in this research because it was considered more conducive to stress concentration than the present detail.

OBJECTIVE

The objective of this research is to determine experimentally the live load stresses in the cover plate termination region from which the stress-frequency curves for in-service loading can be obtained. Once these stress-frequency curves are determined, laboratory tests may be designed to use these fatigue data in determining the permissible stress for the cover plate cutoff points.

Although it was not the intent of this research to evaluate load distribution to the longitudinal stringers, this is inherent any time an experimental stress is compared with a theoretical stress. As a part of the load distribution problem, the impact characteristics and composite section properties were studied. Therefore, the problem of load distribution is an objective of this research, though an indirect one.

STRAIN EQUIPMENT

The objective of this research required not only that the magnitude of the stress be determined but also that a complete stress-time curve be constructed for the passage of each vehicle over the bridge. In other words, an instrument was required which could record the stresses continuously over an extended period of time.

The term "stress analysis" is inaccurate, because although one speaks of measuring stresses actually strains must be measured and converted to stresses. Of the many varied ways of measuring strains, the requirement of a continuous record of strain dictated the type of strain gage and limited the variation in types of strain recorders.

To measure the strains, standard SR-4 strain gages were used. The types of SR-4 gages used were A-11 and A-5. The resistance to the ground of the SR-4 gages was as follows: the A-11 gages 50,000 to 100,000 ohms; the A-5—100,000 to 1,000,000 ohms.

The strain readings were recorded by a Brush universal amplifier (BL-520) and a Brush direct-writing recorder (BL-274). This equipment produces a continuous record of strain for which the time base can be varied by the speed of the recording paper. The speeds available vary from 1 to 250 mm per sec. For a check of the time base as determined by the speed of the paper, a 1-sec timer was used to actuate an event marker on the edge of the record. The Brush universal amplifiers have a number of attenuator settings which vary from 1 microinch per inch of strain per attenuator-line to 1,000 microinch per inch of strain per attenuator-line, and therefore allow a wide choice of amplification of the strain to best use the recording paper.

STRUCTURE

The test bridge was selected because of its location, accessibility, and its similarity to the type of bridge currently being built in Iowa's primary road system (Fig. 1). The bridge is located on US 30 one mile east of Ames, Iowa. Highway 30 crosses the Skunk River at this point, and the bridge is often referred to as the "Skunk River" bridge. The structure has longitudinal steel wide-flange stringers constructed integrally with a reinforced concrete slab roadway. Shear lugs were provided to insure composite action between the stringers and the concrete roadway slab. The steel diaphragms are spaced at about 18-ft, 6-in. centers. The bridge has four 12-ft lanes and a 2-ft safety curb on both sides.

LOADINGS

Controlled Load

Two types of loading were necessary for the data required. The first type was a standard controlled load needed to evaluate the load distribution and impact stresses. This loading was used also to evaluate the stress distribution around the cover plate termination area. The vehicle used in this loading is a tandem axle, International L-190 van-type truck (Fig. 2). This truck used to check the Iowa State Highway Commission scales, has a wheel base of 14 ft, 8 in. and a tread of 6 ft. It weighs 40,650 lb with 31,860 lb on the rear axle.

The "static" tests were performed by the controlled loading vehicle creeping across the bridge with the motor idling. This loading was applied on all 14 test "lanes" on the bridge (Fig. 3). The moving load tests were conducted at vehicle speeds beginning at 10 mph and increasing by approximately 10-mph increments up to the maximum attainable speed of approximately 50 mph. The maximum speed was limited by the vehicle and the terrain. These moving load tests were conducted on only 4 of the 14 test "lanes" The speed of the test vehicle was detemined by two air hose switches connected to a speed indicator on the roadway at one end of the structure. The indicator is the property of the Safety Department of the Iowa State Highway Commission. During the moving load tests, the vehicle's speed was constant over the entire length of the bridge, and the vehicle did not vary from the assigned "lane." Each of the 14 "lanes" used was marked by a painted stripe along which the left front tire of the truck was run. During the speed runs the variation to one side or the other of the vehicle was never more than 1½ in.

Random Load

For the random load test, the actual in-service traffic was recorded. In this traffic were trucks, semi-trucks, buses, cars, and miscellaneous vehicles. The stresses resulting from this traffic were recorded, and the type, direction, and highway lane-of travel of the vehicles were noted on the record. The record was obtained for a period of 4 hr a day for 2 days. The operating periods were staggered so that the two 4-hr periods together covered a period from 10:00 a.m. to 5:30 p.m.

TEST RESULTS

Stress Distribution in the Cover Plate Termination Area

The distribution of stress in the cover plate termination region was determined firs

This was required so that a location could be established for an indicator gage which would yield repeatable results, would not be affected by stress raisers, and could be correlated with the stresses at points of stress concentration.

Figure 4b and 4c shows the longitudinal stress variation as contour lines on the cover plate termination area. These lines were constructed by assuming that the strain varied linearly between the 19 strain gage locations used. This is, of course, an approximation, but it gives an indication of the variation of the stresses. This approximate anomaly picture was used only to determine the best place for the single strain gage. This gage was used as an indicator for each cover plate termination area for the measurement of the strains during the moving load tests. This point was chosen because a center line location was desirable due to the symmetry of the detail. The distance from the end of the cover plate is large enough that the strain measured is not at the point of maximum stress concentration and yet close enough to indicate the response of the cover plate termination detail to various moving loads.

The location chosen for the individual gage was 2½ in. away from the end of the cover plate along the center line of the flange. All the cover plate termination areas in one quadrant of the bridge plan were instrumented with a single gage located at that point. This particular point is indicated in Figure 4 by 100 percent, inasmuch as it was used as a base for the percentage contour line.

Stress-Frequency Curves

The stress history of a structure can be shown best by a continuous record of stress measured over a period of time. This picture of the stress variations is, however, not satisfactory for the most concise indication of the susceptibility of a structure to fatigue. The factors affecting fatigue are the intensity of stress and the number of times the stress is repeated. Therefore, the stress history of a structure, from the fatigue aspect, is most easily shown by a stress-frequency curve. The data for this curve is obtained from a continuous strain record.

A typical continuous strain record curve shows the variation of strain as a vehicle passes over the structure (Fig. 5). To construct a stress-frequency curve from this record, the number of times the strain record exceeds each stress level in the rising direction is plotted on abscissa of the stress-frequency diagram (Fig. 6).

The Random Traffic.—To obtain the in-service stress history of the cover plate termination areas, which was the primary objective of this research, a continuous record of strain was obtained for a given period of time. Once this was obtained the stress-frequency curves for this traffic were constructed to show the cyclical stress repetition occurring in these areas of potential fatigue failures. These stress-frequency curves or stress histories of the traffic sampled, show the susceptibility of the cover plate termination region to fatigue failure under in-service conditions. The data for this information were obtained by recording the strain at the "indicator" gages located 2½ in. from the end of the long cover plates in one quadrant of the bridge plan. Thus because of bi-lateral and bi-longitudinal symmetry the strains recorded are typical of all the long cover-plate termination regions of this structure.

The random traffic sampled was typical mid-week primary road traffic. The sample was obtained on the morning of Tuesday, July 29, and the afternoon of Wednesday, July 30, 1958. The time factor for the random samples is equivalent to 7½ hr of continuous sampling from 10:00 a.m. to 5:30 p.m. In terms of the number of vehicles the sample is the result of 253 vehicles which includes semi-trucks, conventional single-unit trucks, and buses.

The average maximum strain produced by individual automobiles traveling across the bridge was approximately five microinch per inch. This is less than 1/10 of the average maximum strain produced by trucks and buses. Because of the small strain produced by individual automobiles this strain was insignificant in its effect on the fatigue life of the bridge. Therefore, the stress-frequency curves in Figure 7 include only the trucks and buses and combination of automobiles with trucks and buses and are incomplete in the range of ± 5 microinch per inch, or ± 150 psi.

Only when an automobile was immediately preceded by a large truck, especially a

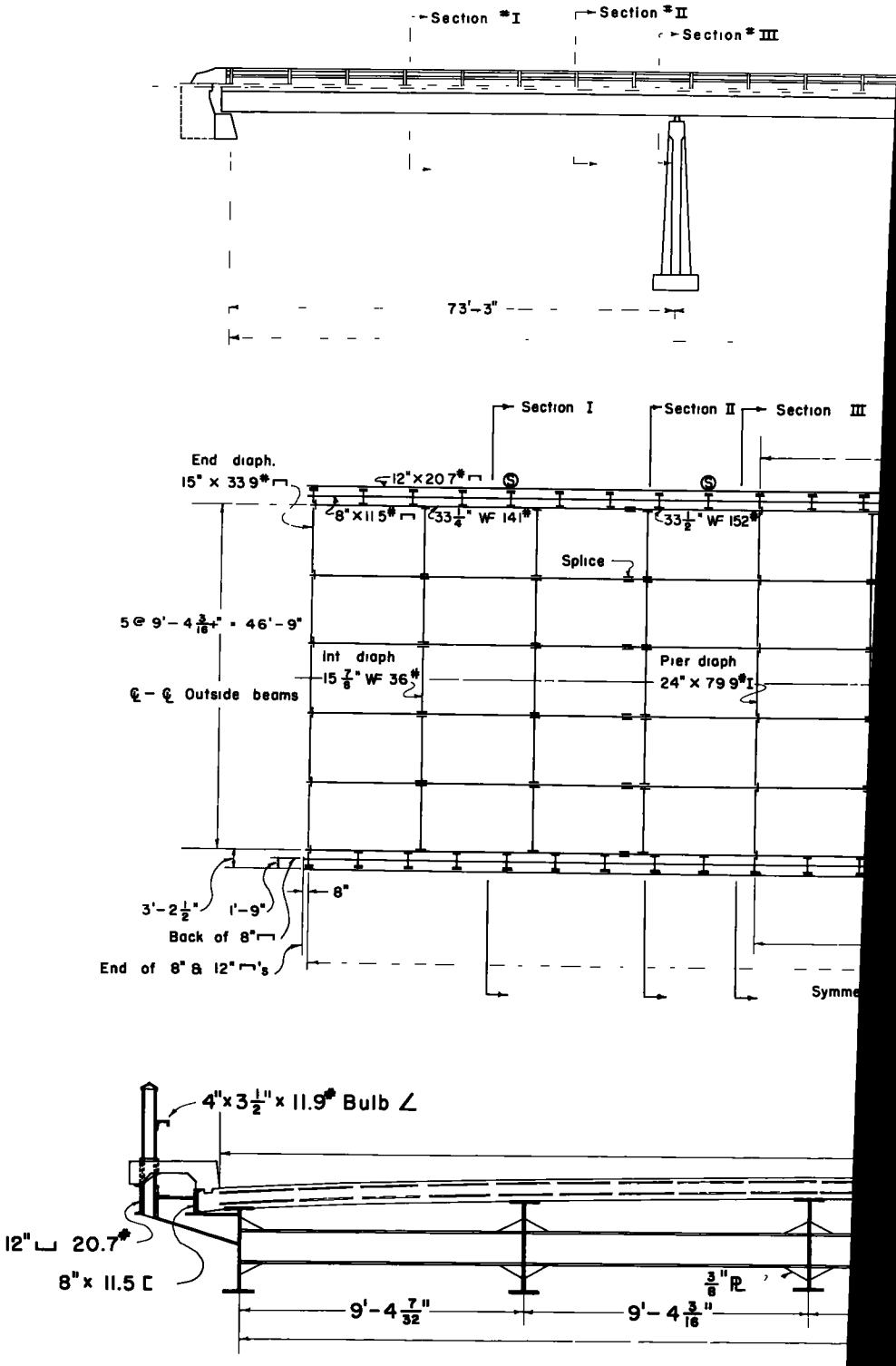

Figure 1. Elevation, p

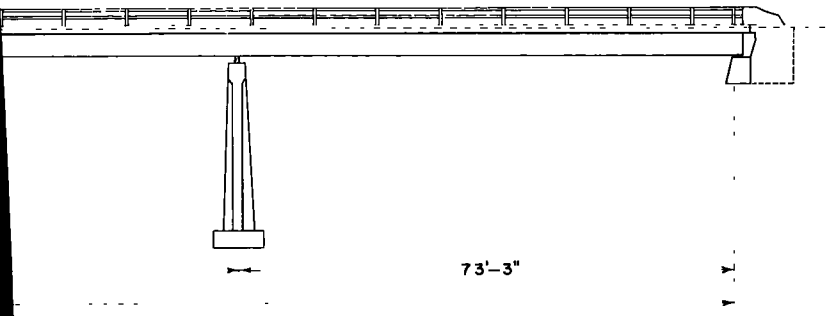

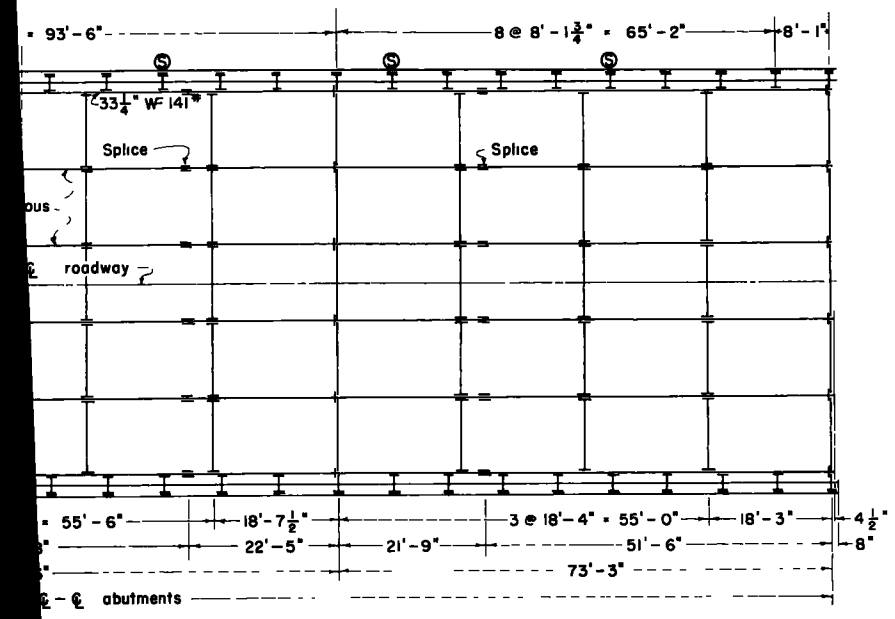

lan

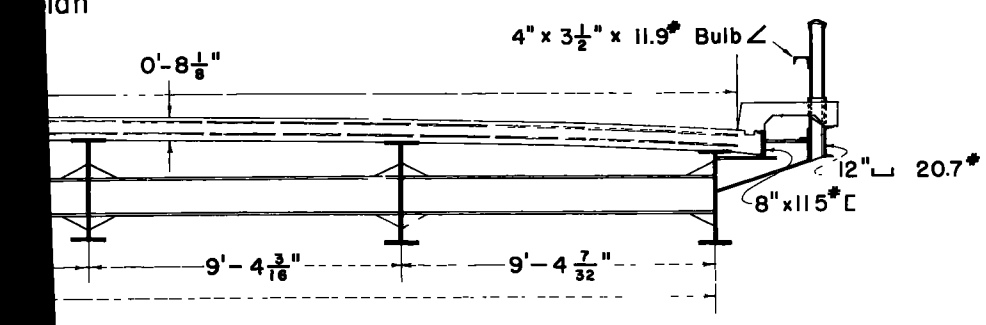

on of the test bridge.

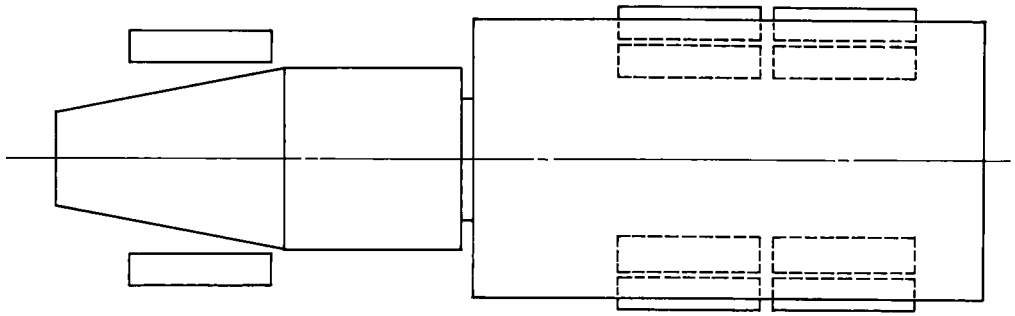

Top view

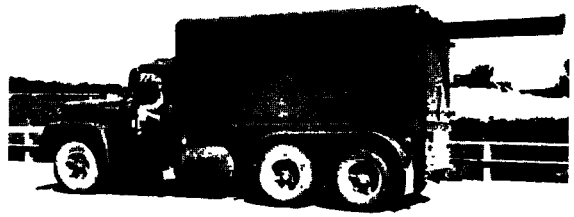

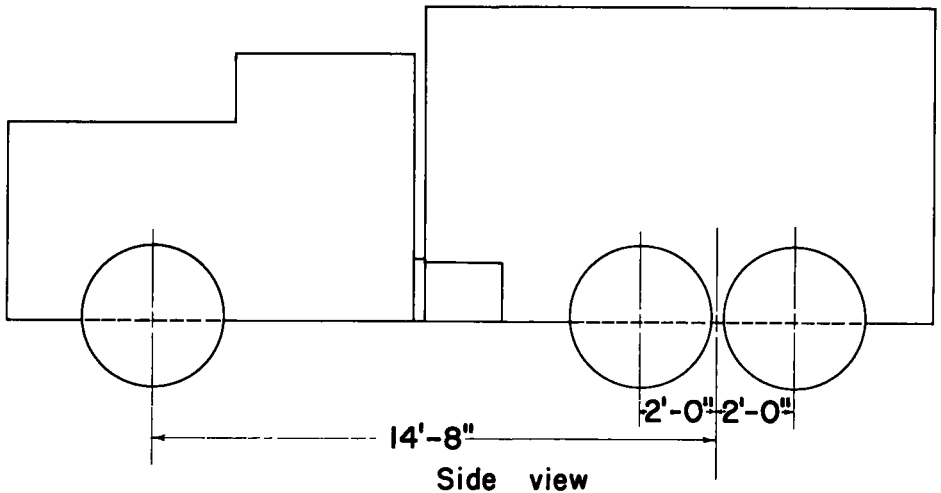

Side view

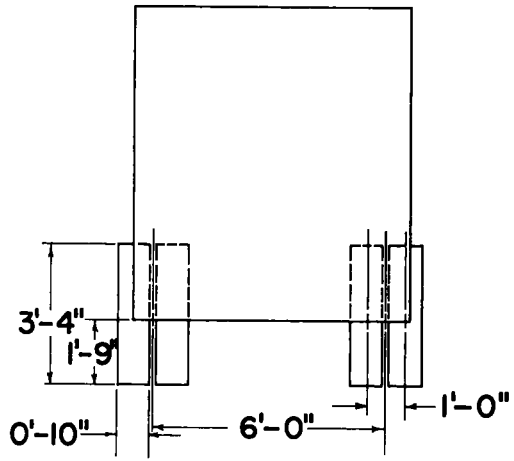

Rear view

Figure 2. The standard (H-20) loading vehicle.

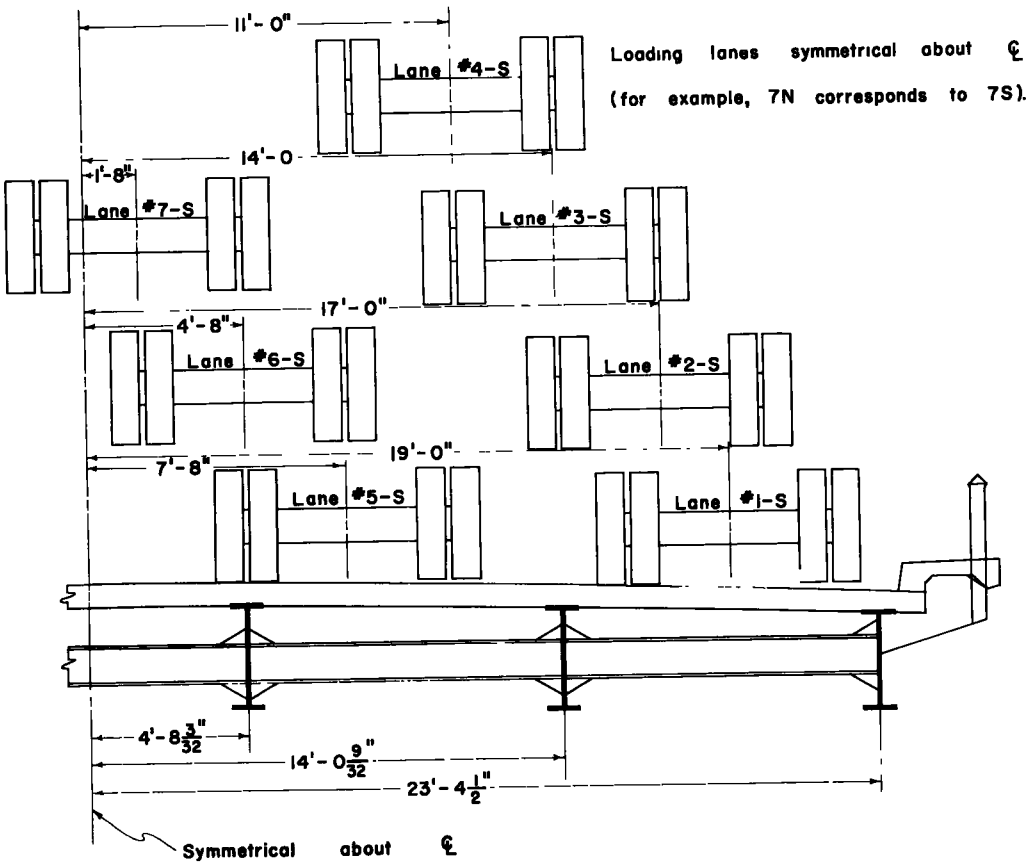

Figure 3. Cross-section showing 14 "lanes".

semi-truck, was the strain produced by an automobile significant. The vibratory motion produced by the truck was often amplified by the automobile, but in most cases the automobile only caused the vibration to continue for a longer period at the same amplitude as that produced by the truck. The period of this bridge vibration is 0.313 sec. This frequency of vibration was often superimposed in a slower vibration of 3.4 sec (Fig. 8). This "beat" or superposition of two frequencies resulted usually in the stringers which are not directly below the load, but adjacent to the "loaded" stringer. The vibration which results from this "beat" causes rather large strains, which are repeated an average of thirty times during the course of the vibration caused by one truck.

The largest strain recorded was 60 microinch per inch, which corresponds to stress of 1,800 psi. This stress was not repeated more than nine times during the 7½ hr of strain recording. This stress is, of course, in addition to the dead load stress which varies between 4,000 and 5,000 psi for the stringers subjected to this maximum repeated live load stress. The dead load stresses are shown for each different cover plate cut-off point as the equilibrium or zero live load stress ordinate on the stress-frequency diagrams (Fig. 7). The cut-off design stress for the test bridge cover plates are based on the equation

$$f_s = 18,000 - 5\left(\frac{L}{b}\right)^2$$

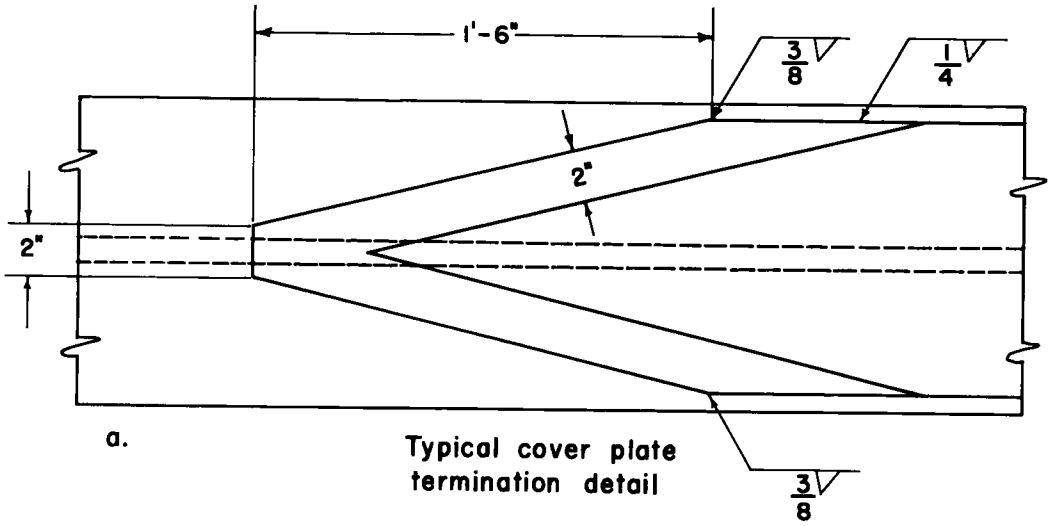

a. Typical cover plate termination detail

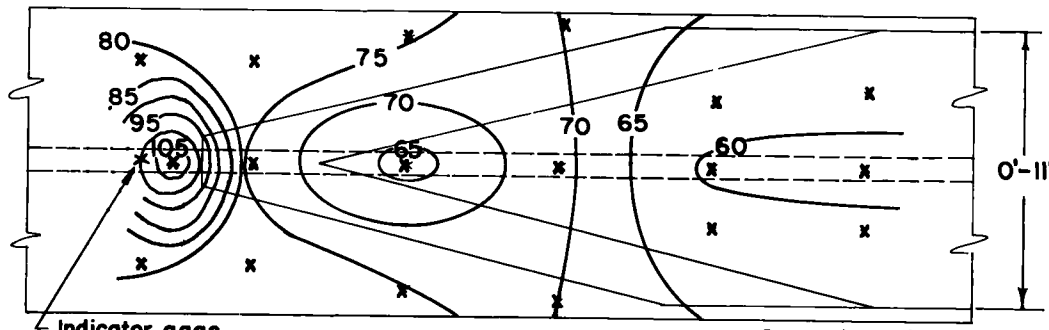

b. Long cover plate

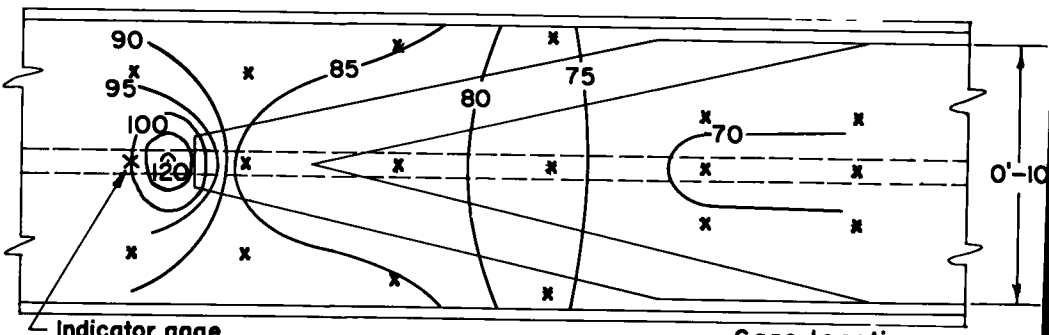

c. Short cover plate

Figure 4. Typical cover plate termination detail (at top), and longitudinal stress contours shown as a percentage of the indicator gage stress.

This equation yields an allowable stress of 16,190 psi for the outer stringers and 16,355 psi for the inner stringers. After lengthening the cover plates 18 in. for the tapered cut-off detail and rounding off the length to the nearest ½ ft, the resulting maximum design live (H-20) and dead load stress at the end of the cover plates varies from 12,300 psi to 12,700 psi for the inner stringers and 13,300 psi to 13,600 psi for the outer stringer.

The Standard Truck.—The standard truck was used as the controlled loading to study the effects of speed and position of the vehicle on the bridge structure.

Speed.—Figure 9 shows the stress-frequency curves for the indicator gage on the inside stringer at the end of the long cover plate. The moving load for these curves was the standard truck. The only variable in the data used to construct these stress-frequency curves was the speed of the vehicle. The increased number of repetitions of a given stress is indicative of the increased vibration which accompanies an increase in speed. The increase in the ordinate of each curve is an indication of the amount of impact which resulted from the moving load. Although the curves show an increase in the repetition of stress as the speed increases, it is apparent that the speed which produces the maximum number of oscillations is not necessarily the maximum speed. The final answer as to the most critical speed was beyond the scope of this research, but it is believed that the maximum vibration for a given structure is a function of speed, length of truck, and continuity of traffic.

Position.—The amount of vibration in the bridge structure is the determining factor in the amount of repetition of stress. It was found that in the bridge investigated, which has a 48-ft roadway, the lane in which the truck was traveling vibrated less than the unloaded lanes (Fig. 10). In the stringer directly below the loaded lane and the stringer below the adjacent unloaded lane, the loaded stringer has the larger stress. However, the greatest number of repetitions in stress occur in the unloaded stringer.

The position of the load used in the construction of these stress-frequency curves is shown in Figure 11. One wheel passed directly along the "loaded" stringer. The distribution of total live load to the "loaded" and "unloaded" stringers was approximately 37 and 14 percent, respectively.

Composite Section

In the typical continuous stringer highway bridge the moment of inertia of the wide flange section and cover plates at the pier is approximately the same as the moment of inertia of the composite stringer. This leads to an often used simplified analysis of live loads which assumes that the moment of inertia is constant throughout the length of the bridge. This assumption could make a considerable difference in the calculated live load moments. Therefore, to evaluate the correctness of the uniform section assumption, the prop-

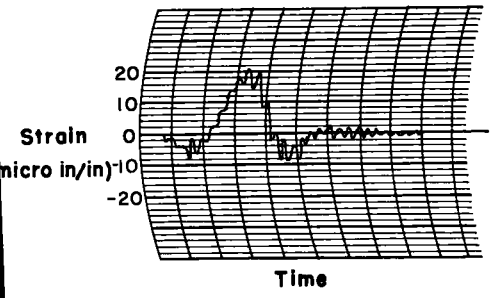

igure 5. Typical continuous strain record.

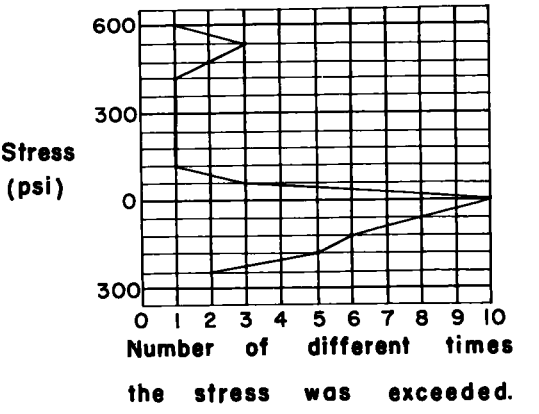

Figure 6. Stress-frequency curve for typical strain record.

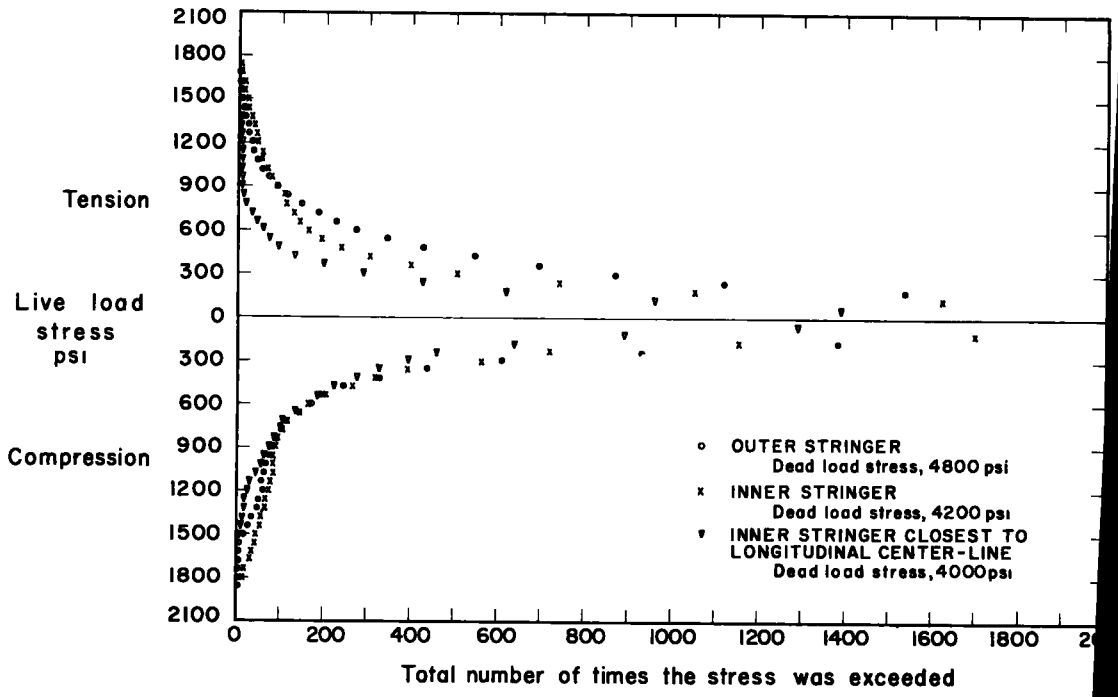

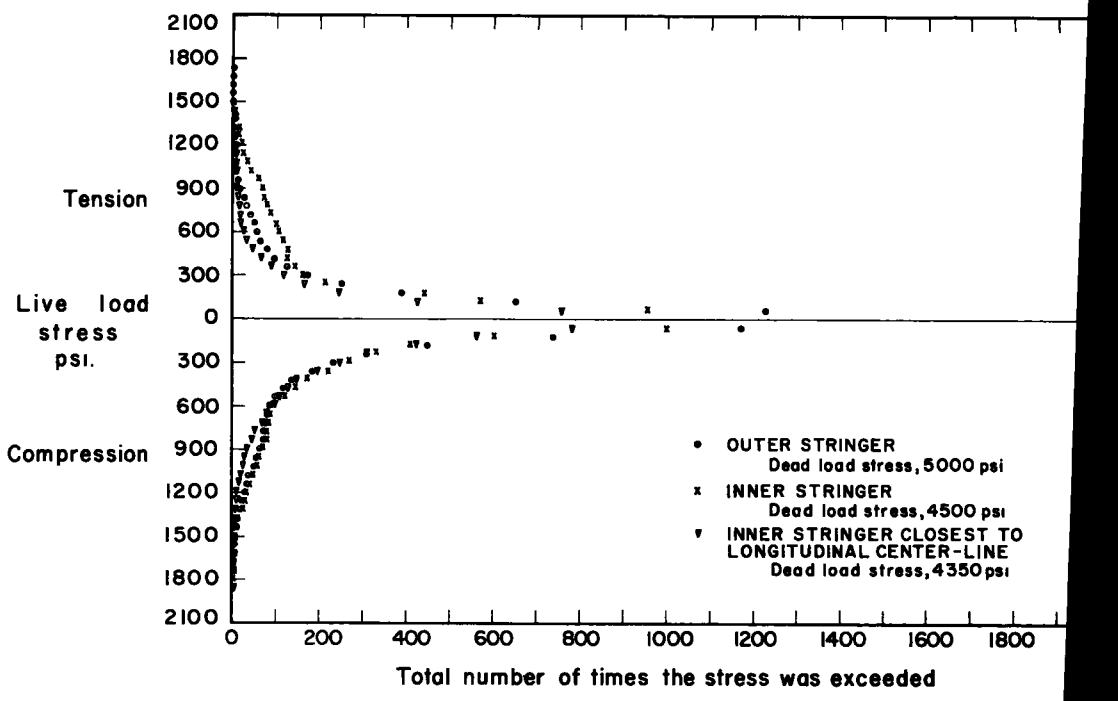

Figure 7. Stress frequency curves for the end span (at top) and stress frequency curve for the center span.

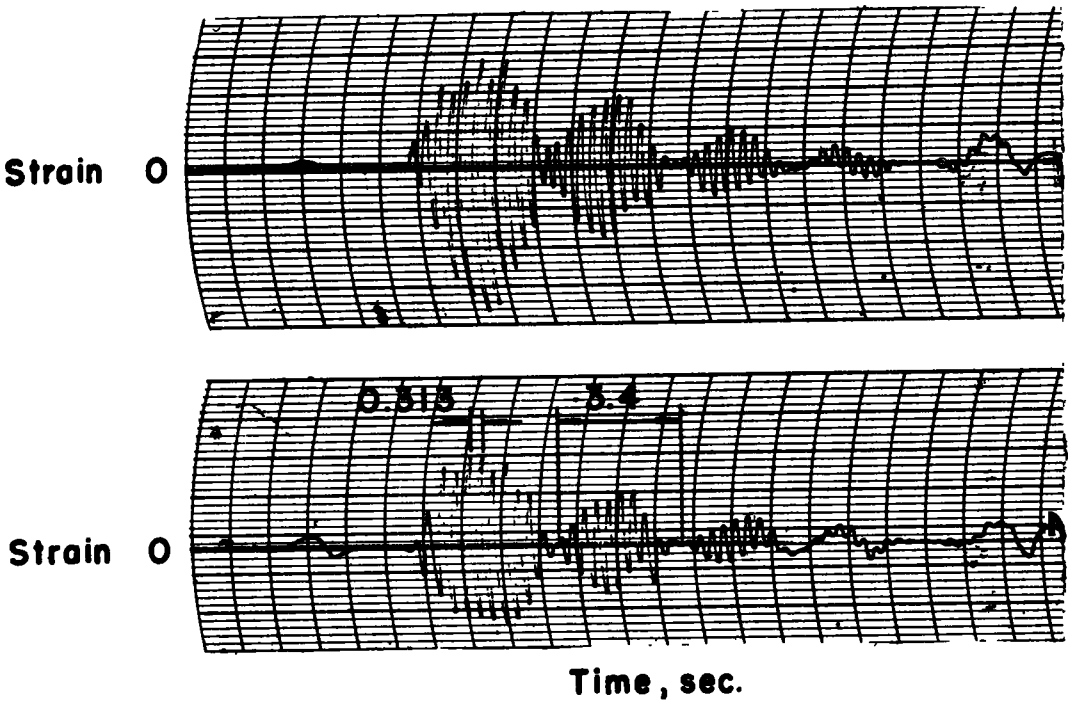

Figure 8. Beat frequency vibration due to moving loads.

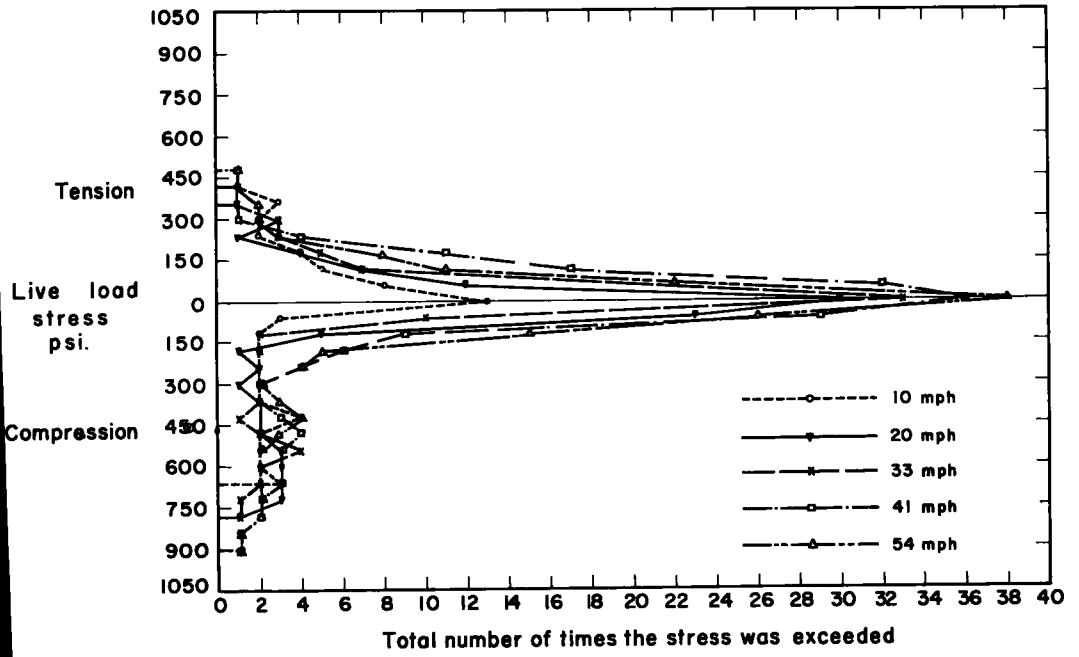

Figure 9. Effect of speed on stress frequency.

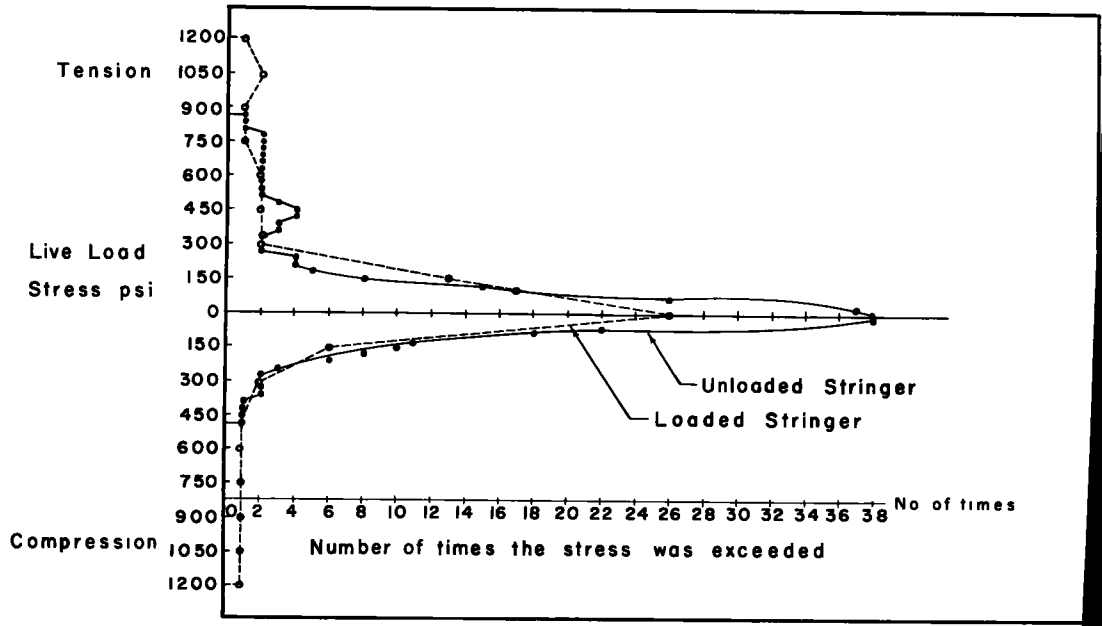

Figure 10. Stress-frequency curve for loaded and unloaded stringers.

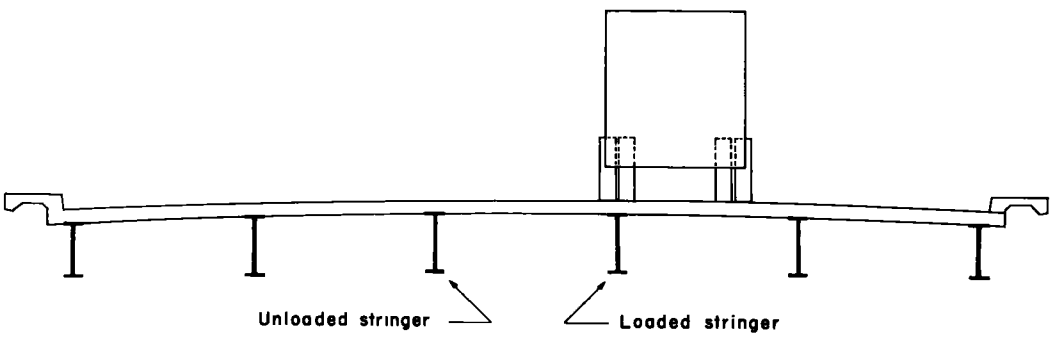

Figure 11. Position of the load with respect to the loaded and unloaded stringers.

erties of the stringer cross-section were determined at three places along the bridge. These three sections are (a) a typical positive moment section, (b) a section in which there are extreme reversals in moment, and (c) a typical negative moment section (sections I, II, and III, Fig. 1).

All three sections are located in the exterior span of the three-span bridge. Section I is located at point 0.4L of the end span from the abutment; this is approximately the point of maximum positive moment. Section II is located 17 ft from the pier and is just beyond the cover plate cutoff point. Section III is located 3 ft from the pier, near the point of maximum negative moment and yet away from the influence of the reaction and the pier diaphragm.

Another purpose of investigating the properties of the stringer cross-sections was to evaluate the actual moments of inertia and section moduli of all the stringers at one section of the bridge. This was necessary before the experimental load distribution data could be reduced and compared with the design data.

It was found that the sum of the measured strains at the bottom fiber for all the stringers at the cross-section of section I was 200 microinch per inch $\pm$ 5 percent, re

gardless of the lateral position of the load vehicle on the roadway. This seemed to indicate that the section moduli were the same for all the stringers and the lateral spreading of the load was not affected by the position of the load, or that these two factors combined so that the final result was a constant. To investigate the mechanics of the distribution of load more thoroughly, the neutral axes were determined for each of the stringers at this cross-section of the bridge. One-half of the bridge was instrumented at section I for the determination of the neutral axes of the stringers. Five SR-4 strain gages were positioned on each steel stringer. One gage was located at the center of gravity of the rolled section, and the other four gages at the extreme fibers and the quarter points of the rolled section. The locations of the neutral axes were then used to determine the amount of concrete slab which was working compositely with the steel stringers. Inasmuch as the roadway surface was spalled, the top ½ in. of the slab was disregarded in these calculations. The moment of inertia was then determined using the necessary amount of slab. A modular ratio of 10 was used in these calculations.

The experimentally located neutral axes varied considerably from the calculated location based on the specifications, and it did not depend on the load or the type of bending moment, either positive or negative. A number of readings were taken with different vehicles going in either direction across the bridge. The experimentally determined neutral axis varied less than four percent of the depth for any particular stringer.

Section I.—At Section I, the point of maximum positive moment, the position of the experimentally determined neutral axis varied for the two inner stringers, although they are both 36 WF 194 rolled sections. This position of the neutral axis was, in both cases, closer to the wide-flange centroidal axis than the calculated location based on specifications. This resulted in the stringer closest to the longitudinal center line of the bridge using 35.0 percent less slab than allowed by the specifications. The location of the neutral axis for the outer stringer, a 33 WF 141 rolled section, was found to be farther from the wide-flange centroidal axis than the calculated location based on specification. This indicates that the outer stringer has more slab acting compositely with the stringer than is available according to the specifications. Using only the roadway slab in the reduction of neutral axis data, the slab required by the outer beams exceeds the amount remaining after the portion needed by the inner beams is subtracted from the total roadway. A more realistic approach for justifying the position of the neutral axis in the exterior beam is the use of some portion of the sidewalk and curb in addition to the slab as the composite beam. This presents the problem of what amount of each of these parts to use in the composite beam. If only the curb directly above the roadway slab is used, 10 ft, 2 in. of roadway slab is required to complete the composite section. This is an unrealistic quantity of slab because the stringers are 9 ft, 4 7/32 in. center to center. This indicates that an arbitrary maximum amount of slab should be used with the sidewalk and curb. The limiting width of slab acting with the rolled section was taken as one-half the distance to the next stringer plus the overhanging slab under the curb. In addition to this slab, 22½ in. of sidewalk curb were required by the experimentally determined position of the neutral axis.

The moments of inertia of the composite stringers at section I resulting from these calculations were 27,050 in. (4), 26,580 in. (4), and 24,500 in. (4) for the three stringers on one side of the longitudinal center line (beginning with the outer stringer). The section moduli show more similarity than the moments of inertia. The composite section moduli are, respectively, from outer to inner stringer, 856 in. (3), 892 in. (3), and 876 in. (3) or a variation from the average of ± 2 percent (Fig. 12).

Section II.—Section II, 17 ft, 0 in. from the pier, is near the dead load contra-flexure point and is subjected to extreme variations in the live load bending moment. Because the section is just outside the cover plate cutoff point, the results indicate the effect of the cover plates on the neutral axis in an area where an abrupt change is theoretically indicated but actually incongruous. The position of the neutral axis of the outer stringer indicates that only a small portion of the sidewalk and curb acts in addition to the arbitrary maximum amount of roadway slab (the arbitrary maximum width for

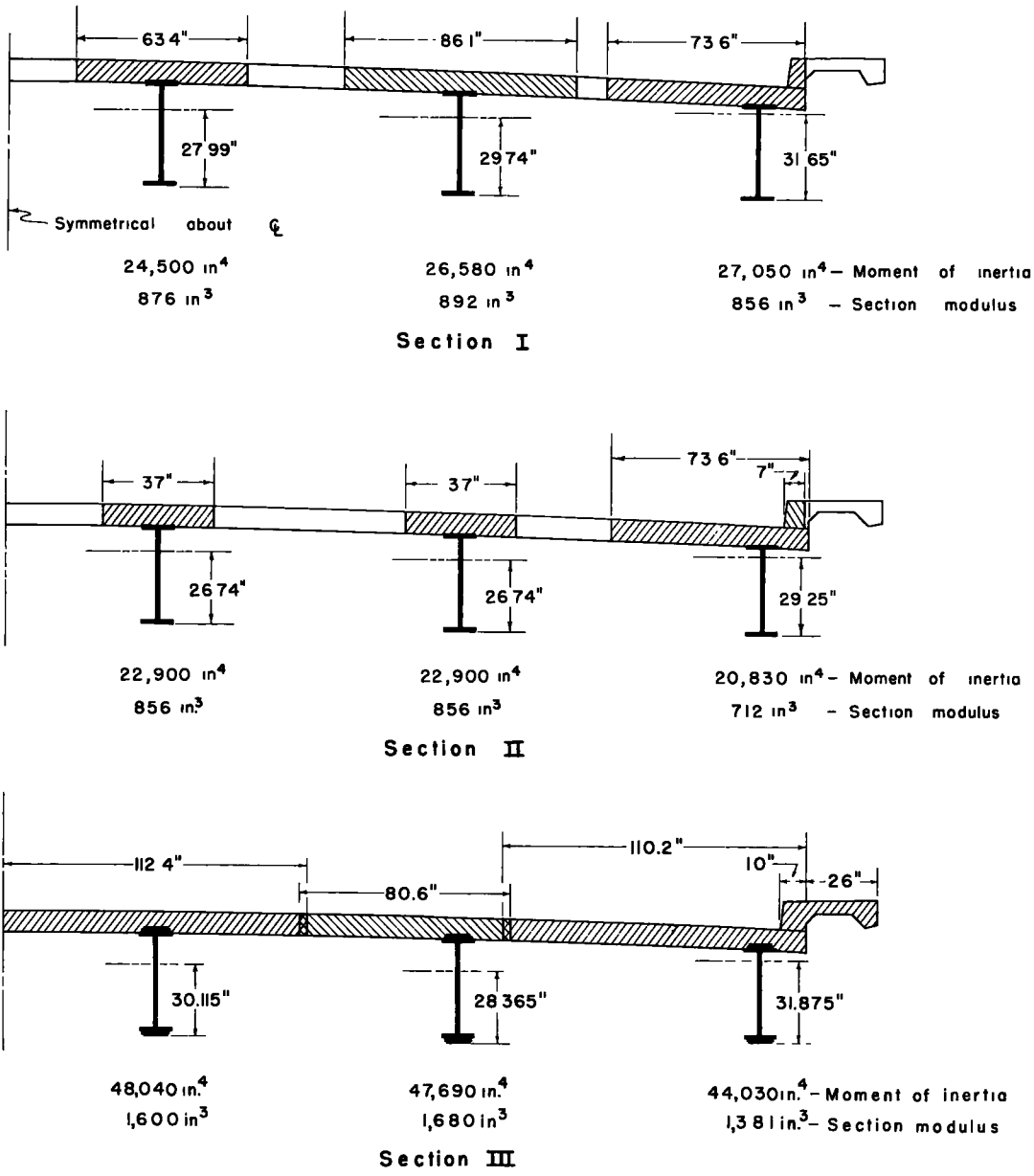

Figure 12. A cross-section of the bridge at sections, I, II, and III showing the composite moments of inertia, section moduli, and the effective slab.

the slab extends to the midpoint between beams). The moment of inertia of the composite stringer is 22.9 percent less at this section than at section I. This is the result of lower position of the neutral axis which, of course, results in a smaller composite section. One factor affecting this is the size of the rolled section. The outer stringer changes from a 33 WF 141 to a 33 WF 152 at a splice on both sides of the pier. Thus, section II is a larger (33 WF 152) wide flange than section I. Thus, the neutral axis will move toward the center of gravity of the rolled section as this rolled section

becomes larger. Also, the cover plates, which terminate nearby, have a tendency to bring the neutral axis closer to the centroid of the rolled section. However, the extent of this effect is unknown.

The inner stringers at section II, both 36 WF 194 rolled sections, have neutral axes closer to the wide-flange centroidal axes than observed at section I. This resulted in an average reduction in moment of inertia of 10.2 percent. The position of the neutral axis was the same for both inner stingers at section II.

A comparison of the moments of inertia and section moduli of the stringers at section II shows a variation of $\pm$ 4.6 percent in the moments of inertia while the section moduli varied $\pm$ 9.2 percent. The moments of inertia are 20,830 in. (4) for the outer stringer and 22,900 in. (4) for the inner stringers. The section moduli are 712 in. (3) and 856 in. (3) for the outer and inner stringers, respectively.

Section III.—The third section at which the neutral axes were found was 3 ft, 0 in. from the pier. This section is near the point of maximum negative moment but should not be affected by the reaction of the pier or by the pier diaphragm. The location of the neutral axis of the outer stringer at this point corresponds approximately to the location of the neutral axis at section II (at the end of the long cover plates). But, because of the cover plates, two plates on the top and bottom flanges, the required amount of composite concrete is increased, and, of course, the moment of inertia is greatly increased. The position of the neutral axis of the outer stringer required that more than all the sidewalk be used in addition to the maximum amount of roadway slab (the arbitrary maximum width of slab extends to the midpoint between beams). Therefore, in addition to all the sidewalk and curb 110.2 in. of roadway were used in the calculations. The resulting moment of inertia and section modulus of the outer beam were 44,030 in. (4) and 1,381 in. (3), respectively.

The inner stringers at section III also exhibit a large amount of composite action. The inner stringer closest to the longitudinal center line required 80.6 in. of slab and the other interior stringer required 112.4 in. of slab. The locations of the neutral axes at section III of the inner stringers corresponds approximately to the locations of neutral axes at section II. Again because of the cover plates, the size of the composite section is considerably greater. The moments of interia for the two inner stringers are 48,040 in. (4) and 47,690 in. (4), the latter being the stringer closest to the longitudinal center line. The section moduli are 1,600 in. (3) and 1,680 in. (3), for these two stringers, respectively.

The total width of roadway slab required at section III exemplifies the composite action situation in the section of negative bending. The total width of roadway required by all three stringers is 25 ft, 3 in. plus the sidewalk and curb. This required slab exceeds the total slab available by 10 in. over the entire width of the bridge. Thus, it is evident that composite action occurs at the pier, and this action should be considered in design if a true analysis is desired.

These neutral axes results are incomplete for the determination of the variations in cross-section along the entire length of the bridge. They do show, however, that the final composite cross-section varies greatly at different sections along the bridge stringers. The variations in moments of inertia and section moduli along the outer span of the three-span bridge can be shown most clearly by reducing the actual values to unit values. Using the moment of inertia and section modulus of the outer stringer at section I as a base, the ratio of the values at sections II and III, respectively, to the values at section I are:

RATIO OF MOMENTS OF INERTIA

Stringer	Section		
	I	II	III
Outer	1.0	0.77	1.62
Inner	0.981	0.846	1.77
Inner (closest to longitudinal center line)	0.906	0.846	1.76

RATIO OF SECTION MODULI

Stringer	Section		
	I	II	III
Outer	1.0	0.83	1.61
Inner	1.04	1.0	1.96
Inner (closest to longitudinal center line)	1.02	1.0	1.87

The moment of inertia of the composite outer stringer is 8 percent smaller than the moment of inertia of the composite inner stringer even though the moment of inertia of the outer stringer rolled section is an average of 35 percent smaller than the moment of inertia of the inner stringer rolled section. The difference is in the amount of composite slab assumed by each of the respective stringers and the sidewalk and curb which act with the outer stringer.

Load Distribution

Of particular interest to the design engineer is how the vehicle loads are distributed to the supporting beams. A number of research programs have been conducted on this subject (3, 4, 5). The results of some of these projects are in the recent revision of the American Association of State Highway Officials design specifications. Although the primary intent of this research was not to evaluate load distribution to the longitudinal stringers, this problem was encountered in this research when an analysis of the experimental stresses was made.

The complexity of the slab-stringer-type bridge does not lend itself conveniently to an exact solution. The slab, which is the roadway, also acts as an integral part of the longitudinal stringers. The continuity of slab over the stringers and the unequal deflections of the stringers combine to make load distribution a function of many variables. Therefore, the results contained in this report are for one bridge and cannot be considered conclusive for all slab-stringer bridges.

The 48-ft wide roadway has resulted in longitudinal distribution of the concentrated wheel loads over a very wide area. This yields a total moment at any one cross-section of the bridge which results from a relatively concentrated load, if a stringer is directly beneath the wheels, and a distributed load on the other stringers. This distributed load is probably a function of the lateral distance from the wheel to the stringers.

The moments in the bridge stringers at section I were determined by measuring the outer fiber flexural strains at that cross-section and multiplying each strain by the modulus of elasticity of steel and the section modulus of the corresponding beam. The total moment at this section is then the sum of these moments.

Because the section moduli of the stringers at section I are almost equal, and because the sum of the experimentally measured strains for all the stringers at section I are also constant regardless of the lateral position of the load, as previously hypothesized, the lateral spreading of the load was not affected by the lateral position of the load on the roadway.

It was found that, regardless of the lateral position of the loading vehicle on the roadway, the total moment of all the stringers at section I varied only $\pm$ 2.2 percent from an average of 424 kip ft for the vehicle traveling toward the abutment (west to east) and only $\pm$ 1.5 percent from an average of 431 kip ft for the vehicle traveling toward the pier (east to west). These moments occur with the rear axle of the vehicle at section I.

The theoretical moment at section I which results from the standard vehicle traveling toward the abutment, assuming a constant cross-section and no longitudinal distribution is 550 kip ft. The corresponding total experimentally determined moment of 424 kip ft is 77.1 percent of this theoretical value. Similarly, the theoretical moment at section I resulting from the standard vehicle traveling toward the pier, again assuming a uniform cross-section and no longitudinal distribution, is 564 kip ft. The experimental moment of 431 kip ft is 76.5 percent of this theoretical moment. This percentage corresponds very closely with the previous one.

The difference between the experimental and theoretical moments is the result of the longitudinal distribution of load and the variation in cross-section. The longitudinally distributed load extends over the entire length of the stringer farthest from the wheel load and over a smaller portion of a stringer closer to the wheel load, and like the variations in cross-section, this would tend to decrease the positive moment.

By using the individual moment of each stringer as a percent of the total moment, the variation in the lateral distribution of load can be determined for the stringers. This assumes the moment diagram for all the stringers are indentical in shape, similar to the design assumptions. Figure 13 shows the static load distribution at section I (approximately the point of maximum positive bending moment) as a percent of load carried by each stringer. The cross-section of the bridge is shown at the top of the graphs, and the position of the truck is indicated on each particular graph.

In obtaining the maximum distribution of load to the various stringers, the static load distribution curves were used with the assumption that superposition is valid (6). The largest number of standard vehicles which contribute to the load in each respective stringer were superimposed on the bridge roadway. Each vehicle was limited in its lateral movement to the width of its lane less approximately 2 ft for clearance. This could be accomplished by using the experimental lane data without any need for interpolation. Three trucks were used for the outer stringers and four vehicles were used in the computation of the maximum load on the inner stringers.

By loading lanes 1-S, 5-S, and 6-N the roadway is loaded to produce the greatest load in the outer stringer while keeping the trucks approximately within 2 ft of the edge of their respective lanes (Fig. 13). To improve the accuracy of the results the percent distribution values were averaged with the corresponding values for the other outer stringer using lanes 1-N, 5-N, and 6-S. The resulting average load distributed to an outer stringer is 64.15 percent of a standard vehicle. This corresponds to a wheel load distribution factor of 1.283.

The lanes loaded to produce the largest load in the inner stringer immediately adjacent to the outer stringer are lanes 2-S, 5-S, 2-N, and 6-N for this stringer on the south, and 2-N, 5-N, 2-S, and 6-S for this stringer on the north (Fig. 13). Averaging these two values, the average percent of a standard vehicle distributed to each of these stringers is 78.45 percent. This corresponds to a wheel load distribution factor of 1.569.

The lanes loaded to produce the largest load in the inner stringer closest to the longitudinal center line are lanes 2-S, 6-S, 6-N and 2-N for both the stringers on the north and on the south of the longitudinal center line. The average percent of a standard vehicle distributed to each of these stringers is 78.5 percent. The wheel load distribution factor for these stringers is therefore 1.570, which is very close to the wheel load distribution factor for the other inner stringers.

These distribution factors are for approximately 77 percent of a unit vehicle load as a result of the variation in cross-section and the longitudinal distribution. A comparison of these values can now be made with the AASHO design specification load factors.

The specifications require that a load factor of S/5.5 be used in determining the fraction of a wheel load applied to an interior (inner) stringer. For this bridge the load factor for an inner stringer is 1.70.

The fraction of a wheel load applied to the outer stringers by the AASHO specifications shall not be less than "the reaction of the wheel load obtained by assuming the flooring to act as a simple beam between stringers" or the fraction of a wheel load found by

$$\frac{S}{4.0 + 0.25S} \qquad 6 \text{ ft} \leqq S \leqq 14 \text{ ft}$$

The first criteria results in a load factor of 1.06 while the second criteria results in a load factor of 1.475. Thus, the second load factor governs.

Investigating the problem of load distribution further, another method of analysis was used to determine the theoretical amount of wheel load distributed to the outer stringers. This is a method which makes use of the formula usually associated with eccentric column analysis (7). The formula is

$$f = \frac{P}{A} \pm \frac{Pey}{I}$$

or

$$W_n = I_n \left[\frac{P}{\Sigma I} \pm \frac{PeC_n}{\Sigma Iy^2} \right]$$

in which

P = total load,
e = eccentricity of load,
C_n = distance of Nth girder from centroid of I's,
ΣI = sum if I's for all girders,
ΣI_y^2 = sum of the moments of inertia of I's,
I_n = moment of inertia of Nth girder, and
W_n = load carried by Nth girder.

This formula is used by the Iowa State Highway Commission to determine the amount of load distributed to the outer stringers. A unit moment of inertia is assumed for each stringer so that it is not necessary to approximate the relative sizes of stringers prior to the analysis. It was found that for the bridge tested, the experimental moments of inertia varied less than 6 percent at the 0.4L point (section I). Thus, the use of unit moments of inertia is a good approximation for this bridge. By placing three vehicles in the position for a maximum load on an outer stringer and using the foregoing method of analysis, a theoretical design load factor of 1.64 is found. This value corresponds to the loading which produces the largest experimental load. However, a design loading of four vehicles would be used by the Iowa State Highway Commission, and this results in a design load factor of 1.452 for the outer stringer.

The Effect of Impact on Load Distribution.—It has been suggested by one author that the increase in stress due to impact for highway bridges "might be almost any value between 10 percent and 200 percent of the amount given by the specifications" and that an over-all impact factor might be apportioned to the stringers individually (7). This suggestion and others dealing with impact seem to indicate that the simplicity with which impact is handled in design, has resulted in large inequities in the actual stresses produced in different type bridges under similar loads (8). From the data obtained during this research an analysis of impact and the effect on the distribution of loads may be made.

Moving load tests were performed using 4 of the 14 test lanes. Speed increments of 10 mph were used up to the maximum speed obtainable from the vehicle (approximately 50 mph). The vehicle used was the standard H-20 truck. The stress resulting from the moving vehicle was obtained as a continuous strain time record. A similar record of the vehicle moving slowly across the bridge had been obtained. This was considered the static stress with no impact. The effect of the dynamic loads is considered to be the variation from this static strain record. This variation appeared as a transient vibration superimposed on the static strain record. The amount of the impact resulting from this moving load cannot be considered to be the maximum. The maximum amount of impact for this bridge would probably result from a truck-trailer combination with the maximum trailer length. This is a surmise in a relatively unexplored area that needs further research. The importance of the data presented here is not in the quantitative but instead in the qualitative aspect. The way in which the impact affects the distribution of load and the way in which the impact per se is distributed is the objective of this data.

The distribution of load to the various stringers for a vehicle traveling on the experimental lanes at various speeds is shown in Figure 14. At the top of the graph is the bridge cross-section with the vehicle position located. Each part of the graph indicates the load distribution for a different speed. The solid line indicates this dynamic load distribution for the vehicle at Section I, and the dotted line represents the value obtained from the static tests at the same section. The static test values were determined from the strain time curve obtained by the vehicle moving slowly across the

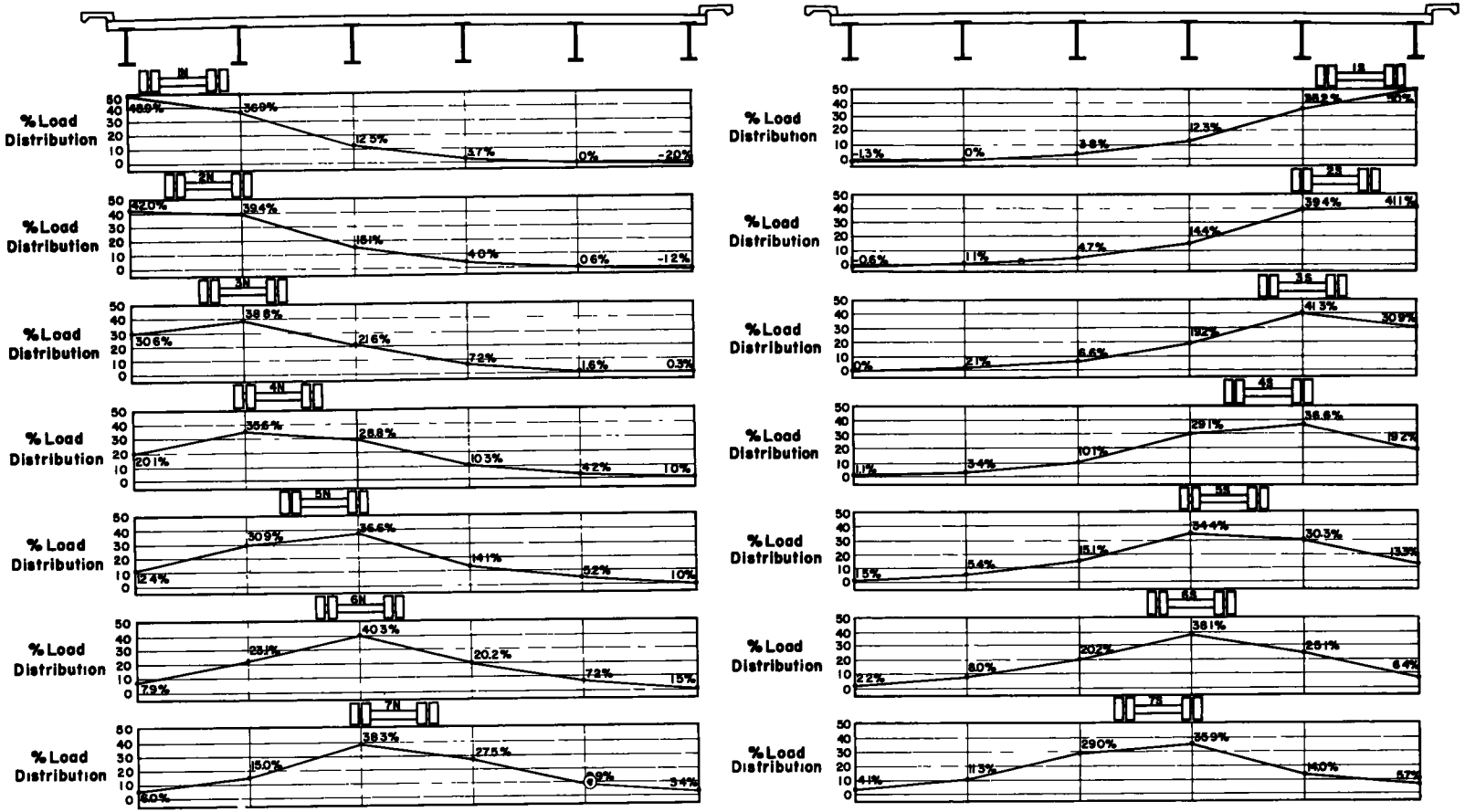

Figure 13. Static load distribution at section I.

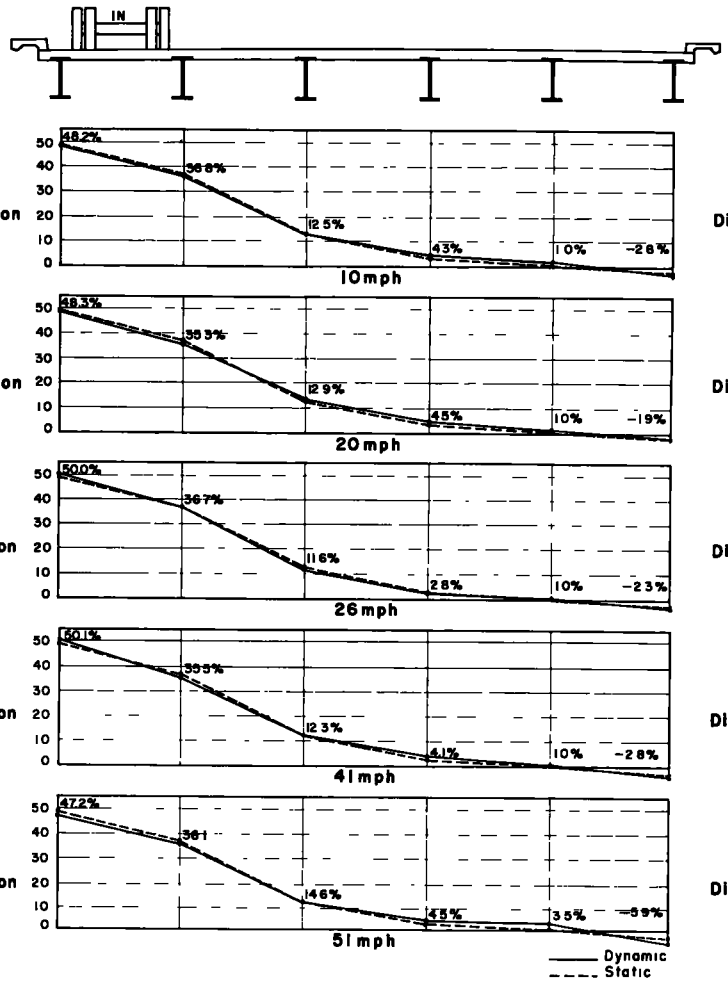
IN
% Load Distribution
48.2%
36.8%
12.5%
4.3%
1.0%
-2.8%
10 mph
48.3%
35.3%
12.9%
4.5%
1.0%
-1.9%
20 mph
50.0%
36.7%
11.6%
2.8%
1.0%
-2.3%
26 mph
50.1%
35.5%
12.3%
4.1%
1.0%
-2.8%
41 mph
47.2%
36.1
14.6%
4.5%
3.5%
-5.9%
51 mph
Dynamic
Static

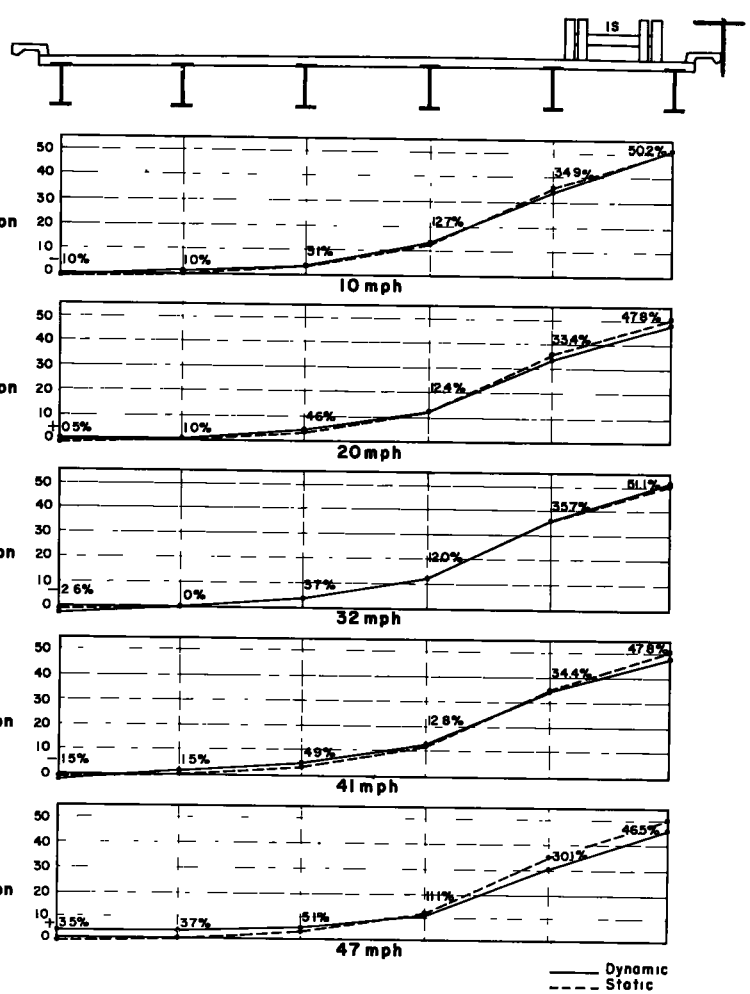
IS
% Load Distribution
1.0%
1.0%
3.1%
12.7%
34.9%
50.2%
10 mph
0.5%
1.0%
4.6%
12.4%
33.4%
47.9%
20 mph
2.6%
0.0%
3.7%
12.0%
35.7%
51.1%
32 mph
1.5%
1.5%
4.9%
12.8%
34.4%
47.8%
41 mph
3.5%
3.7%
5.1%
11.1%
30.1%
46.5%
47 mph
Dynamic
Static

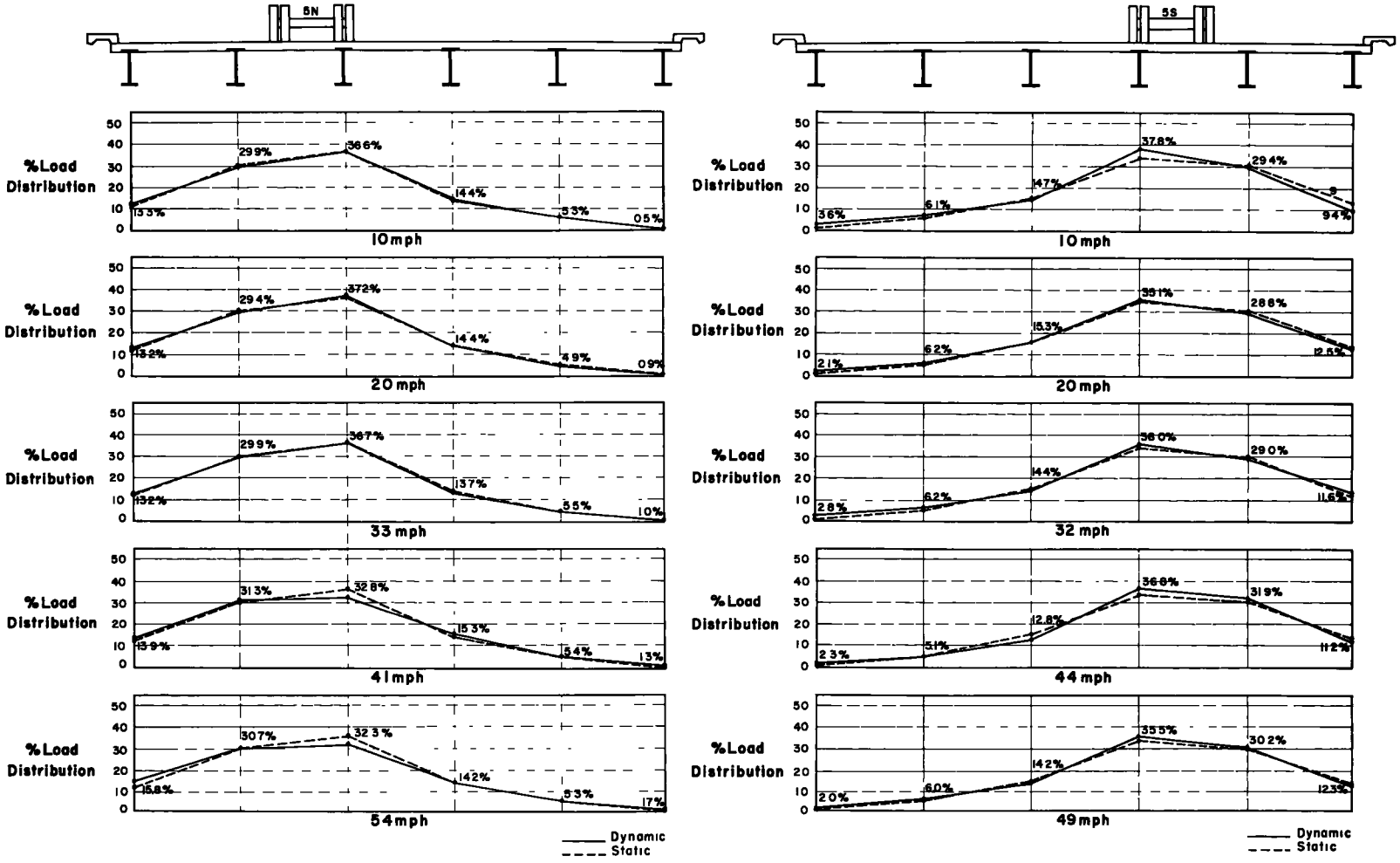

Figure 14. The effect of speed on the distribution of load; the percent figure applies to the dynamic load only.

bridge. This is the same static load distribution curve shown in Figure 13. The resulting variations between the dynamic and static load distribution curves are very small.

Shown in Figure 15 is the impact or increase in stress which is shown as a percentage ratio of the dynamic moment to the static moment. This value for the individual stringers is shown beneath the respective stringers. The total impact in the bridge cross-section is a percentage ratio of the total dynamic moment to the total static moment in the bridge cross-section. The total impact is shown at the right of each graph. The individual impact values vary considerably and in some cases are less than 100 percent, or less than the static value. This indicates that the dynamic moment was smaller than the static. Also, the impact ratio for some stringers is shown as infinity which results from a zero static live load moment. The total bridge impact values also vary considerably, but their tendency is to increase as the speed increases. The vehicle is shown on the bridge cross-section at the top of the figures in the position for which the underlying series of dynamic results were obtained.

The impact values obtained for the individual stringers cannot be compared with the total bridge impact values. These two values vary considerably and are the basis of many contradictory conclusions.

SUMMARY AND CONCLUSIONS

The structure tested in this research program was a three-span continuous composite steel stringer bridge typical of the type used by the Iowa State Highway Commission on primary and interstate highways. Some detail changes have been made by the I. S. H. C. bridge design section in this type since this bridge was built. However, the results obtained in this research are at least qualitatively applicable, and some are quantitatively applicable to the continuous composite steel stringer bridges being designed.

Stress Frequency and Fatigue

The stress-frequency curves obtained in this research indicate that the number of cycles of repetition is large, although the corresponding stress is rather small. Approximately the largest repeated live load stress produced was 1, 800 psi and this was not repeated more than nine times in the 7½-hr sampling period. The stringers with the largest dead load stress which were subjected to this maximum repeated live load have a stress variation pattern of 4, 500 ± 1, 800 psi, or a maximum stress of 6, 300 psi and a minimum of 2, 700 psi. A comparison of this data with the results of other fatigue tests (1) can be made to determine if the fatigue strength of these cover plate termination areas might be critical. Using a summation (2) of fatigue data for "beams with partial length cover plates attached with continuous fillet welds," a fatigue strengt of 11, 500 ± 2, 500 psi is indicated for 2, 000, 000 cycles of zero to maximum stress. Assuming the ultimate strength of structural steel is 60, 000 psi, and using Goodman's equation, an indication is obtained of how the fatigue strength of "beams with partial length cover plates attached with continuous fillet welds" compares with the experimental results of the stress-frequency data for the structure tested. By using the mo critical fatigue strength of 9, 000 psi, (11, 500 - 2, 500) and assuming that the dead load stress level is 4, 200 psi, the repeated amplitude of stress for fatigue to be critic is ± 4, 425 psi. Alternately, assuming a repeated amplitude of stress of ± 1, 800 psi and the same fatigue strength as mentioned, the dead load stress level for critical fatigue is 37, 300 psi. Because the dead load stress level for most bridges will correspond closely to the value for the bridge tested, and because it is not likely that the dead load stress level will be increased in the future, a closer look at the critical repeated amplitude is necessary.

From the experimental results it is possible to obtain an average repeated amplitude of ± 5, 890 psi by placing eighteen H-20 trucks on the test structure. This does not include the dynamic effect that such a combination of vehicles might produce but on the other hand it requires a spacing of vehicles of 7. 33 ft. This hypothetical case shows that it is possible for the critical fatigue amplitude to be exceeded, although th

possibility of it occurring often enough to produce a fatigue failure is at the present absurd.

The previous simple calculations seem to indicate that the cover plate termination regions investigated are not critical due to fatigue considerations. However, the fatigue strength based on the Illinois fatigue tests should not be applied without some concern about the difference between the fatigue tests and the actual bridge stringers which are being compared. The comparison of the experimental fatigue results with the actual stress frequency of the bridge stringers is based on a phenomenon first studied by Wohler (9) and later formulated by Gerber and Goodman. All these results are based on the idea that the range of stress necessary to produce failure decreases as the mean stress increases. This permits a comparison of the zero to maximum stress condition of the experimental fatigue results with a mean stringer stress of 4,200 psi plus or minus the live load stress amplitude in the bridge stringer. However, other investigators have shown that there is no general law connecting the mean stress and the stress range. It is necessary, therefore, to obtain experimental fatigue data for the range of stress at the critical regions of the bridge stringers before their fatigue life can be determined with any certainty. For additional accuracy in the correlation of experimental fatigue tests with the actual bridge stringer data, the experimental stress cycle during the fatigue test should be varied periodically to correspond with the actual stress variations. This fatigue test, with varying amplitudes of stress, would estimate service life under service stresses. To correlate this experimental fatigue test with the actual service stress condition, a previously determined stress-frequency curve is converted to a stepped curve with a logarithmic scale, and this is converted in turn to the variable stress fatigue program required for testing.

Each variable stress fatigue program is one series of stress cycles. These stress cycles are continued, one series after another, until failure occurs. In a second program all the stresses are multiplied by a constant factor, thus a curve similar to the usual endurance curve is obtained which relates stress level to the life of the specimen. This curve could be used to determine an allowable design stress, after the application of a safety factor.

A stress frequency curve in Figure 7 is converted to a stepped curve in Figure 16, and the resulting variable stress fatigue program is in Figure 17. Only with the results from a variable stress fatigue experiment based on a program similar to that in Figure 17 will the designer ever know whether bridge structures have a finite fatigue life, at which point they will require extensive repair, or whether the cover plate termination stresses are ultra-conservative.

Variations in Cross-Section

It has been shown that there is composite action even in the cross-sections subjected to negative bending. This occurs even though a maximum live load tensile strain of 60 microinch per inch was experimentally determined in the extreme top fiber of the roadway slab. This corresponds to a stress of approximately 180 psi. Therefore, it is not unrealistic to assume that there is complete action all along the stringer.

It might be possible by using this composite action judiciously to attach the cover plates to the lower flange only or even to omit them entirely. For instance, if the same amount of slab acted compositely with an inner stringer without cover plates as with an inner stringer with cover plates, the composite moment of inertia would exceed by 10 percent the theoretical moment of inertia of the non-composite wide flange with cover plates.

The data and results for the composite cross-sections also indicate that the assumption that the final moments of inertia of the stringers are constant throughout the length of the bridge is very much in error. The positive moment regions have composite action as assumed in design, and the resulting moments of inertia correspond closely to the theoretical moment of inertia of the wide-flange sections with cover plates and no composite actions. However, the composite action at the supports increases the moment of inertia 148 percent for the outer stringers and 85 percent for the inner stringers. Therefore, the final ratio of the moment of inertia at the negative moment

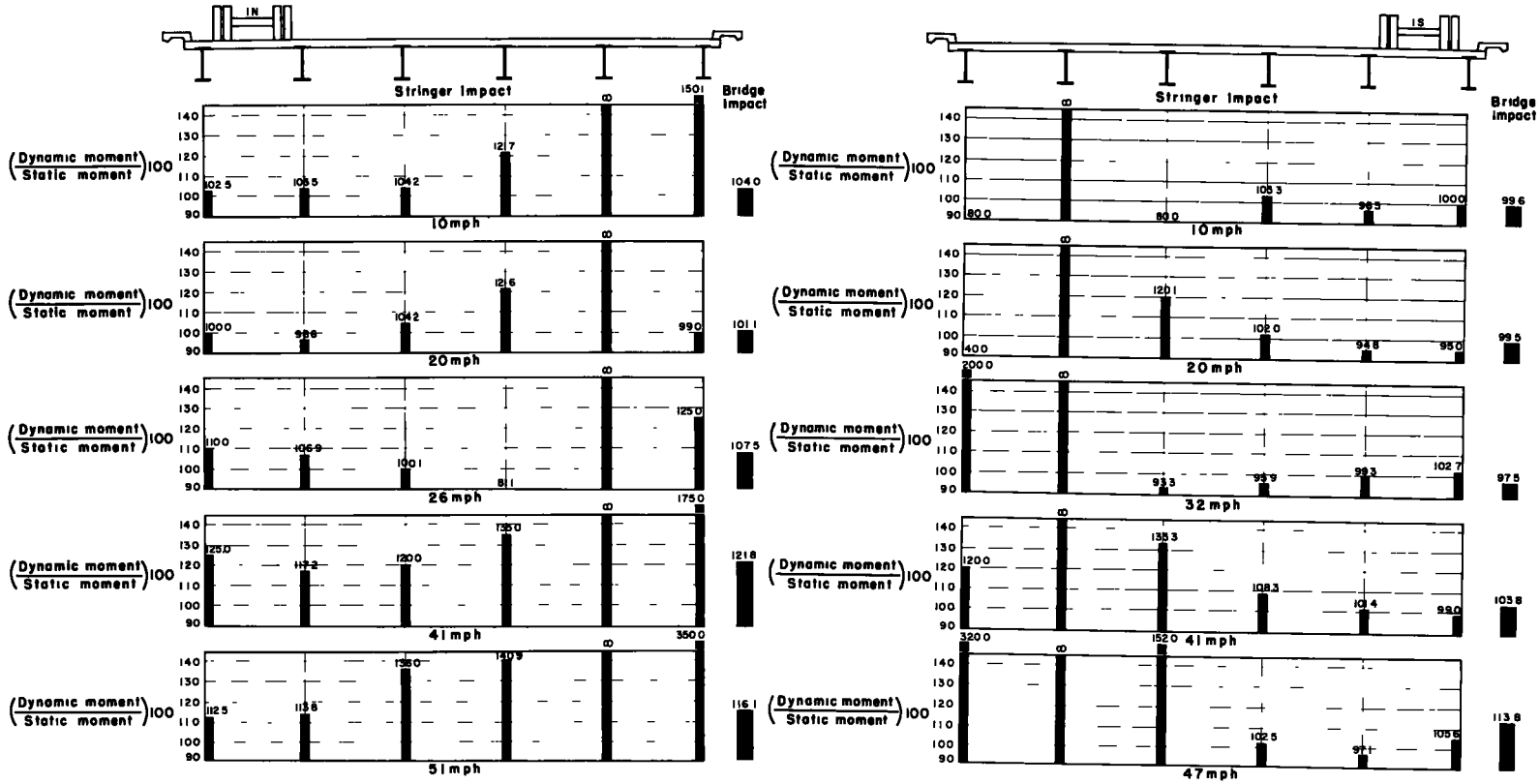
1N
Stringer Impact
Bridge Impact
(Dynamic moment / Static moment)100
10 mph
20 mph
26 mph
41 mph
51 mph
1S
47 mph

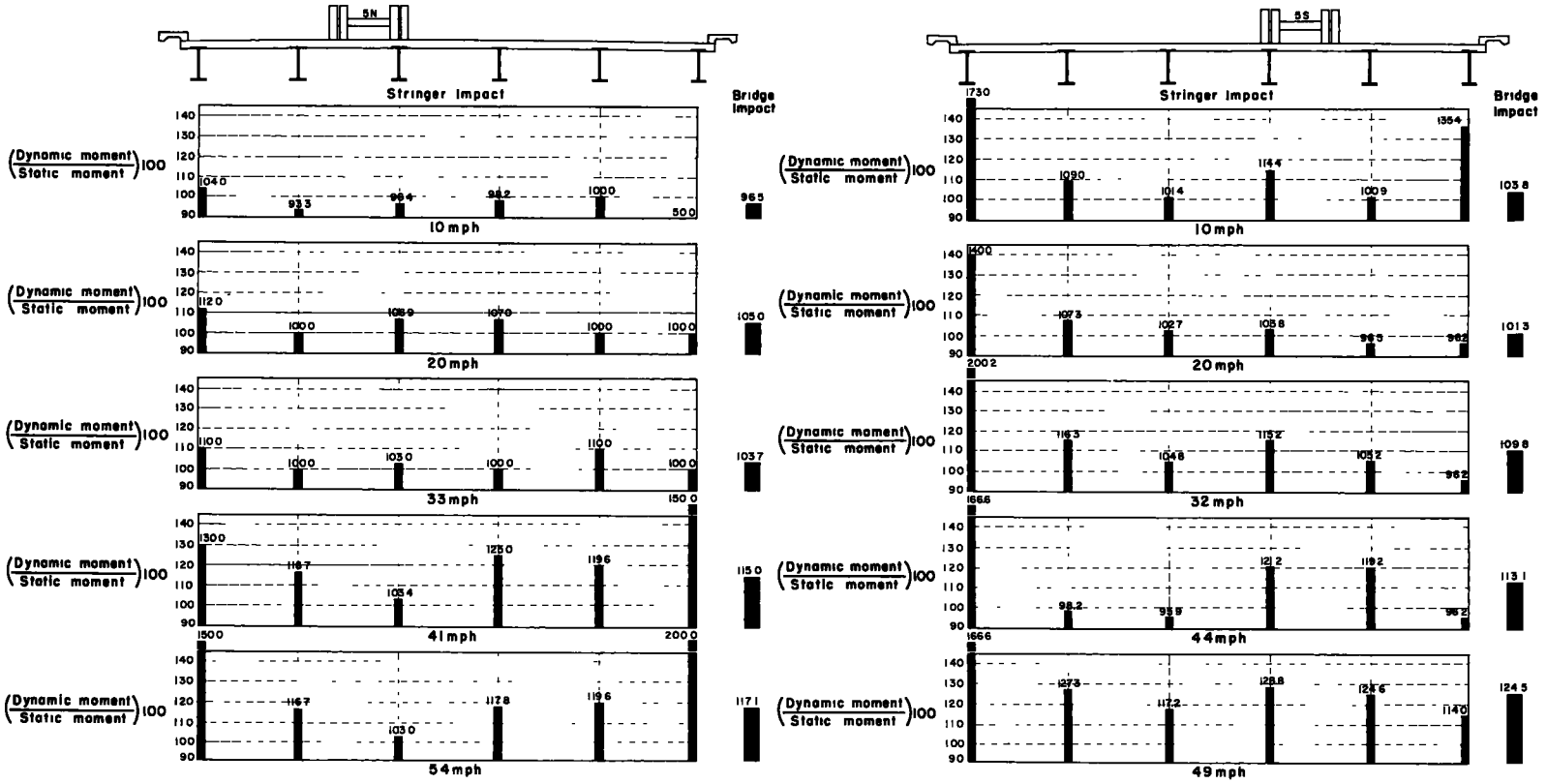

Figure 15. Percent impact for each stringer and for the whole bridge.

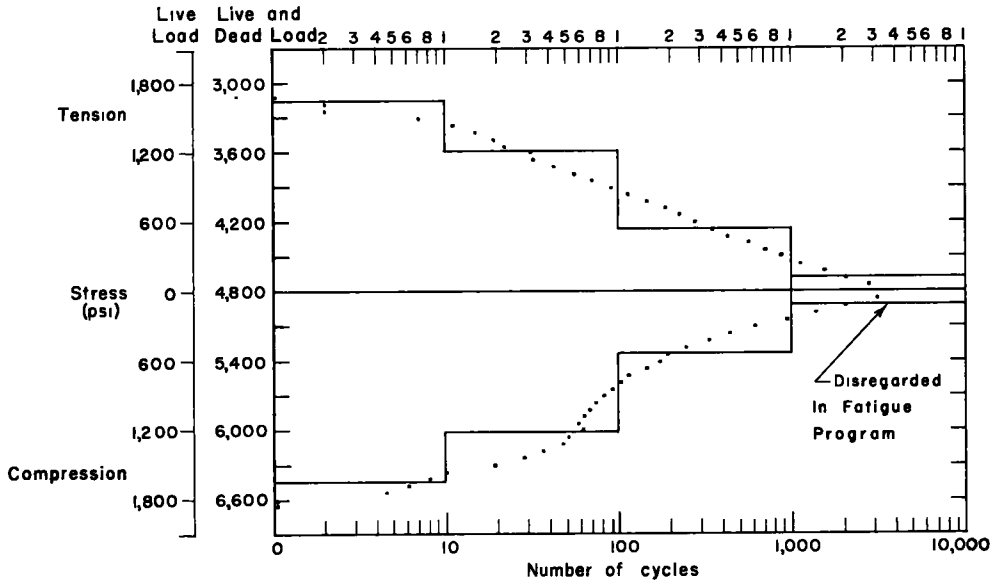

Figure 16. A stepped stress frequency curve for the cover plate termination detail of the outer stringer in the end span.

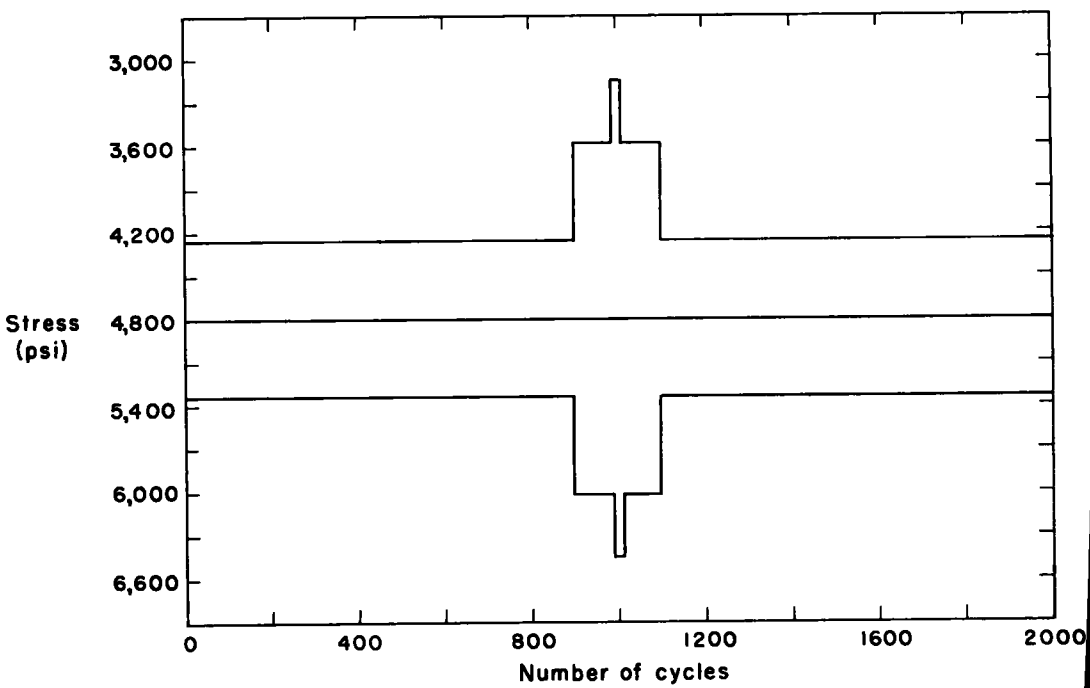

Figure 17. A stress fatigue program for the outer stringer in the end span.

section with respect to the moment of inertia at the positive moment section is an average of 1.79 for all the stringers. This indicates the error in the live load moments which are based on a constant moment of inertia.

These data also indicate the large increase in the moment of inertia of the outer stringer due to the sidewalk and curb. A comparison between the non-composite outer and inner stringers at the pier shows that the numerical moment of inertia of the outer wide flange is 65 percent of the moment of inertia of the inner wide flanges. When composite action is considered, the moment of inertia of the outer stringer is only 8 percent less than the value of the moment of inertia of the inner stringers. Similarly, at the positive bending section the composite action limited by specifications results in the moment of inertia of the outer section being 60 percent of that of the inner section. The actual composite sections, including the effect of the sidewalk and curb on the outer stringer, results in the moment of inertia of the outer stringer being approximately 6 percent more than that of the composite inner stringers. It is clear from the foregoing discussion that the stringers tend to use the amount of slab necessary to equalize the moments of inertia at the various cross-sections.

Load Distribution

The load distribution data show quite clearly the error introduced by assuming that no longitudinal load distribution occurs. The error is increased further by the variation in moments of inertia. The large composite moment of inertia in the negative bending area (section III) tends to increase the negative moment at the pier. It is possible for this to decrease the positive moment at section I 3 to 5 percent. Therefore, inasmuch as the experimental moment was found to be 23 percent less than the theoretical moment, it can be assumed that about 20 percent of the reduction in the experimentally determined moment can be attributed to longitudinal distribution of the wheel loads.

If the longitudinal distribution of load is disregarded, the lateral load distribution factors agree rather closely with the values specified by the American Association of State Highway Officials. The experimental lateral load distribution factors of 1.57 for the inner stringers is 7.6 percent less than the AASHO design load factor of 1.70. Similarly, the experimental load distribution factor of 1.283 for the outer stringer is 13 percent less than the AASHO load factor of 1.475. The other method which makes use of the eccentrically loaded column formula results in a lateral load distribution factor, as used by the Iowa State Highway Commission, of 1.452 (7). Here, the experimental value of 1.283 is 11.6 percent less than this design value. Thus, the relatively small irregularities in lateral load distribution are overshadowed by the initial assumption that there is no distribution of longitudinal load.

Impact

The data indicate the dynamic moments and how they are distributed in the bridge cross-section. The stringers with the largest load percentagewise have an increase in moment; however, the increase in percentage is often larger in the stringers with less moment. This results from the vibrational amplitude of the stringers depending more on their mass than on their static load. Therefore the moment resulting from the vibration of the stringers with a smaller static moment shows the largest increase in percentage.

It is apparent that the distribution of load undergoes no large change as a result of the vibrational impact. The greatest change occurs when the truck is in the outer lane and produces an upward or negative moment in the extreme opposite outer stringer. The dynamic effect of the truck is a vibration superimposed on the static load distribution. Thus, when the vibrational amplitude causes the greatest increase in moment, the sign of the dynamic vibratory moment is opposite to the sign of the static moment in this outer stringer. The result is an apparent decrease in moment in the extreme opposite outer stringer and therefore a small change in the load distribution percentages. Even so, the dynamic load distribution percentages were always within 5 percent of the static load distribution percentages. As a result, the change in the dynamic load distribution was always well within the difference between the experimental and design load distribution factors.

The total impact in the bridge shows an increase with speed, the amount of impact depending on whether or not the amplitude of vibration coincides exactly with the maximum moment in the bridge stringers. The maximum total bridge impact measured was 24.5 percent. This corresponds to a specification impact value for the outer span of 23.2 percent.

The individual stringer impact values depend on the amplitude of the vibratory moment and the static moment level. For the most heavily loaded stringers, the maximum impact values are somewhat similar to the maximum bridge impact values. The largest impact value in a heavily loaded stringer is 28.8 percent. This is similar to the maximum percentage for the total bridge.

It is difficult to determine what value of impact might be suitable for design. The two values compared in this study are the individual stringer impact percentages and the total bridge impact percentages. These two values vary considerably and would probably vary more if a more critical, in terms of vibration, truck-trailer combination had been used.

ACKNOWLEDGMENTS

The authors wish to express their appreciation to the Iowa Highway Research Board who sponsored this project. The cooperation and assistance of Mark Morris, Director of Highway Research, Neil Welden, Bridge Engineer, and Carl Schach, Traffic and Safety Engineer, all of the Iowa State Highway Commission, are especially appreciated.

REFERENCES

1. Wilson, W.M., "Flexural Fatigue Strength of Steel Beams." Eng. Exp. Sta., Bull. 377, University of Illinois, Urbana (1948).
2. Hulsbos, C.L., and Hanson, J.M., "Factors Influencing the Fatigue Strength of Steel Beams in Highway Bridges." Progress Report to Iowa Highway Research Board, Iowa Eng. Exp. Sta., Iowa State Univ. (March 1958).
3. Siess, C.P., and Veletsos, A.S., "Distribution of Loads to Girders in Slab and Girder Bridges: Theoretical Analyses and Their Relation to Field Tests." HRB Rev. Rpt. 14-B (1952).
4. Holcomb, R.M., "Distribution of Loads in Beam and Slab Bridges." Iowa Highway Research Board, Bull. No. 12, Ames (1959).
5. Newmark, N.M., "Design of I-Beam Bridges." Proc. ASCE (March 1948).
6. Caughey, R.A., and Senne, J.H., "Distribution of Loads in Beam and Slab Bridge Floors." Final Report to Iowa Highway Research Board, Iowa Eng. Exp. Sta., Iowa State Univ. (Sept. 1959).
7. Wise, J.A., "Dynamics of Highway Bridges." HRB Proc., 32: 180-187 (1953).
8. "Vibration and Stresses in Girder Bridges." HRB Bull. 124 (1956).
9. Timoshenko, S., "Strength of Materials, Part II, Advanced Theory and Problems." D. Van Nostrand Co., Inc., New York (1956).

Rapid Method for Estimating Maximum Bending Stress in Simple-Span Highway Bridges

HENSON K. STEPHENSON, Research Engineer, Texas Transportation Institute and Professor of Civil Engineering, Agricultural and Mechanical College of Texas, College Station

This paper presents a new and rapid method for estimating maximum combined bending stresses in simple-span beam bridges produced by dead load, live load and impact. The maximum live load and impact stresses are those resulting from any heavy vehicle type or loading found on the highway.

The procedure for estimating the total maximum stress in simple-span bridges—of given construction type and design designation—is accomplished in two simple steps: (a) convert any particular vehicle under consideration into its equivalent H truck loading on any span, as may be desired, by use of the conversion coefficients given in Table 1; and (b) once the H-equivalency of a given vehicle has been determined for a given span then its stress-producing effects may be determined from charts similar to those shown in Figures 3 to 14, inclusive, depending on the span and loading conditions.

THE METHOD presented for estimating the maximum combined bending stresses roduced by dead load, vehicle loads and impact in simple-span beam bridges results om three rather simple but important observations. Briefly, these observations are:

1. It has been shown that any heavy vehicle may be converted into an equivalent H uck loading that will produce the same maximum bending moment on a given span as e particular vehicle under consideration (1, 4, 5, 7). Equivalent H truck loadings, erefore, provide a convenient means for describing or evaluating the stress-produc- effects of any particular vehicle on a given span. It might be added that heavy ve- cles also may be converted into any other equivalent design loading on the basis of oments, shears or any other stress function as may be desired (1, 2, 3).
2. It has been found, for any simple-span beam bridge of given length, that the per- nt of total design moment per beam caused by dead load remains about the same, respective of the lateral spacing of the beams (4, 7). Similarly, for a given span, percent of total design moment (or stress) per beam caused by live load plus impact o remains about the same, irrespective of the beam spacing (4, 7). For a given span, refore, it follows that the percentage of total design moment (or stress) caused by e and dead loads, respectively, is about the same per foot width of bridge or per 10- ane as it is per beam, irrespective of the beam spacing. These findings permit the e and dead load design moments (or stresses) per beam or per 10-ft lane to be gen- lized for simple-span beam bridges of given construction type and design designa- as shown in Figure 2.

3. For a given bridge the maximum dead load stress is a fixed and definite percent of the total design stress; also, the maximum live load plus impact stress caused by a given vehicle will vary directly with the weight or H-equivalency of that particular vehicle. From these and the preceding observations it has been shown that the total maximum stress caused by dead load, vehicle load and impact in a given bridge may be expressed by a simple straight-line equation in which the total maximum stress is a function of the H-equivalency of the vehicle under consideration (4, 7). It is usually more convenient though to convert this total maximum stress into the ratio that it bears to the allowable stress for which the bridge was designed. This ratio is referred to herein as the design stress ratio. The variations of this design stress ratio with equivalent H truck loadings on various spans are as shown in Figures 3 - 14 inclusive.

DEVELOPMENT OF METHOD FOR ESTIMATING MAXIMUM BENDING STRESSES

The bridges used herein for illustrating the method are of H 15 design and consist of a concrete deck of minimum thickness supported by unencased steel beams. It is also assumed that the supporting steel beams are so spaced that the maximum live load bending stress produced in an interior stringer by a single vehicle in one lane only, will amount to C = 75 percent of that produced by indentical vehicles in each lane simultaneously. This means that if the given bridge were loaded with vehicles having identical H-equivalencies, one in each lane, the maximum live load stress produced in a typical interior stringer would be $\frac{4}{3}$ or 133 percent of that produced by only one of these vehicles in one lane only.

The reason for selecting this light type of construction is that the ratio of dead load stresses to total design stresses is smaller than would be the case for any of the heavie types of construction, such as reinforced concrete deck girder spans. Consequently, any conclusions arrived at concerning the stress-producing effect of a given vehicle or vehicles on any particular bridge are on the conservative rather than the unsafe side. Although the discussion and illustrative examples given herein are confined to bending moments and bending stresses in simple-span steel beam bridges of H 15 design, the method is equally applicable to bridges of other construction types and design designation.

Once the percent of total design stresses caused by live load plus impact and dead load have been determined for bridges of a given type and design designation similar t those given in Figure 2 it is convenient to consider the method for estimating total maximum bending stress in a given bridge in two parts, as follows: (1) determination of equivalent H truck loadings, and (2) evaluation of total maximum stress caused by a given equivalent H truck loading on a given span corresponding with specified loading conditions.

The nomenclature and definitions used herein are assembled in Appendix A for convenience of reference.

EQUIVALENT H TRUCK LOADINGS

Any heavy vehicle may be converted into an equivalent H truck loading that will pro duce the same maximum bending moment on a given span as the particular vehicle un consideration. Heavy vehicles also may be converted into any other equivalent desig loading on the basis of moments, shears or other stress function on various span leng as may be desired (1, 2, 3).

The H-equivalency of a given vehicle on a given span may be determined on an exa basis by finding the maximum moment caused by this particular vehicle on the given span and then selecting the standard H truck designation in tons that would produce th same maximum moment. The procedure for any other stress function would be simi

It has been found, however, from numerous investigations of actual vehicles, irrespective of the number of spacing of axles, that any normal distribution of load among the axles of a given vehicle will produce slightly less moment on a given span t the same load would produce if it were uniformly distributed over a length, L, equal the wheel base length of the vehicle under consideration (5, 7). This means that the maximum moment caused by any given vehicle on a given span can be estimated quit

easily and accurately—but a little on the safe side—by the moment formula resulting from the uniform load of length, L, and weight, W, on span, S (Fig. 1). This loading results in the following formula for maximum moment:

$$M = \frac{W}{4}\left(S - \frac{L}{2}\right) \quad (1)$$

Eq. 1 provided the basis for calculating the coefficients given in Table 1 for converting heavy vehicles of given weight and wheel base length into equivalent H truck loadings on various span lengths.

The determination and use of the coefficients given in Table 1 can be illustrated by comparing the maximum moment caused by a heavy vehicle weighing 20 tons and having a total wheel base length of 28 ft with that caused by an H 20 truck on a 50-ft simple span. According to Eq. 1 the moment caused by the heavy vehicle would be 360.0 kip-feet. This compares with a moment of 445.6 kip-feet caused by an H 20 truck on a 50-ft span. The 20-ton heavy vehicle with 28-ft wheel base, therefore, causes 80.79 percent as much moment as the H 20 truck on this 50-ft span.

This means that a vehicle, with a 28-ft wheel base, will cause 0.8079 times as

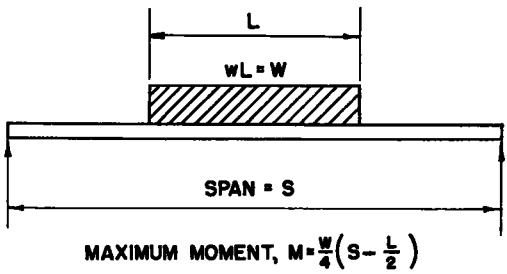

Figure 1. Maximum moment caused by a gross weight of W, uniformly distributed over a length L, on a span length of S.

TABLE 1

COEFFICIENTS FOR CONVERTING ANY HEAVY VEHICLE OF GIVEN WEIGHT AND WHEEL-BASE LENGTH INTO EQUIVALENT H TRUCK LOADINGS ON SIMPLE SPANS

Wheel Base, L (ft)	Coefficient								
	20-Ft Span	30-Ft Span	40-Ft Span	50-Ft Span	60-Ft Span	70-Ft Span	80-Ft Span	90-Ft Span	100-Ft Span
4	1.1250	1.1354	1.0982	1.0772	1.0638	1.0541	1.0473	1.0416	1.0373
8	1.0000	1.0543	1.0404	1.0323	1.0271	1.0231	1.0204	1.0179	1.0161
12	0.8750	0.9732	0.9826	0.9874	0.9905	0.9921	0.9936	0.9942	0.9949
16	0.7500	0.8921	0.9248	0.9425	0.9538	0.9611	0.9667	0.9706	0.9738
20	0.6250	0.8110	0.8670	0.8977	0.9171	0.9301	0.9398	0.9469	0.9526
24	-	0.7299	0.8092	0.8528	0.8804	0.8991	0.9130	0.9232	0.9314
28	-	0.6488	0.7514	0.8079	0.8437	0.8681	0.8861	0.8995	0.9102
32	-	-	0.6936	0.7630	0.8070	0.8371	0.8593	0.8759	0.8891
36	-	-	0.6358	0.7181	0.7704	0.8061	0.8324	0.8522	0.8679
40	-	-	0.5780	0.6732	0.7337	0.7751	0.8056	0.8285	0.8467
44	-	-	-	0.6284	0.6970	0.7440	0.7787	0.8048	0.8256
48	-	-	-	0.5835	0.6603	0.7130	0.7519	0.7812	0.8044
52	-	-	-	-	0.6236	0.6820	0.7250	0.7575	0.7832
56	-	-	-	-	0.5869	0.6510	0.6982	0.7338	0.7621
60	-	-	-	-	0.5503	0.6200	0.6713	0.7102	0.7409

OTE: The H-equvalency of any vehicle of given weight and wheel base length on a iven span, is equal to the weight of the vehicle times the conversion coefficient for at span corresponding to the given vehicle's wheel base length. For example, a 20-n vehicle with a 28-ft wheel base on a 50-ft span would have an H-equivalency of 20.0 0.8079 = 16.16 tons or correspond with an equivalent H 16.16 truck loading.

much moment on a 50-ft span as a standard H truck of equal weight. It also means that a vehicle of given weight, with a 28-ft wheel base, will cause as much moment on a 50-ft span as a standard H truck weighing 80.79 percent as much. This 20-ton vehicle, with a 28-ft wheel base on a 50-ft span, therefore, would have an H-equivalency of 20.0 x 0.8079 = 16.16 tons or correspond with an equivalent H 16.16 truck on that span.

Design Stress Relationships in Simple-Span Steel Stringer Bridges of H 15 Design

As previously stated, it has been found that for any simple-span beam bridge of given length, the percent of total design stress (or moment) per beam caused by dead load remains about the same, irrespective of the lateral spacing of the beams (4, 7). Similarly for a given span, the percent of total design stress per beam caused by live load plus impact also remains about the same, irrespective of the beam spacing. For a given span, therefore, it follows that the percent of total design stress (or moment) caused by live and dead loads, respectively, is about the same per foot width of bridge or per 10-ft lane as it is per beam, irrespective of beam spacing. These findings permit the live and dead load design stresses (or moments) per beam or per 10-ft lane to be generalized for simple-span beam bridges, of given construction type and design designation, similar to those shown in Figure 2.

With design stress information for simple-span bridges, of given construction type and design designation, similar to that given in Figure 2, it has been shown that the total maximum stresses caused by dead load, vehicle load and impact for a given bridge may be expressed by a simple straight-line equation in which the total maximum stress or design stress ratio is a function of the H-equivalency of the vehicle under consideration (4, 7). Design stress ratio for a given member is defined as the ratio of actual total maximum stress caused by dead load, vehicle load and impact in the member, to the maximum allowable stress used for the design of that member.

A further discussion of design stress ratios is given in Appendix B. Also in Appendix B is given the development of the straight-line equations for estimating design stress ratios (or maximum stresses) caused by dead load, vehicle loads and impact for given spans corresponding with various loading conditions. The development of the straight-line equations in Appendix B follows rather closely the development of similar equations previously presented (4, 7).

Estimating Maximum Bending Stresses Caused by Equivalent H Trucks

Inasmuch as Figure 2 gives the ratio of dead load stress to total design stress, R_D, and the ratio of live load plus impact stress to total design stress, R_L, it will be seen that the equivalent H truck loading corresponding with any degree of overstress or understress (design stress ratio, Q) and loading conditions may be determined by Eq. 12. Tables 2 through 5 give the equivalent H truck loadings, in tons, required to produce maximum bending stresses in an interior stringer, cor-

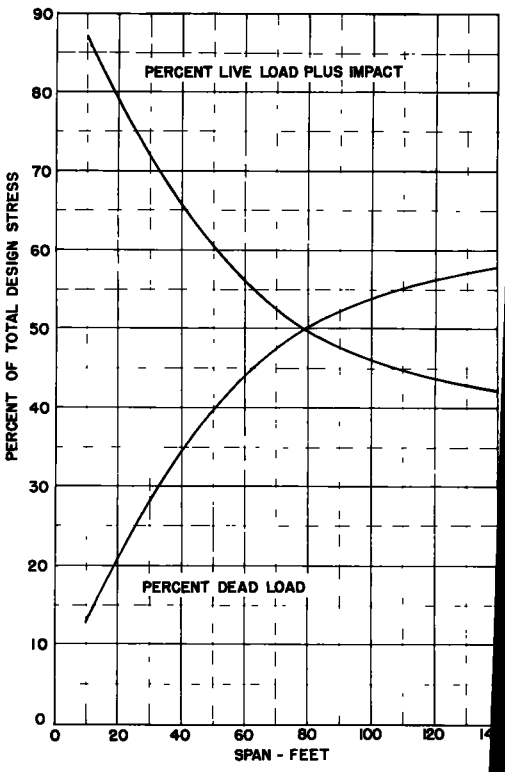

Figure 2. Estimated percent of total design stresses represented by live load plus impact and dead load stresses for simple-span beam bridges of H 15 design

responding to a given design stress ratio, for four different conditions of loading.

Referring to Eq. 13, it will be seen that the design stress ratio, Q, is a linear equation. For any given member of a particular bridge it will also be seen that the change in Q varies directly with the values of H, C, and K' in Eq. 13. This is illustrated in Figures 3 to 14. Figures 3 to 8 give the design stress ratios produced by equivalent H trucks on simple-span steel stringer bridges of H 15 design with one vehicle in each lane and varying allowance for impact. Figures 9 to 14, give the design stress ratios produced by equivalent H trucks on simple-span steel stringer bridges of H 15 design with one vehicle in one lane only and varying allowance for impact.

On a 50-ft span, for example, Figure 5 shows that one equivalent H 30 truck in each lane simultaneously (C = 1.00) with full allowance for impact would result in a maximum design stress ratio Q = 1.60. This means that the maximum stress produced in one of the interior steel stringers by such a loading would be 160 percent of the basic allowable design stress, or an overstress of 60 percent. However, if the speed of these equivalent H 30 trucks were reduced to about 5 mph, which would result in little or no impact, it will be seen that the maximum amount of overstress in an interior stringer would be reduced to about 32 percent.

Similarly, on a 50-ft span Figure 11 shows that one equivalent H 30 truck in one lane only (C = 0.75) with full allowance for impact would result in a maximum design stress ratio, Q = 1.31, or an overstress of about 31 percent. However, if the speed of this equivalent H 30 truck were reduced so as to result in little or no impact, the maximum amount of overstress in an interior stringer would only amount to about 10 percent. These illustrations should be sufficient to show the value and utility of the stress data to be obtained from Figures 3 through 14.

Summary of Method

The preceding discussion shows that the maximum combined bending stresses caused by dead load, live load, and impact in simple-span beam bridges may be estimated rather quickly in two simple steps as follows:

TABLE 2

EQUIVALENT H TRUCK LOADING IN EACH LANE WITH FULL ALLOWANCE FOR IMPACT REQUIRED TO PRODUCE MAXIMUM STEEL STRESS CORRESPONDING TO GIVEN DESIGN STRESS RATIO

= I				K' = 1.00 + I = K						C = 1.00
	Value of Factor									
actor	10-Ft Span	20-Ft Span	30-Ft Span	40-Ft Span	50-Ft Span	60-Ft Span	70-Ft Span	80-Ft Span	90-Ft Span	100-Ft Span
$_L$	0.870	0.790	0.715	0.654	0.603	0.558	0.522	0.498	0.478	0.460
	1.30	1.30	1.30	1.30	1.286	1.27	1.256	1.244	1.232	1.222
M_D	11.7	41.5	95.9	178.5	283.0	421.0	610.0	820.1	1062.6	1344.8
KM_L	78.0	156.0	240.5	337.4	429.8	531.5	666.1	813.6	973.0	1145.6
M_T	89.7	197.5	336.4	515.9	712.8	952.5	1276.1	1633.7	2035.6	2490.4
esign ress tio, Q	Equiv. H Truck Loading									
.50	23.6	24.5	25.5	26.5	27.4	29.1	32.2	35.2	38.2	41.4
.40	21.9	22.6	23.4	24.1	24.9	26.4	29.0	31.7	34.3	37.1
.30	20.2	20.7	21.3	21.9	22.5	23.6	25.9	28.1	30.4	32.8
.20	18.5	18.8	19.2	19.6	20.0	20.9	22.7	24.6	26.5	28.5
.10	16.7	16.9	17.1	17.3	17.5	18.1	19.6	21.1	22.6	24.2
.00	15.0	15.0	15.0	15.0	15.0	15.4	16.4	17.6	18.7	19.8
.90	13.3	13.1	12.9	12.7	12.5	12.6	13.3	14.0	14.8	15.5
.80	11.6	11.2	10.8	10.4	10.0	9.8	10.1	10.5	10.9	11.2
70	9.8	9.3	8.7	8.1	7.5	7.1	7.0	7.0	7.0	6.9
60	8.1	7.4	6.6	5.8	5.0	4.3	3.8	3.5	3.1	2.6
50	6.4	5.5	4.5	3.5	2.6	1.6	0.7	-	-	-

TABLE 3

EQUIVALENT H TRUCK LOADING IN EACH LANE WITH NO ALLOWANCE FOR IMPACT REQUIRED TO PRODUCE MAXIMUM STEEL STRESS CORRESPONDING TO GIVEN DESIGN STRESS RATIO

$\Gamma = 0.00$ $K' = 1.00 + 0.00 = 1.00$ $C = 1.00$

	Value of Factor									
Factor	10-Ft Span	20-Ft Span	30-Ft Span	40-Ft Span	50-Ft Span	60-Ft Span	70-Ft Span	80-Ft Span	90-Ft Span	100-Ft Span
R_L	0.870	0.790	0.715	0.654	0.603	0.558	0.522	0.498	0.478	0.460
K	1.30	1.30	1.30	1.30	1.286	1.27	1.256	1.244	1.232	1.222
M_D	11.7	41.5	95.9	178.5	283.0	421.0	610.0	820.1	1062.6	1344.8
KM_L	78.0	156.0	240.5	337.4	429.8	531.5	666.1	813.6	973.0	1145.6
M_T	89.7	197.5	336.4	515.9	712.8	952.5	1276.1	1633.7	2035.6	2490.4
Design Stress Ratio, Q	Equiv. H Truck Loading									
1.50	30.7	31.8	33.2	34.4	35.3	37.0	40.4	43.8	47.1	50.6
1.40	28.5	29.4	30.4	31.4	32.1	33.5	36.5	39.4	42.3	45.3
1.30	26.3	26.9	27.7	28.4	28.9	30.0	32.5	35.0	37.5	40.1
1.20	24.0	24.4	25.0	25.5	25.7	26.5	28.6	30.6	32.7	34.8
1.10	21.8	22.0	22.2	22.5	22.5	23.0	24.6	26.2	27.8	29.5
1.00	19.5	19.5	19.5	19.5	19.3	19.5	20.6	21.8	23.0	24.2
0.90	17.3	17.0	16.8	16.5	16.1	16.0	16.7	17.5	18.2	19.0
0.80	15.0	14.6	14.1	13.5	12.9	12.5	12.7	13.1	13.4	13.7
0.70	12.8	12.1	11.3	10.6	9.7	9.0	8.8	8.7	8.6	8.4
0.60	10.5	9.6	8.6	7.6	6.5	5.5	4.8	4.3	3.8	3.2
0.50	8.3	7.2	5.9	4.6	3.3	2.0	0.9	-	-	-

TABLE 4

EQUIVALENT H TRUCK LOADING IN ONE LANE WITH FULL ALLOWANCE FOR IMPACT REQUIRED TO PRODUCE MAXIMUM STEEL STRESS CORRESPONDING TO GIVEN DESIGN STRESS RATIO

$\Gamma = I$ $K' = 1.00 + I = K$ $C = 0.7$

	Value of Factor									
Factor	10-Ft Span	20-Ft Span	30-Ft Span	40-Ft Span	50-Ft Span	60-Ft Span	70-Ft Span	80-Ft Span	90-Ft Span	100-F Span
R_L	0.870	0.790	0.715	0.654	0.603	0.558	0.522	0.498	0.478	0.4
K	1.30	1.30	1.30	1.30	1.286	1.27	1.256	1.244	1.232	1.2
M_D	11.7	41.5	95.9	178.5	283.0	421.0	610.0	820.1	1062.6	1344.8
KM_L	78.0	156.0	240.5	337.4	429.8	531.5	666.1	813.6	973.0	1145.6
M_T	89.7	197.5	336.4	515.9	712.8	952.5	1276.1	1633.7	2035.6	2490.4
Design Stress Ratio, Q	Equiv. H Truck Loading									
1.50	31.5	32.6	34.0	35.3	36.6	38.8	42.9	46.9	51.0	55.
1.40	29.2	30.1	31.2	32.2	33.2	35.1	38.7	42.2	45.8	49.
1.30	26.9	27.6	28.4	29.2	29.9	31.5	34.5	37.5	40.6	43.
1.20	24.6	25.1	25.6	26.1	26.6	27.8	30.3	32.8	35.4	38.
1.10	22.3	22.5	22.8	23.1	23.3	24.1	26.1	28.1	30.1	32.
1.00	20.0	20.0	20.0	20.0	20.0	20.5	21.9	23.4	24.9	26.
0.90	17.7	17.5	17.2	16.9	16.7	16.8	17.7	18.7	19.7	20.
0.80	15.4	14.9	14.4	13.9	13.4	13.1	13.5	14.0	14.5	15.
0.70	13.1	12.4	11.6	10.8	10.0	9.5	9.3	9.3	9.3	9.
0.60	10.8	9.9	8.8	7.8	6.7	5.8	5.1	4.6	4.1	3.
0.50	8.5	7.3	6.0	4.7	3.4	2.1	0.9	-	-	-

TABLE 5

EQUIVALENT H TRUCK LOADING IN ONE LANE WITH NO ALLOWANCE FOR IMPACT REQUIRED TO PRODUCE MAXIMUM STEEL STRESS CORRESPONDING TO GIVEN DESIGN STRESS RATIO

I' = 0.00 K' = 1.00 + 0.00 = 1.00 C = 0.75

Factor	Value of Factor									
	10-Ft Span	20-Ft Span	30-Ft Span	40-Ft Span	50-Ft Span	60-Ft Span	70-Ft Span	80-Ft Span	90-Ft Span	100-Ft Span
R_L	0.870	0.790	0.715	0.654	0.603	0.558	0.522	0.498	0.478	0.460
K	1.30	1.30	1.30	1.30	1.286	1.27	1.256	1.244	1.232	1.222
M_D	11.7	41.5	95.9	178.5	283.0	421.0	610.0	820.1	1062.6	1344.8
KM_L	78.0	156.0	240.5	337.4	429.8	531.5	666.1	813.6	973.0	1145.6
M_T	89.7	197.5	336.4	515.9	712.8	952.5	1276.1	1633.7	2035.6	2490.4

Design Stress Ratio, Q	Equiv. H Truck Loading									
1.50	41.0	42.4	44.2	45.9	47.0	49.3	53.9	58.4	62.8	67.4
1.40	38.0	39.1	40.6	41.9	42.8	44.6	48.6	52.5	56.4	60.4
1.30	35.0	35.9	36.9	37.9	38.5	40.0	43.3	46.7	50.0	53.4
1.20	32.0	32.6	33.3	34.0	34.2	35.3	38.1	40.8	43.6	46.4
1.10	29.0	29.3	29.7	30.0	30.0	30.7	32.8	35.0	37.1	39.3
1.00	26.0	26.0	26.0	26.0	25.7	26.0	27.5	29.1	30.7	32.3
0.90	23.0	22.7	22.4	22.0	21.4	21.3	22.3	23.3	24.3	25.3
0.80	20.0	19.4	18.7	18.1	17.2	16.7	17.0	17.4	17.9	18.3
0.70	17.1	16.1	15.1	14.1	12.9	12.0	11.7	11.6	11.4	11.2
0.60	14.1	12.8	11.5	10.1	8.7	7.4	6.4	5.7	5.0	4.2
0.50	11.1	9.5	7.8	6.1	4.4	2.7	1.2	-	-	-

1. Convert the heavy vehicle under consideration into its equivalent H truck loading on a given span by use of the appropriate coefficient in Table 1.
2. With the H-equivalency found in the first step, an estimate of the bending stresses caused by it on the given span may be read directly from the appropriate chart given in Figures 3 through 14, depending on the span length and loading conditions.

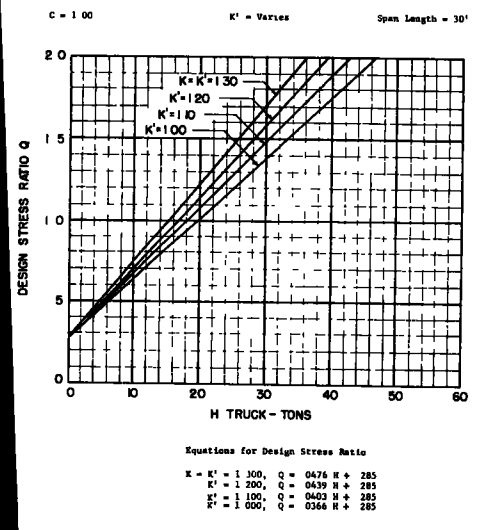

Figure 3. Design stress ratio produced by equivalent H trucks on simple-span bridges of H 15 design with one vehicle in each lane and varying allowance for impact.

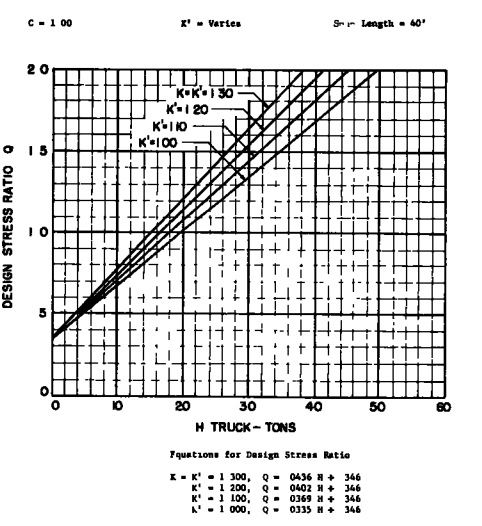

Figure 4. Design stress ratio produced by equivalent H trucks on simple-span bridges of H 15 design with one vehicle in each lane and varying allowance for impact.

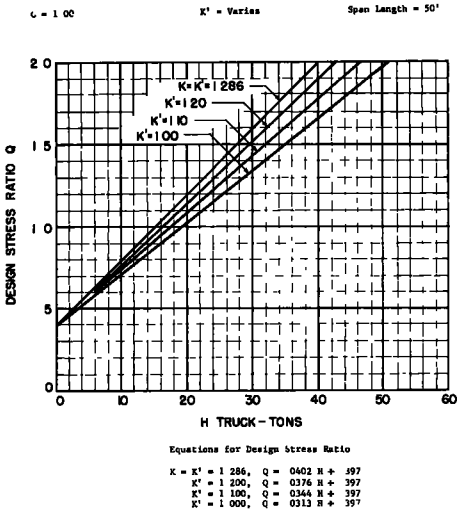

Figure 5. Design stress ratio produced by equivalent H trucks on simple-span bridges of H 15 design with one vehicle in each lane and varying allowance for impact.

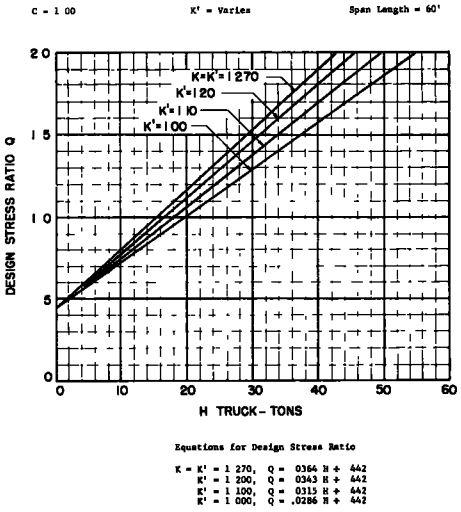

Figure 6. Design stress ratio produced by equivalent H trucks on simple-span bridges of H 15 design with one vehicle in each lane and varying allowance for impact.

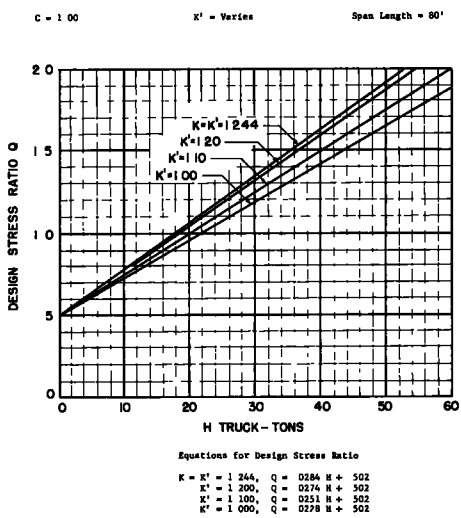

Figure 7. Design stress ratio produced by equivalent H trucks on simple-span bridges of H 15 design with one vehicle in each lane and varying allowance for impact.

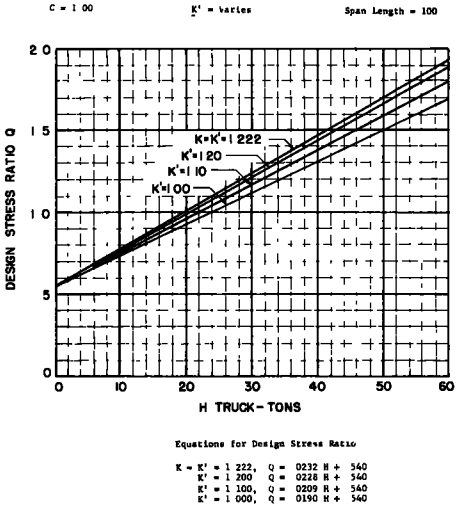

Figure 8. Design stress ratio produced by equivalent H trucks on simple-span bridges of H 15 design with one vehicle in each lane and varying allowance for impact.

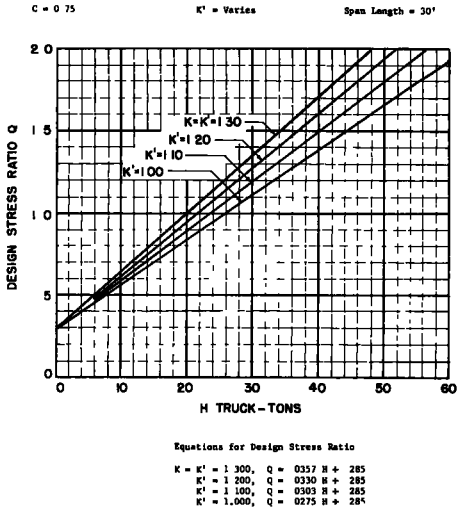

Figure 9. Design stress ratio produced by equivalent H trucks on simple-span bridges of H 15 design with one vehicle in one lane only and varying allowance for impact.

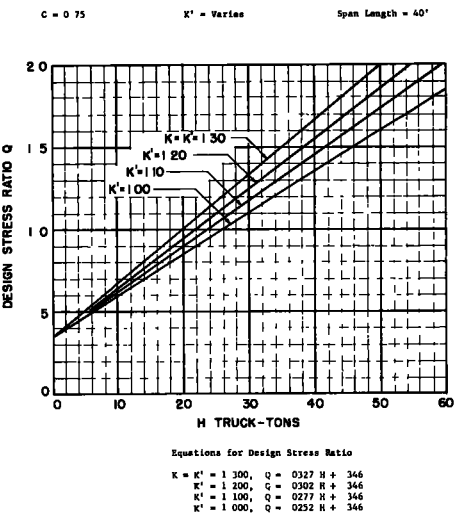

Figure 10. Design stress ratio produced by equivalent H trucks on simple-span bridges of H 15 design with one vehicle in one lane only and varying allowance for impact.

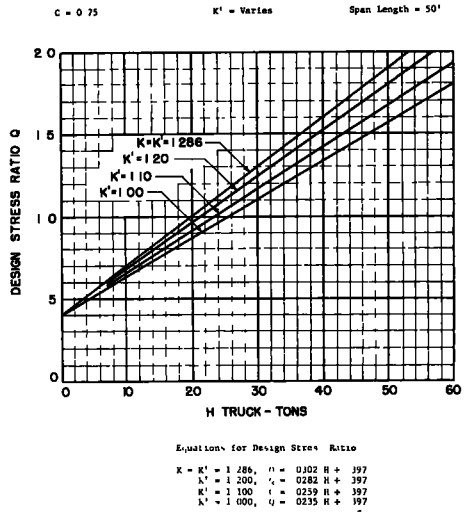

Figure 11. Design stress ratio produced by equivalent H trucks on simple-span bridges of H 15 design with one vehicle in one lane only and varying allowance for impact.

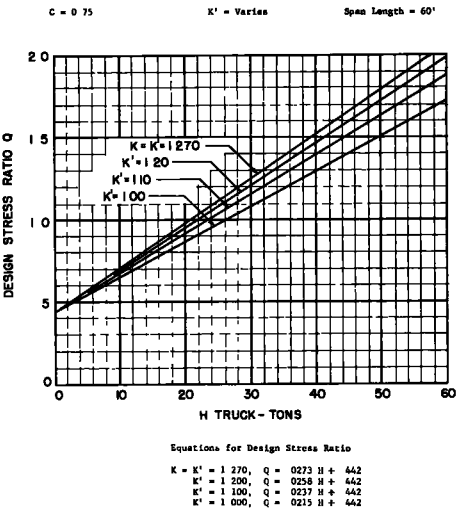

Figure 12. Design stress ratio produced by equivalent H trucks on simple-span bridges of H 15 design with one vehicle in one lane only and varying allowance for impact.

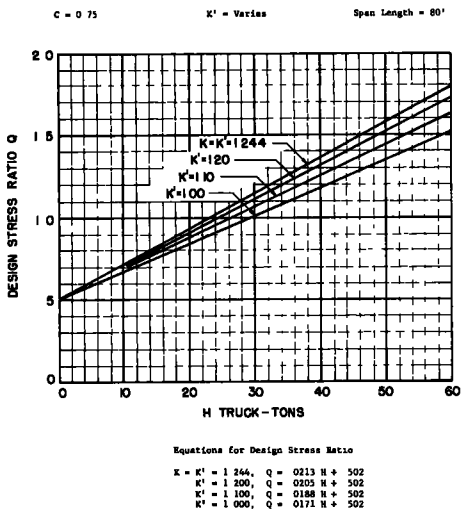

Figure 13. Design stress ratio produced by equivalent H trucks on simple-span bridges of H 15 design with one vehicle in one lane only and varying allowance for impact.

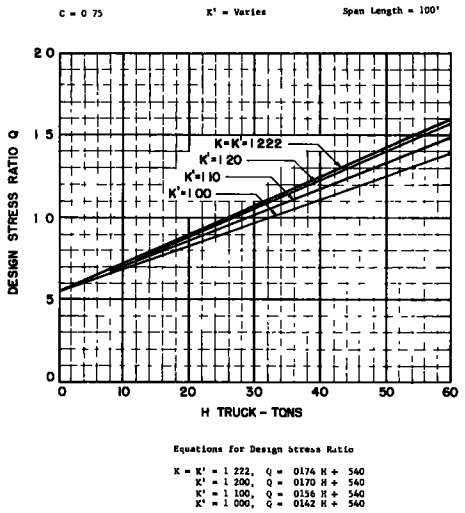

Figure 14. Design stress ratio produced by equivalent H trucks on simple-span bridges of H 15 design with one vehicle in one lane only and varying allowance for impact.

REFERENCES

1. Stephenson, H.K., and Cloninger, K., Jr., "Method of Converting Heavy Motor Vehicle Loads into Equivalent Design Loads on the Basis of Maximum Bending Moments." Bull. 127, Texas Eng. Exp. Sta. (1952).
2. Stephenson, H.K., and Cloninger, K., Jr., "Method of Converting Heavy Motor Vehicle Loads into Equivalent Design Loads on the Basis of Maximum Shears." Bull. 131, Texas Eng. Exp. Sta. (1953).
3. Stephenson, H.K., and Cloninger, K., Jr., "Method of Converting Heavy Motor Vehicle Loads into Equivalent Design Loads on the Basis of Maximum Floor Beam Reactions." Bull. 135, Texas Eng. Exp. Sta. (1954).
4. Stephenson, H.K., and Cloninger, K., Jr., "Stress Producing Effects of Equivalent Design Loads on Modern Highway Bridges." Bull. 132, Texas Eng. Exp. Sta. (1953).
5. Stephenson, H.K., "Determination of Permissible Vehicle Weights on Bridges of H Loading Design." AASHO Proc., pp. 145-185 (1949).
6. Stephenson, H.K., "Highway Bridge Live Loads Based on Laws of Chance." Paper 1314, Jour. Structural Div., ASCE, Vol. 83, No. ST4 (July 1957).
7. Stephenson, H.K., "Frequencies of Various Levels of Stress in Highway Bridges." HRB Proc., 38:113-148 (1959).

Appendix A

NOMENCLATURE AND DEFINITIONS

C = coefficient which represents the fractional part of the total live load stress, in a given member, produced by one or more lanes loaded, C = 1.00 if a stringer bridge is loaded with identical vehicles, one in each lane and so placed to produce maximum stress. For a steel stringer bridge, if one vehicle in one lane only would produce 75 percent as much stress in an interior stringer as identical vehicles in each lane it would mean that C = 0.75.

f = unit stress in pounds per square inch or unit stress as may be defined, f_D = unit stress resulting from dead load; f_L = unit stress resulting from live load; f_T = maximum total design stress; f_H = stress resulting from vehicle or vehicles weighing H tons each.

H = equivalent H truck in tons. For example, if a given vehicle produces the same maximum moment (or other stress function) in a given member as a standard H truck weighing 23.6 tons, it would be rated as an equivalent H 23.6 truck loading in which case H = 23.6 tons.

I = impact fraction (maximum 0.30 or 30 percent) as determined by the AASHO formula I = 50/ (S + 125) in which S = length in feet of the portion of the span which is loaded to produce the maximum stress in the member.

I' = impact fraction assumed in connection with the determination of the stress-producing effects of any given vehicle under consideration. For example, if the speed of a given vehicle were limited to about 5 mph, this impact fraction might be considered so small as to be negligible, in which case I' might be assumed equal to zero. Depending on traffic and conditions, therefore, the impact fraction, I' could be assumed at any reasonable value between zero and the full impact allowance, I, as defined by the AASHO design specifications.

K = (1.00 + I) = coefficient by which the design live load moment (shear, or other stress function is multiplied to obtain the live load plus impact moment (shear or other stress function) used for design. Thus, KM_L would be equal to the live load plus impact moment used for design; similarly KV_L would be equal to the live load plus impact shear used for design.

K' = (1.00 + I') = coefficient by which the live load moment (shear, or other stress function) produced by a given vehicle is multiplied to obtain the live load plus impact moment (shear, or other stress function) produced on a given span or in a given member by the vehicle under consideration. Thus, $K'M_H$ would be equal to the live load plus impact moment produced on a given span by any particular vehicle having an H-equivalency of H tons.

M_D = dead load moment as included in total design moment.

M_H = moment in an interior stringer (or other member) resulting from equivalent H trucks weighing H tons each. Likewise M_H represents the moment for 1 lane produced by equivalent H truck weighing H tons.

$M_{H(1)}$ = moment for one lane produced by a standard H truck weighing 1 ton.

M_L = live load moment as included in total design moment.

M_T = moment used for design or total design moment.

Q = design stress ratio. This term refers to the ratio of total maximum stress, caused by dead load, vehicle load and impact, to total design stress in any particular member of part of a given highway bridge.

R_D = (M_D/M_T) = ratio of dead load moment M_D (shear, or other stress function) to total moment M_T used for design. In terms of shear this ratio would be $R_D = (V_D/V_T)$, and for other stress functions it would be similar.

$R_L = (KM_L/M_T)$ = ratio of live load plus impact moment, KM_L, (shear, or other stress function), used for design, (to the total design moment, M_T, or total moment (shear, or other stress function) used for design. In terms of shear, this ratio would be $R_L = (KV_L/V_T)$, and for other stress functions it would be similar.
S = span length (usually in feet).
V = shear force.

Appendix B

DEVELOPMENT OF EQUATIONS FOR DESIGN STRESS RATIOS

Design Stress Ratios

Design stress ratios, Q, refer to the ratios of total actual stresses to total design stresses in any particular member or part of a given highway bridge. For example, consider a 50-ft simple-span steel stringer bridge with concrete deck of H-15 design. If the design calculations for this bridge show that the dead load produces a maximum stress of 7.20 ksi and the design live load plus impact produces a maximum stress of 10.80 ksi in an interior stringer, the total design stress for this stringer is 7.20 + 10.80 = 18.00 ksi.

If further calculations indicate that a particular heavy vehicle load would produce a maximum live load plus impact stress of $K f_H = 16.20$ ksi (see Appendix A for nomenclature) it will be seen that the maximum total actual stress in this stringer would be 7.20 + 16.20 = 23.40 ksi. So, the ratio of total actual stress to total design stress for this situation results in a design stress ratio of Q = 23.40/18.00 = 1.30. This means that the heavy vehicle under consideration would result in total actual stresses 1.30 times as much as the total basic design stress of 18.00 ksi for which this stringer was designed or an overstress of 30 percent in excess of the basic design permitted by the AASHO design specifications.

Each of the many heavy vehicle types and loadings has one thing in common—the capacity to induce a stress (bending, shear, or direct stress) of definite and calculable magnitude at any particular point in a given bridge. Consequently a bridge of given type and span can be made to serve as a sort of weighing device by which the maximum stress (bending, shear, or direct stress) produced by any given heavy vehicle can be directly compared with that produced by any other vehicle or arbitrarily standardized loading. However, rather than directly comparing the actual stresses produced by a given heavy vehicle with those produced by others, it is more convenient to appraise the stress-producing effects of a given vehicle if they are expressed in terms of some arbitrary or standardized loading on a simple span of given length.

For this purpose a standard H truck, H-S truck, or any other arbitrary loading, could be used. The standard H truck loading is used herein as a basis for measuring the stress-producing characteristics of all other vehicles because the load-carrying capacities of most existing highway bridges are rated in terms of the H loading design. And, as previously mentioned, bending moment is the stress function used to illustrate the method for measuring overstress because it is the bending stresses that ordinarily determine the load-carrying capacity of most highway bridges.

On a 50-ft simple span, for example, if it were determined that a given heavy vehicle produced a maximum live load moment of 445.6 kip-ft, with no allowance for impact, it would be found to be the same as the maximum live load moment produced by a H-20 truck on the same span. Based on its capacity to produce bending stresses in a simple span of 50 ft the given vehicle would be converted into or rated as an equivalent H truck load weighing 20 tons, or simply an equivalent H-20 truck loading. In a similar manner, if a given heavy vehicle produced as much direct stress in a particular member of a given through truss bridge as an H-21.6 truck, it would be rated as an equivalent H-21.6 truck loading insofar as its capacity to produce direct stress in that particular member is concerned. The logic would be similar for any type of stress or stress function at any point that might be of interest in any type of simple-span or continuous bridge. The manner in which these equivalent design loads can be used for

determining the degree of overstress, or design stress ratio, produced by any given vehicle at some particular point in a given bridge is presently explained.

Development of Equations

The stress relationships in the 50-ft simple-span steel stringer bridge of H-15 design referred to previously provides a convenient basis for illustrating the development of equations relating to design stress ratios. A study of the stresses in this bridge, and how they are related to each other, shows how such relationships provide a basic and necessary tool for the further investigation of maximum stresses in highway bridges (also see 4). For this 50-ft bridge the design calculations show that the dead load produces a maximum stress of 7.20 ksi and the design live load plus impact produces a maximum stress of 10.80 ksi, or a maximum total design stress of 7.20 + 10.80 = 18.00 ksi, in a typical interior stringer. In accord with the nomenclature given in Appendix A, it will be seen from these data that the dead load ratio, R_D, which is defined as the ratio that the maximum dead load stress, f_D, bears to the maximum total design stress, f_T, would be

$$R_D = \frac{f_D}{f_T} = \frac{M_D}{M_T} = \frac{7.20}{18.00} = 0.400 \qquad (2)$$

Similarly, it will be seen that the live load ratio, R_L, which is defined as the ratio that the maximum live load plus impact stress, Kf_L (moment, $K M_L$; shear, $K V_L$; or other stress function), bears to the maximum total design stress, f_T (moment, M_T; shear, V_T; or other stress function) would be

$$R_L = \frac{K f_L}{f_T} = \frac{K M_L}{M_T} = \frac{10.80}{18.00} = 0.600 \qquad (3)$$

But because the sum of the design dead load, live load and impact stresses for a given member is equal to the total design stress, the sum of the dead load and live load ratios must equal 1.00, and it follows that

$$R_D + R_L = \frac{f_D + K f_L}{f_T} = \frac{7.20 + 10.80}{18.00} = 0.400 + 0.600 = 1.00 \qquad (4)$$

Similarly, if these ratios were defined in terms of moments for an interior stringer or in terms of moments for a full lane, which would be proportional to those in the stringer, their values would remain the same and their sum equal 1.00. Thus

$$R_D + R_L = \frac{M_D + K M_L}{M_T} = 0.400 + 0.600 = 1.00 \qquad (5)$$

In Eq. 4 the maximum stress, f_L, in one of the interior stringers is produced by the standard design live loading (without impact), which for this 50-ft span consists of one standard H-15 truck in each lane, simultaneously: K is the coefficient by which the live load stress, f_L, is increased to include the specified allowance for impact. That is,

$$K = 1.00 + I \qquad (6)$$

which I is the impact fraction as determined by the AASHO formula

$$I = 50/(S + 125) \qquad (7)$$

and S is the length in feet of the span which is loaded to produce maximum stress in the member under consideration (for simple spans, S = full length of span).

For the 50-ft simple span the impact would amount to I = 50/(50 + 125) = 0.286, which in turn would result in a coefficient K = 1.00 + 0.286 = 1.286. As previously stated, the design live load plus impact produces a maximum stress in an interior stringer of $K f_L$ = 10.80 ksi. Inasmuch as this value includes an allowance of 28.6

percent for impact, it will be seen that the design live load stress without impact would be $f_L = 10.80/1.286 = 8.40$ ksi.

It was also stated previously that further calculations indicated that a particular heavy vehicle would produce a maximum live load plus impact stress of $K f_H = 16.20$ ksi in the most highly stressed interior stringer of that 50-ft simple-span steel stringer bridge. The next question would be: What is the H-equivalence of this particular vehicle on a 50-ft span? In other words, a standard H truck of what weight would be required to produce a live load plus impact stress of 16.20 ksi in the most highly stressed interior stringer? This question can be answered by referring to previous calculations which show that the design live load plus impact produces in this same interior stringer a maximum stress of $K f_L = 10.80$ ksi. The design live load in this consists of one H-15 truck in each lane simultaneously. For this bridge, too, it was assumed that a single vehicle in one lane only would produce 75 percent as much stress in an interior stringer as that produced by identical vehicles, one in each lane simultaneously. On this basis, therefore, a single H-15 truck on this bridge in one lane only would produce in the same interior stringer a live load plus impact stress of $C K f_L = 0.75 \times 1.286 \times 1.286 \times 8.40 = 8.10$ ksi.

Now if a single H-15 truck, in one lane only, produces a maximum live load plus impact stress of this magnitude, by direct proportion one can find the equivalent H truck required to produce a corresponding stress of $K f_H = 16.20$ ksi, or $K f_H / C K f_L = 16.20/8.10 = 2.00$ times as much live load plus impact stress as a single H-15 truck. Therefore, this given heavy vehicle would be rated as an equivalent H-30 truck on a 50-ft span. Symbolically, the equivalent H truck rating (KHT) for this particular vehicle would be $EHT = 15(K f_H / C K f_L) = 15(16.20/8.10) =$ Equivalent H-30 truck.

Based on the foregoing discussion of dead load, design live load, impact and actual live load plus impact stresses, and how they may be related for determining the design stress ratios which result from actual vehicle loadings, it is now possible to write a general expression for determining the design stress ratio (4, 7) produced by a vehicle of given H-equivalency on a span of given length. In terms of stress produced by vehicles of given H-equivalency, the design stress ratio would be

$$Q = R_D + R_L \frac{K' f_H C}{K f_L} \tag{8}$$

Similarly, if the stress function were in terms of maximum bending moments produced by vehicles of given H-equivalency, the design stress ratio would be

$$Q = R_D + R_L \frac{K' M_H C}{K M_L} \tag{9}$$

in which

$$K' = 1.00 + I' \tag{10}$$

is the coefficient by which the actual live load stress (moment or other stress function) is multiplied to obtain the live load plus impact stress (moment or other stress function) produced on a given span by a given vehicle under consideration; and I' is the impact fraction assumed in connection with the stress-producing effects of any given vehicle under consideration. Depending on the speed of the vehicle under consideration and other traffic conditions, the impact fraction I', could be assumed at any reasonable value between zero and the full impact allowance, I, as defined by the AASHO design specifications.

In Eq. 8, if f_H represents the maximum live load stress in an interior stringer resulting from identical vehicles of given H-equivalency, one in each lane simultaneously, the coefficient C = 1.00 (or 100 percent) of the potential stress that would result from identical vehicles of given H-equivalency, one in each lane simultaneously. But if only one of these vehicles were placed in one lane only, C would be less than 1.00, and in the foregoing examples it has been assumed that C = 0.75 for the case of one vehicle

one lane only. Here, it will be remembered that C is a function of the stringer spacing and for all lanes loaded, C = 1.00. Similarly, in Eq. 9, if M_H represents the maximum live load moment in an interior stringer resulting from identical vehicles of given H-equivalency, one in each lane simultaneously, C = 1.00. But if only one of these vehicles were placed in one lane only, this coefficient would be less than one, say C = 0.75, as has been assumed previously.

Likewise, if M_H represents the moment for one lane produced in a given span by a vehicle of given H-equivalency and M_L represents the live load moment for one lane produced by the design live load, the ratio M_H/M_L would be the same as would obtain if M_H were defined as the moment in an interior stringer resulting from vehicles of given H-equivalency, one in each lane simultaneously and M_L the moment in the same stringer resulting from the design live load in each lane simultaneously. Therefore, Eq. 9 provides a general expression for determining design stress ratios resulting from heavy vehicle loadings.

Use of Eq. 8 or Eq. 9

To illustrate the use of Eq. 8 or Eq. 9 for determining design stress ratios, suppose it is desired to determine the design stress ratio resulting from the live load plus impact stress of 16.20 ksi produced in an interior stringer by the equivalent H-30 truck in one lane only on the 50-ft span referred to earlier. Now is K' = K = 1.286, and this stress of 16.20 ksi is 75 percent of what it would be if each lane were loaded, then if vehicles with identical H-equivalencies were placed one in each lane simultaneously, the maximum actual live load stress in an interior stringer would be $K'f_H = 16.20/0.75 = 21.60$ ksi.

With this information it is now possible by use of Eq. 8 to determine the design stress ratio in an interior stringer of this 50-ft span. Therefore, by Eq. 8 it will be found that the design stress ratio for this situation is

$$Q = 0.400 + 0.600\left(\frac{21.60 \times 0.75}{10.80}\right) = 0.400 + 0.900 = 1.300$$

This shows that the given vehicle, which turned out to be an equivalent H-30 truck, would result in a design stress ratio of 1.30 or an overstress of 30 percent in an interior stringer if this vehicle were the only one on the span at one time.

What would the design stress ratio be if vehicles of idential H-equivalencies (equivalent H-30 trucks) were placed one in each lane simultaneously? An equivalent H-30 truck in each lane simultaneously on this 50-ft span would, by Eq. 8, result in a design stress ratio of

$$Q = 0.400 + 0.600\left(\frac{21.60 \times 1.00}{10.80}\right) = 1.60$$

In other words, on this 50-ft span of H-15 design, an equivalent H-30 truck in each lane simultaneously would produce a maximum stress in an interior stringer 60 percent in excess of the basic design stress, or a maximum actual stress of 1.60 x 18.00 = 28.80 ksi.

Evaluating H-Equivalencies

For any given span, if M_H is the moment for one lane produced by a single equivalent H truck weighing H tons and $M_H(1)$ the moment for one lane produced by a standard truck weighing 1.0 tons, then the H rating or H-equivalency in tons for any particular vehicle on a given span would be

$$H = M_H/M_{H(1)} \tag{11a}$$

$$M_H = H\, M_{H(1)} \tag{11b}$$

Substitution of Eq. 11b in Eq. 9 gives

$$H = \frac{K\, M_L\, (Q - R_D)}{C\, K'\, M_{H(1)}\, R_L} \tag{12}$$

an equation for determining the equivalent H truck loading that would be required on a given span to produce a design stress ratio, Q, of specified value.

Ratios Resulting from Equivalent H Truck Loadings

By rearranging Eq. 12 or by substituting the value of M_H, as given by Eq. 11b in Eq. 9, it will be seen that the design stress ratios resulting from various weights of equivalent H trucks and other loading conditions would be

$$Q = R_D + R_L \frac{H\ C\ K'\ M_{H(1)}}{K\ M_L} \tag{13}$$

This shows that the design stress ratio, Q, is a linear equation. Therefore, for any given member of a bridge of given span, Q varies directly with the values of H, C and K' in Eq. 13. Thus, Eq. 13 provides a simple and effective means for estimating the stress-producing effects of heavy vehicle loads on highway bridges of various spans, types of construction and design designation.

The usefulness and variety of information to be obtained from Eq. 13 are discussed and illustrated in the main body of the paper.

Report on Test Pile Program Conducted by Kansas and Missouri State Highway Departments

J.A. WILLIAMS, Bridge Engineer, Missouri State Highway Department

This report presents the primary reasons for development of a test pile program conducted by the Kansas and Missouri State Highway Departments, the procedures followed, and the results obtained in the driving and loading of two groups of four different types of piles. The U. S. Bureau of Public Roads and the two states involved agreed that because of the magnitude of pile requirements for the proposed structure, preliminary studies and investigations to predetermine comparative pile lengths and capacities would be worthwhile. It was hoped to obtain data that would justify the use of design loads for piles in excess of those permitted by the AASHO specifications, and thereby realize an appreciable economic saving in construction costs.

THE PLANNING and construction of structures in urban areas present many complicated and costly problems. The Kansas and Missouri State Highway Departments were confronted with such a problem in providing additional lanes for the existing structure which connects Kansas City, Kans., and Kansas City, Mo. The existing structure at this location consists of a truss over the Kansas River and some 8,000 ft of I-beam spans averaging approximately 45 ft in length. This structure has four 10-ft traffic lanes with a 6 in. wide median dividing the east-and west-bound traffic.

Interstate Route 70 has been routed over this structure and in order to meet Interstate standards, it was necessary to widen the existing structure or build another structure parallel to it. The anticipated traffic requires three lanes in each direction. After a comparative cost estimate was made, the two states agreed that a separate three-lane structure should be constructed parallel, but not tied to the existing structure. The existing structure would carry three lanes of traffic.

The central portion of the proposed structure consists of approximately 3,715 linear feet of which 1,359 ft is in Kansas and 2,356 ft in Missouri. A joint agreement was entered into by the two states and a consulting firm was employed to design and prepare the detail plans. At the time the preliminary plans for the proposed structure were being discussed, structural steel was still scarce and it was agreed to construct a continuously-reinforced concrete tee-girder structure with the spans matching the plan arrangement of the existing structure. Because of the necessity for using short spans, the substructure costs for the proposed structure took on additional importance.

The central portion of the Intercity Viaduct, for which plans were being developed, is located in the flood valleys of the Kansas River and the Missouri River, and not far from the junction of these two rivers. Preliminary sounding information brought out the fact that at the Kansas end of the structure, bedrock was approximately 85 ft below ground elevation and at the Missouri end it was approximately 65 ft to bedrock. The borings showed that the soil classification was fairly uniform for the entire structure,

the top 10 or 15 ft consisting of fine sand, the next 25 ft consisting of silty sand and sandy silt, and the balance consisting of fine to coarse sand and gravel. The bedrock was shale and limestone.

On the basis of this preliminary sounding data, it was evident that the substructure units should be placed on piling. The question then arose as to whether friction piling or point bearing piling would be the more economical. In accordance with AASHO specifications, the maximum assumed design load for a 14-in. cast-in-place concrete friction pile, without the benefit of extensive subsurface investigations or test loads, would be approximately 30 tons. With the benefit of subsurface investigations and past practices in the area, but without test loads, this maximum could conceivably be increased to 45 or 50 tons but normally not in excess thereof. AASHO specifications also limit the maximum design load for steel point bearing piles to 6,000 psi unless test loads indicate that larger loads can safely be sustained.

In view of the large number of substructure units involved in the project and the subsurface conditions as noted in the explorations, it was thought that a test pile program would be of considerable value. A thorough study was made of the proposed test pile program by the two state highway departments, the U.S. Bureau of Public Roads, and the consulting engineer's office. It was then agreed by everyone involved that a test pile program would be beneficial in determining the possible use of pile design loads in excess of those permitted by AASHO specifications and thus reducing the over-all foundation costs.

After a definite decision had been reached by all organizations involved, the consultant was requested to proceed with a test pile program and to investigate subsurface soil conditions in the vicinity of the pile driving site, and to determine the relative driving effort, pile length requirements, and bearing capacities for four types of bearing piles. The program was set up to obtain pertinent information not only for the Intercity Viaduct, but also to obtain additional data on friction piles which at some future time could be added to HRB Special Report 36, covering a study of the comparative behavior of friction piles (1958).

The consultant was authorized to set up a project, prepare specifications, and receive competitive bids for a program to consist of furnishing, driving, and test loading four types of piles and for a split-barrel boring centered in the pile groups at each of two locations. One location was in Kansas and the other in Missouri. The program as originally proposed was to consist of one pile of each type at each of the two locations but to satisfy the various pile manufacturers, three additional piles were added.

Location A, which was in Missouri, called for seven piles. The piles consisted of (1) 14⅛-in. Union Metal Monotube Tapered Steel Pile, (1A) 12¼-in. Union Metal Monotube Tapered Steel Pile, (2) 14⅜-in. Raymond Step Tapered Pile, (3) 12¾-in. Armco Foundation Pipe Pile, (3A) 14-in. Armco Foundation Pipe Pile, (4) 12-in. BP 53 Steel H-Pile, and (4A) 12-in. BP 53 Steel H-Pile Driven to refusal. Piles (1), (1A), (2), (3), (3A), and (4) were driven to a depth of 55 ft below ground level and test loaded. Pile (4A) was driven to bedrock and test loaded.

Location B, which was in Kansas, called for six piles. The piles consisted of (5) 16⅜-in. Raymond Step Tapered Pile, (6) 16¼-in. Union Metal Monotube Tapered Steel Pile, (7) 14-in. Armco Foundation Pipe Pile, (7A) 16-in. Armco Foundation Pipe Pile, (8) 14 BP 73 Steel H-Pile, and (8A) 14 BP 73 Steel H-Pile driven to refusal. Piles (5), (6), (7), (7A), and (8) were driven to a depth of 54 ft 9 in. below ground level and test loaded. Pile (8A) was driven to refusal and test loaded.

Test piles fabricated by the Union Metal Manufacturing Company, Raymond Concrete Pile Company, and Armco Drainage and Metal Products, Inc., were in accordance with manufacturer's standards and met the dimensions listed. The piles were located and driven so that they could be used in the foundation of the permanent structure. The piles were all driven with a Modified Vulcan No. 1 Steam Hammer with a 6,500-ram and a rated energy of 19,500 ft-lb. The test piles were driven in accordance with each respective pile manufacturer's recommended procedure, and each pile was driven to the specified depth without interruption.

After driving all piles at the two locations, the shells for the cast-in-place piles were inspected for shell condition and watertightness and then filled with concrete.

The seven-day compressive strength of the high-early strength concrete used in the piles was determined by testing companion 6- by 12-in. cylinder specimens and found to vary from 4,315 to 4,855 psi.

The contractor elected to apply the test loads concentrically to each test pile by using a 500-ton capacity hydraulic jack. Wide flange beams were secured to anchor piles to serve as a reaction for the jacking operations. Settlement of the pile was measured by two Ames dials reading to 0.001-in. located 180 deg apart, referenced to a fixed beam across the test site. Settlement readings were also made with a wire line arrangement customarily used by contractors.

The following procedure was followed by the contractor in handling the test load applications. The load was applied concentrically not earlier than 48 hr after the driving of the pile to be tested and anchor pile had been completed, and in no case were the cast-in-place piles loaded until the concrete had attained a compressive strength of 3,000 psi. The load was maintained at all times during the test by constant attention to load gage readings and jacking applications.

The load was applied in increments. The first application was approximately 50 tons per pile at Location A and 65 tons per pile at Location B. An increment load of approximately 25 tons per pile was applied not earlier than 1 hr after all measurable settlement of the initial loading had ceased. The least settlement considered measurable was 0.012 in. Additional 25-ton increments of load per pile were added after the measurable settlement of the previous load had ceased. The waiting period after measurable settlement had ceased was increased 1 hr for each additional load increment.

The loading for the first set of tests consisted of two 25-ton increments applied to each pile at Location A and three to each pile at Location B, in addition to the initial 50-ton and 65-ton applications. This made a total load of 100 tons at Location A and 140 tons at Location B. Yield point was reached at Location A by one pile before the 100-ton load was applied. Yield point was reached at Location B by four piles before the 140-ton load was applied. Yield point is defined as where the rate of gross settlement exceeds 0.03- in. per ton for the last increment of load applied.

All friction piles at Location A and B were unloaded after completion of the first test, or after failure, and the recovery noted. The load was removed in increments equal in magnitude to those applied with a 15-min interval between each increment. Immediately after the load was removed, the net recovery was observed and recorded. The recording of the recovery was continued for 3 hr after the load was removed.

The friction piles at Locations A and B that had not failed during the first test were given a second load test. The load was applied in increments of 25 tons. The load increments were applied at 15-min intervals until the magnitude of the previous load had been applied and thereafter at 2-hr intervals until the yield point was reached. After the second test, the piles were again unloaded and the recovery noted.

Pile (4A) at Location A and Pile (8A) at Location B, were the steel H-piles which were driven to refusal on rock. Pile (4A), the 12 BP 53 steel H-pile, was test loaded with an initial load of 50 tons and additional load increments of 25 tons each were applied at 2-hr intervals until the maximum load of 200 tons was applied. The maximum load was maintained for a period of 6 hr before the load was removed and recovery noted. Pile (8A), the 14 BP 73 steel H-pile, was test loaded with an initial load of 75 tons and additional load increments of 25 tons each were applied at 2-hr intervals until the maximum load of 300 tons was applied. The maximum load of 300 tons was maintained for 6 hr before the load was removed and recovery noted.

Borings were made at each of the test pile locations and extended from ground level to bedrock. Borings were made in accordance with the Proposed Method for Penetration Tests and Split-Barrel Sampling of Soil as published in "Procedures for Testing Soils," ASTM Committee D-18 (April 1, 1958). As previously stated, the soil classifications at Location A and Location B were quite similar and consisted of various gradations of sand with mixtures of silt and clay for the first 30 to 40 ft and coarse sand and gravel from there to bedrock. The ground water level was 28 ft below ground surface at Location A and 30 ft below ground surface at Location B.

It is not possible to give a complete summary of the driving record of each pile,

but a summary is given of the load in ton at yield point for each pile as well as the capacity of the pile as computed by the following formula

$$P = \frac{2WH}{2000\,(S+0.1\,\frac{w}{W})} = \frac{19.5}{\frac{12}{B} + \frac{0.1w}{W}}$$

in which

P = capacity in tons;
H = height of fall of the hammer in feet;
S = average penetration in inches per blow;
B = blows per foot of penetration;
w = weight of pile, mandrel and cap in pounds; and
W = weight of striking part of hammer in pounds.

Pile No. 1—14⅛-in. Union Metal Monotube Tapered Steel Pile. Yield point load 115 tons. Formula capacity 48.5 tons. Factor of safety 2.37 (Fig. 1).

Pile No. 1A—12¼-in. Union Metal Monotube Tapered Steel Pile. Yield point load 103 tons. Formula capacity 48.9 tons. Factor of safety 2.11 (Fig. 2).

Pile No. 2—14⅜-in. Raymond Step Tapered Pile. Yield point load 145 tons. Formula capacity 26.0 tons. Factor of safety 5.57 (Fig. 3).

Pile No. 3—12¾-in. Armco Pipe Pile. Yield point load 85 tons. Formula capacity 33.6 tons. Factor of safety 2.53 (Fig. 4).

Pile No. 3A—14-in. Armco Pipe Pile. Yield point load 105 tons. Formula capacity 40.1 tons. Factor of safety 2.62 (Fig. 5).

Pile No. 4—12 BP 53 Steel H-Pile in Friction. Yield point load 110 tons. Formula capacity 26.7 tons. Factor of safety 4.12 (Fig. 6).

Pile No. 4A—12 BP 53 point bearing and driven to refusal at more than 200 tons (Fig. 7).

Pile No. 5—16⅜-in. Raymond Step Tapered Pile. Yield point load 165 tons. Formula capacity 39.8 tons. Factor of safety 4.14 (Fig. 8).

Pile No. 6—16¼-in. Union Metal Monotube Tapered Steel Pile. Yield point load 124 tons. Formula capacity 78 tons. Factor of safety 1.59 (Fig. 9).

Pile No. 7—14-in. Armco Pipe Pile. Yield point load 110 tons. Formula capacity 52.2 tons. Factor of safety 2.11 (Fig. 10).

Pile No. 7A—16-in. Armco Pipe Pile. Yield point load 123 tons. Formula capacit 63.2 tons. Factor of safety 1.95 (Fig. 11).

Pile No. 8—14 BP 73 Steel H-Pile in Friction. Yield point load 116 tons. Formul capacity 43.7 tons. Factor of safety 2.65 (Fig. 12).

Pile No. 8A—14 BP 73 Steel Pile point bearing driven to refusal at more than 300 tons (Fig. 13).

To complete an economic comparison of foundation types, it was necessary to determine appropriate lengths of friction piles required for a selected range of design loads. This range was arbitrarily selected to vary from 30 to 70 tons per pile in 10-ton increments. The length of pile for a given design load had to be determined in so manner from the results of the load tests.

One approach which was considered was to assign friction values to the subsurface soils based on available boring and test data, thus estimating the depth of penetration required to provide the desired design load plus a factor of safety.

The method actually used was based on the Danish Formula wherein the ultimate test loads, plastic set values and driving records obtained during the program were incorporated in the pile length determinations. In arriving at this formula, the resis tance of the embedded surface of the pile is disregarded and it is assumed that the point resistance varies with the downward increment of the pile point. The materials of the pile and the driving cushion are assumed to be perfectly elastic. Inertia force in the soil and energy losses due to irreversible derformations, except of the soil, are disregarded. This formula may be written

$$aWH = \tfrac{1}{2}\,QSo + QS$$

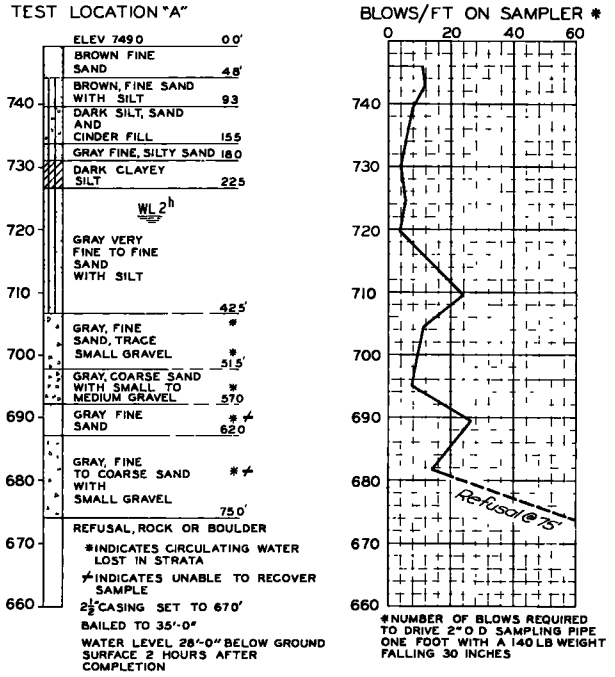

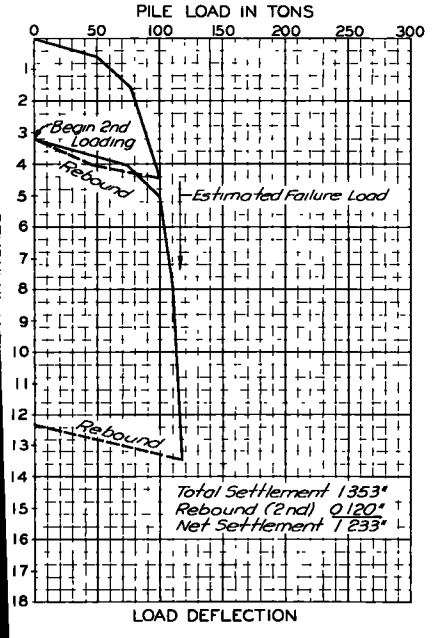

PILE DATA

14B" Union Metal Monotube Tapered Steel Pile composed of following sections:

1-40 foot Type F, 0.14"/foot taper; 7 gauge with 8½" hemispherical tip

1-20 foot Type N, 0.028"/foot taper, 7 gauge heavy duty field Joint-welded

Driven Length	60.0 feet
Loaded Length	56.0 feet
Imbedded Length	55.0 feet
Elevation of Tip	689.5 feet

Pile driven Jan 29, 1959 and filled with concrete Feb 5, 1959, and tested Feb 18, and 19, 1959

DRIVING DATA

Pile driven with Vulcan No 1 with 6,500 Lb ram (Raymond 1-S)

Rated Energy	19,500 Ft Lbs
Weight of Driving cap	1,000 Lbs
Approximate weight of pile at final penetration	1,487 Lbs
Strokes per minute	58
Driving time	13 minutes

gure 1. Intercity viaduct connecting Kansas City, Mo., and Kansas City, Kan. (Test Pile Program, Location A, Pile No. 1).

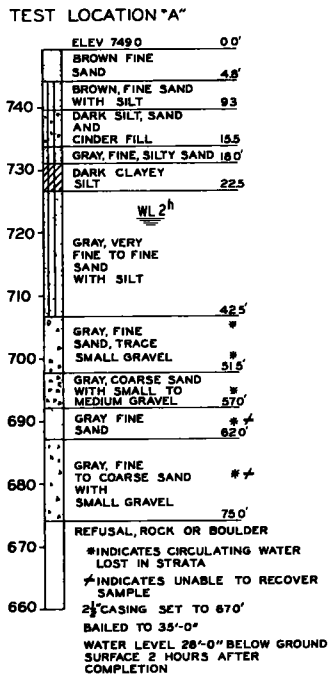

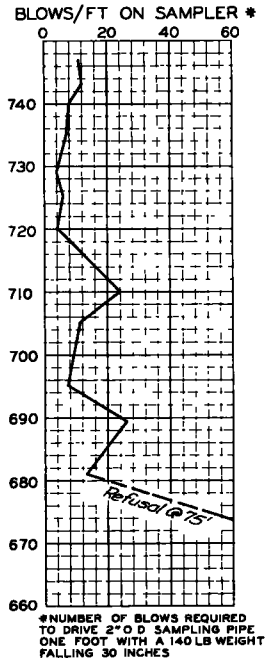

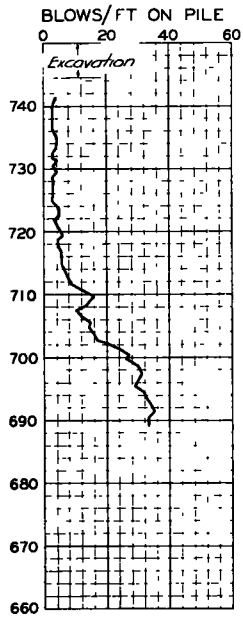

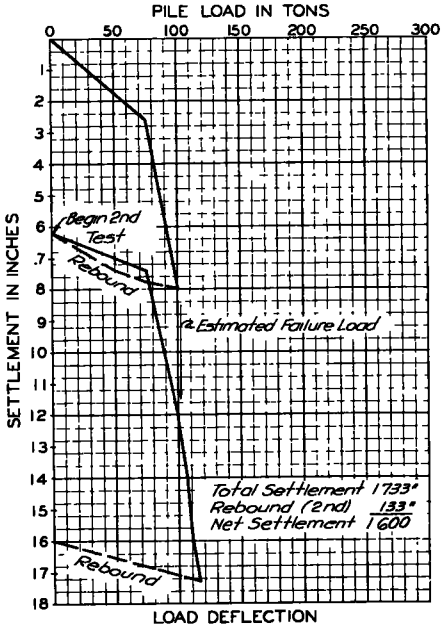

PILE DATA

12¾" Union Metal Monotube Tapered Steel Pile - composed of following sections

1-30 foot Type F, .014"/foot taper, 7 gauge, hemispherical tip

1-30 foot Type N, .0028"/foot taper, 7 gauge

Driven length	60.0 feet
Loaded length	56.2 feet
Imbedded length	55.0 feet
Elevation of tip	689.3

Pile driven Jan 30, 1959 and filled with concrete Feb 5, 1959, and test loaded Feb 16 and 17, 1959

DRIVING DATA

Pile driven with Vulcan No 1 with 6500 Lb ram (Raymond I-S)

Rated Energy	19,500 Ft Lbs
Weight of driving cap	1,000 Lbs
Approximate weight of pile of final penetration	1,383 Lbs
Strokes per minute	58
Driving time	12 minutes

Figure 2. Intercity viaduct connecting Kansas City, Mo., and Kansas City, Kan. (Test Pile Program, Location A, Pile No. 1A).

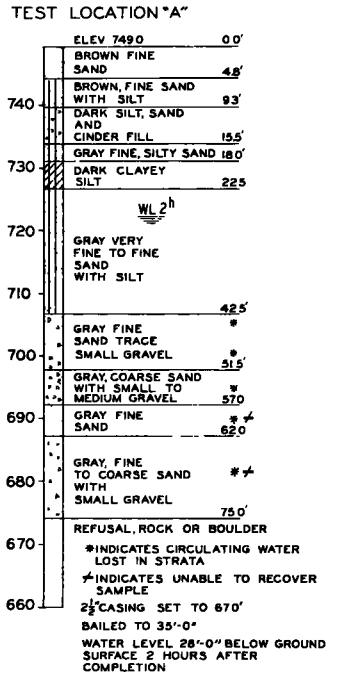

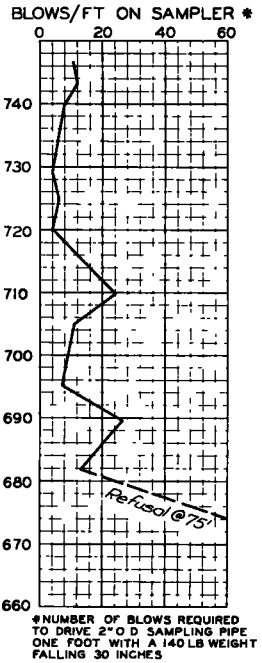

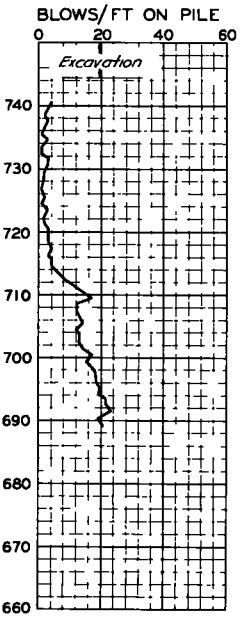

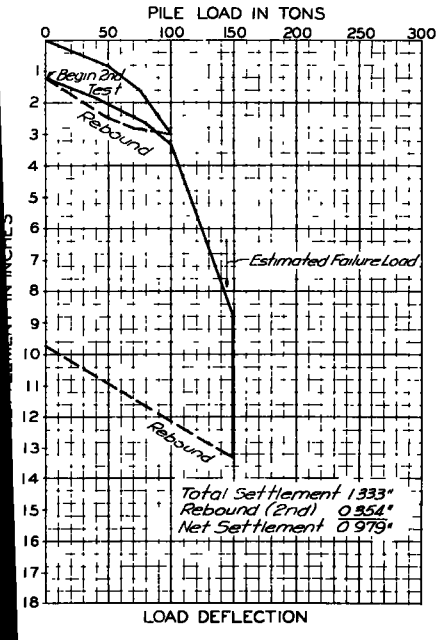

PILE DATA

14⅜" Raymond Step Tapered Pile - composed of following sections:

- 1-8 foot Raymond designation #000 (8⅛" tip diameter, 14 gauge) with welded flat steel plate to close bottom
- 1-8 foot Raymond designation #00 (14 gauge)
- 1-8 foot Raymond designation #0 (14 gauge)
- 1-8 foot Raymond designation #1 (16 gauge)
- 1-8 foot Raymond designation #2 (16 gauge)
- 1-8 foot Raymond designation #3 (16 gauge)
- 1-8 foot Raymond designation #4 (18 gauge)

Driven length	56.0 feet
Loaded length	56.2 feet (Built up)
Imbedded length	55.2 feet
Elevation of tip	689.3

Pile driven Jan 30, 1959 and filled with concrete Feb 5, 1959, and test loaded, Feb 19 and 20, 1959.

DRIVING DATA

Pile driven with Vulcan No 1 with 6500 lb ram (Raymond 1-S)

Rated Energy	19,500 Ft Lbs
Weight of driving cap.	1,000 Lbs
Approximate weight of pile and mandrel at final penetration	8,564 Lbs
Strokes per minute	58
Driving time	10 minutes

igure 3. Intercity viaduct connecting Kansas City, Mo., and Kansas City, Kan. (Test Pile Program, Location A, Pile No. 2).

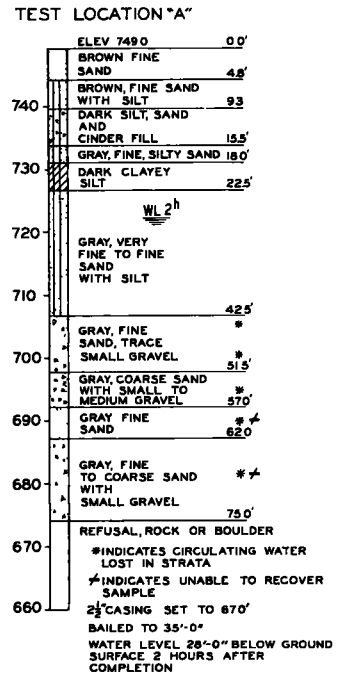

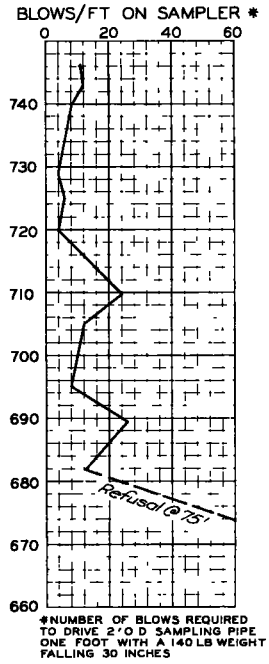

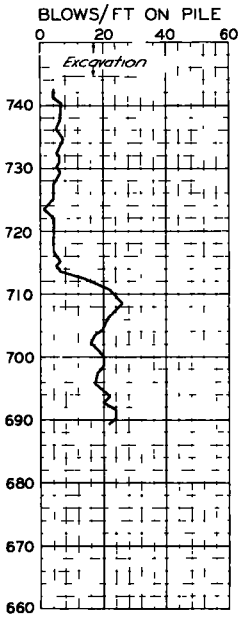

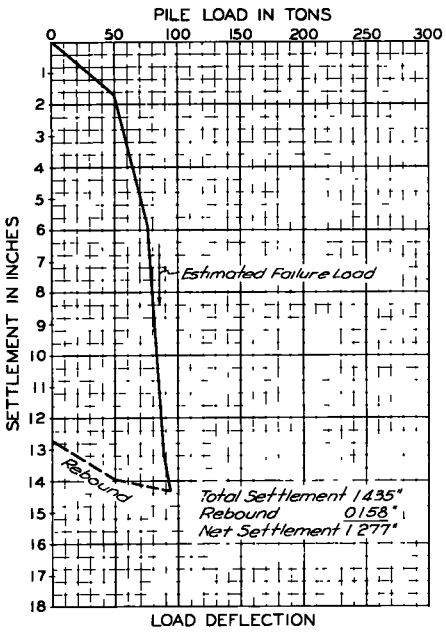

PILE DATA

12¾" Armco Foundation Pipe Pile, spiral welded 60 foot length, ⅜" wall thickness End closed with flat steel plate

Driven length	*60 feet*
Loaded length	*55.6 feet*
Imbedded length	*55.0 feet*
Elevation of tip	*689.9*

Pile driven Jan 30, 1959 and filled with concrete Feb 5, 1959, and test loaded on Feb 12 and 13, 1959

DRIVING DATA

Pile driven with Vulcan No 1 with 6,500 Lb ram (Raymond I-S)

Rated Energy	*19,500 Ft Lbs*
Weight of driving cap	*1,000 Lbs*
Approximate weight of pile at final penetration	*1,510 Lbs*
Strokes per minute	*58*
Driving time	*11 minutes*

Figure 4. Intercity viaduct connecting Kansas City, Mo., and Kansas City, Kan. (Test Pile Program, Location A, Pile No. 3).

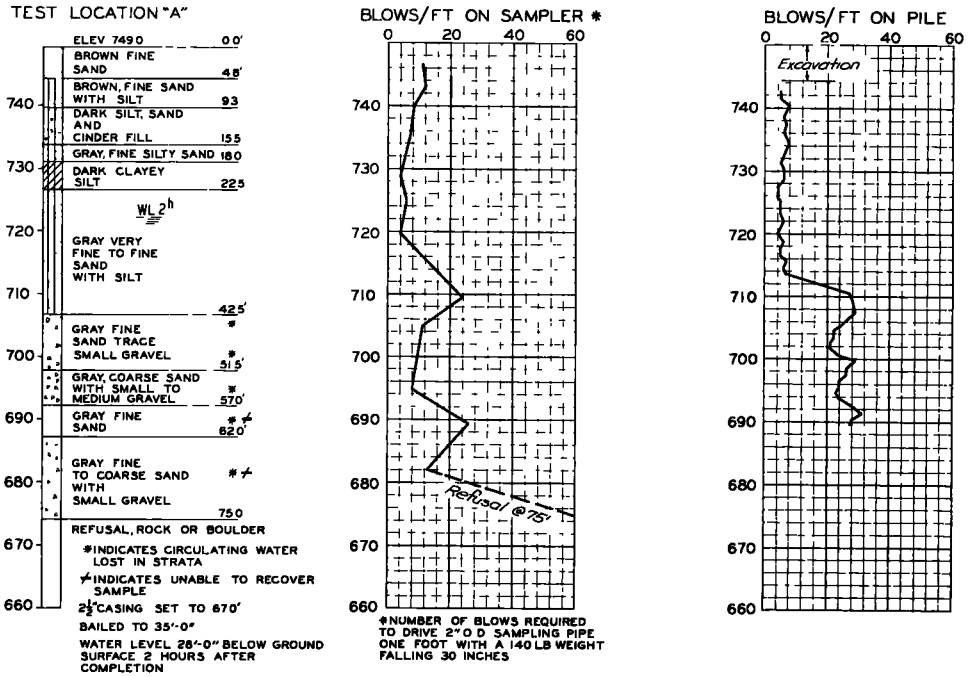

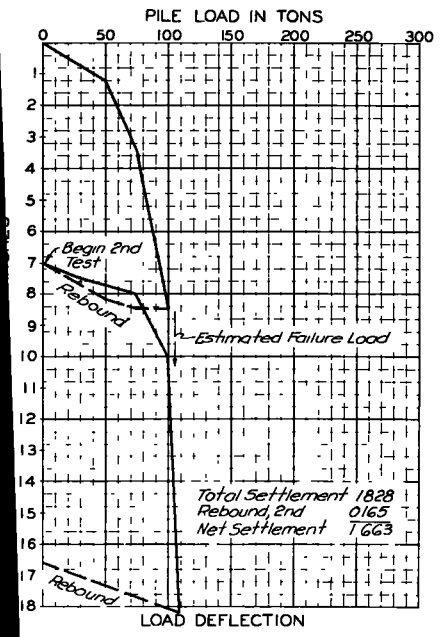

PILE DATA

14" Armco Foundation Pipe Pile, spiral welded
60' length, ¼" wall thickness End closed
with flat steel plate

Driven length	60 feet
Loaded length	55.3 feet
Imbedded length	55.0 feet
Elevation of tip	690.2

Pile driven Jan 30, 1959 and filled with concrete
Feb 5, 1959, and test loaded on Feb 16 and 17, 1959

DRIVING DATA

Pile driven with Vulcan No 1 with 6,500 Lb ram
(Raymond 1-S)

Rated Energy	19,500 Ft Lbs
Weight of driving cap	1,000 Lbs
Approximate weight of pile at final penetration	1,660 Lbs
Strokes per minute	58
Driving time	16 minutes

gure 5. Intercity viaduct connecting Kansas City, Mo., and Kansas City, Kan. (Test Pile Program, Location A, Pile No. 3A).

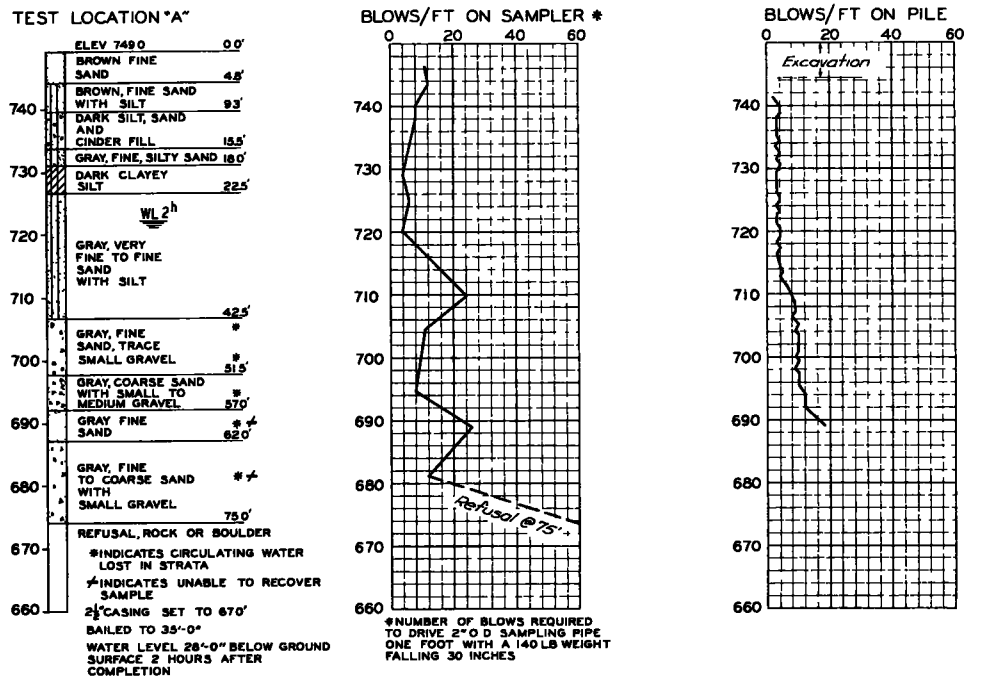

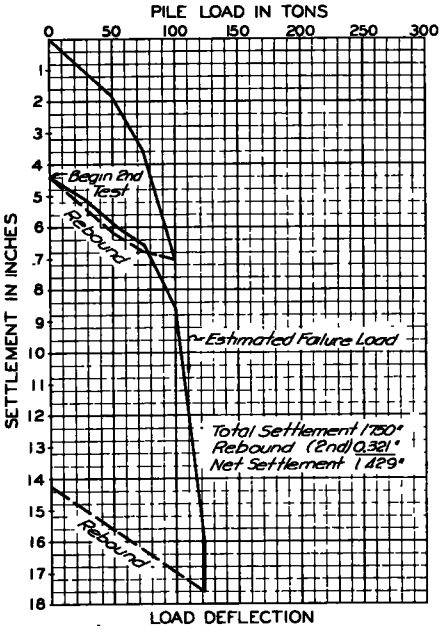

PILE DATA

12" BP 53 Steel H Pile 56 foot length, steel meeting requirements ASTM Desig A-7

Driven length	56 feet
Loaded length	55.7 feet
Imbedded length	55.0 feet
Elevation of tip	693.8

Pile driven Feb 2, 1959, and tested on Feb 13 and 14, 1959

DRIVING DATA

Pile driven with Vulcan No 1 with 6,500 Lb ram (Raymond I-S)

Rated Energy	19,500 Ft Lbs
Weight of driving cap	1,000 Lbs
Approximate weight of pile at final penetration	2,968 Lbs
Strokes per minute	58
Driving time	8 minutes

Figure 6. Intercity viaduct connecting Kansas City, Mo., and Kansas City, Kan. (Te
Pile Program, Location A, Pile No. 4).

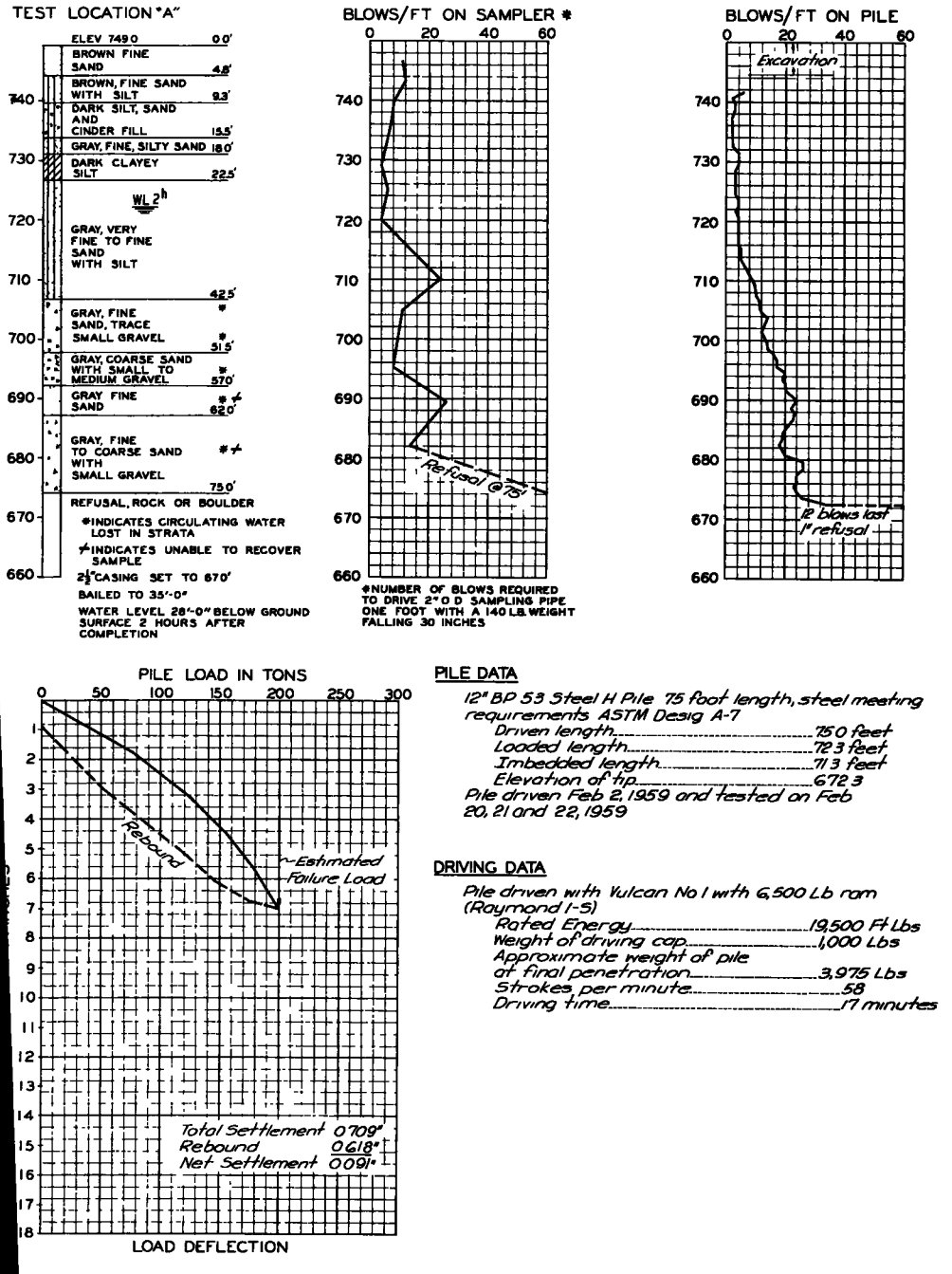

PILE DATA

12" B.P. 53 Steel H Pile 75 foot length, steel meeting requirements ASTM Desig A-7

Driven length	75.0 feet
Loaded length	72.3 feet
Imbedded length	71.3 feet
Elevation of tip	672.3

Pile driven Feb 2, 1959 and tested on Feb 20, 21 and 22, 1959

DRIVING DATA

Pile driven with Vulcan No 1 with 6,500 Lb ram (Raymond I-S)

Rated Energy	19,500 Ft Lbs
Weight of driving cap	1,000 Lbs
Approximate weight of pile at final penetration	3,975 Lbs
Strokes per minute	58
Driving time	17 minutes

ure 7. Intercity viaduct connecting Kansas City, Mo., and Kansas City, Kan. (Test Pile Program, Location A, Pile No. 4A).

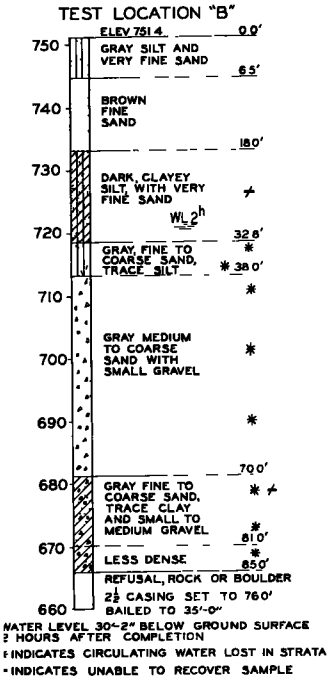

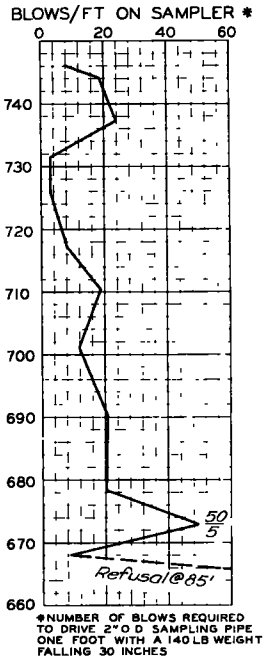

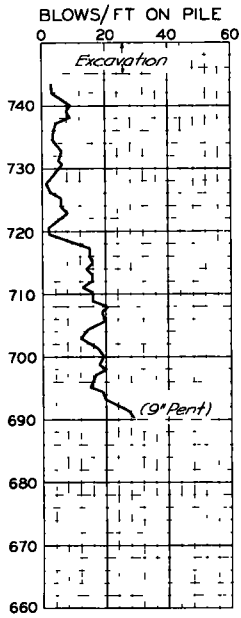

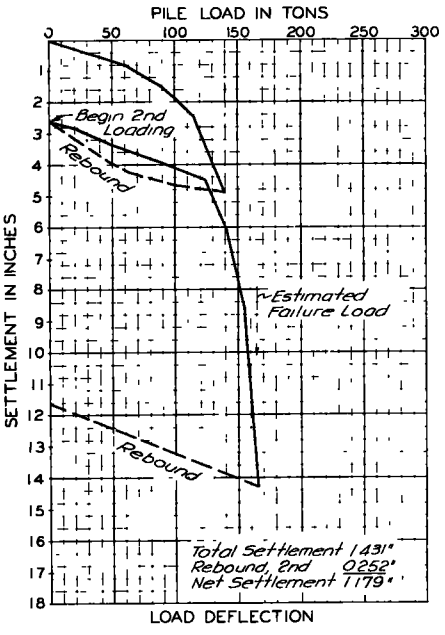

PILE DATA

16⅜" Raymond Step Tapered Pile - composed of following sections

1 - 8 foot Raymond designation #0,*	14 gauge
1 - 8 foot Raymond designation #1,	14 gauge
1 - 8 foot Raymond designation #2,	14 gauge
1 - 8 foot Raymond designation #3,	16 gauge
1 - 8 foot Raymond designation #4,	16 gauge
1 - 8 foot Raymond designation #5,	16 gauge
1 - 8 foot Raymond designation #6,	18 gauge
Driven length	56.0 feet
Loaded length	56.0 feet
Imbedded length	54.8 feet
Elevation of tip	690.7 MSL

Pile driven Feb 11, 1959, filled with concrete Feb 13, 1959 and test-loaded on Feb 25 and 26, 1959

* 1¼" tip diameter with welded flat steel plate to close bottom

DRIVING DATA

Pile driven with Vulcan No 1 with 6,500 Lb ram (Raymond 1-S)

Rated Energy	19,500 Ft Lbs
Weight of driving cap	1,000 Lbs
Approximate weight of pile and mandrel at final penetration	10,048 Lbs
Strokes per minute	58
Driving time	13 minutes

Figure 8. Intercity viaduct connecting Kansas City, Mo., and Kansas City, Kan. (Tes
Pile Program, Location B, Pile No. 5).

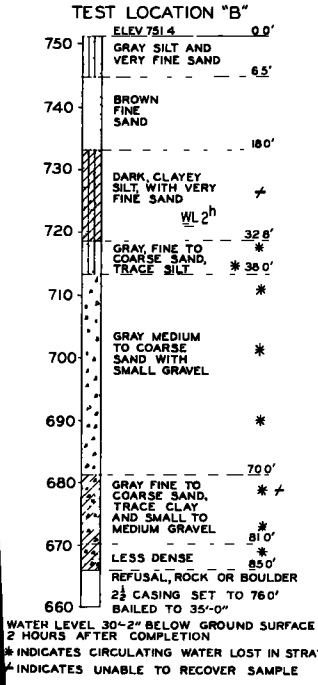

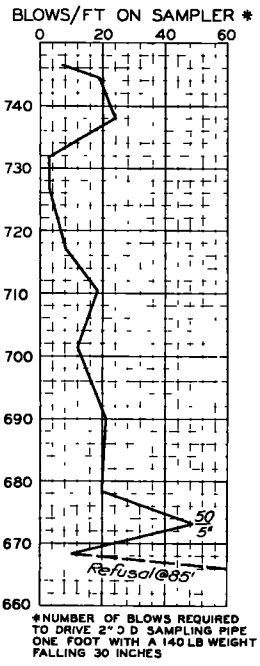

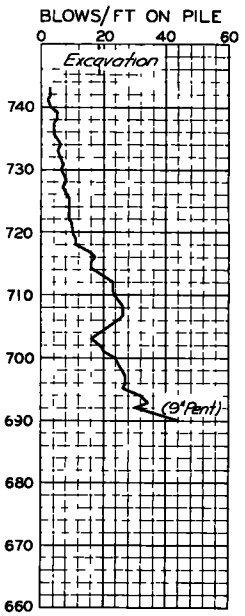

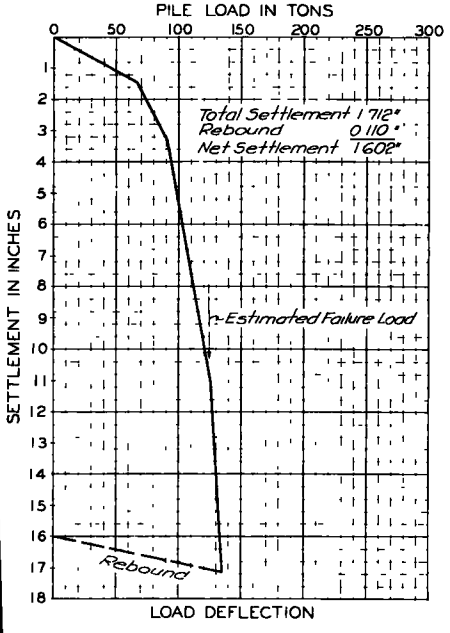

PILE DATA

16¼" Union Metal Monotube Tapered Steel Pile composed of following sections

1-33 foot Type J, 0.25"/foot taper, 7 gauge with hemispherical tip

1-25 foot Type N, 0.28"/foot taper, 7 gauge heavy duty field joint, welded

Driven length	58.0 feet
Loaded length	56.4 feet
Imbedded length	54.9 feet
Elevation of tip	690.6

Pile driven Feb 11, 1959 and filled with concrete Feb 13, 1959, and tested on Feb 27 and 28, 1959

DRIVING DATA

Pile driven with Vulcan No 1 with 6,500 Lb ram (Raymond I-S)

Rated Energy	19,500 Ft Lbs
Weight of driving cap	1,000 Lbs
Approximate weight of pile of final penetration	1,670 Lbs
Strokes per minute	58
Driving time	15 minutes

gure 9. Intercity viaduct connecting Kansas City, Mo., and Kansas City, Kan. (Test Pile Program, Location B, Pile No. 6).

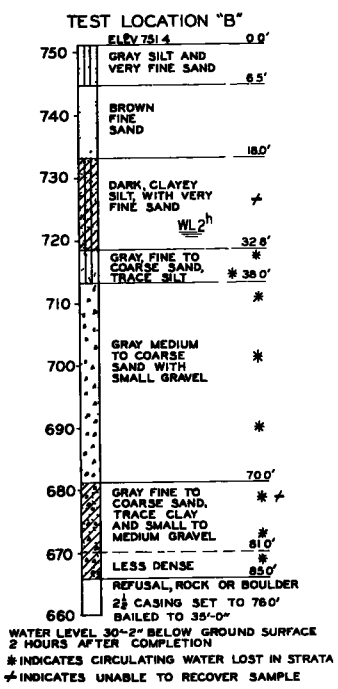

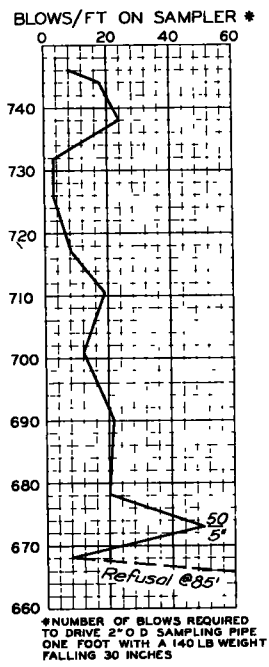

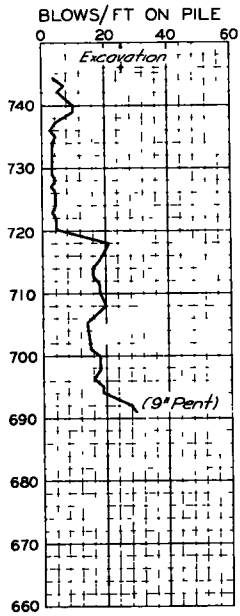

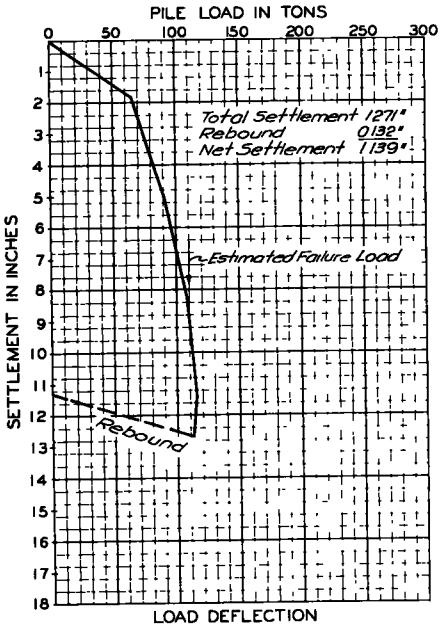

PILE DATA

14" Armco Foundation Pipe Pile, spiral welded
60 foot length, 5/16" wall thickness End closed
with flat steel plate

Driven length	60.0 feet
Loaded length	56.5 feet
Imbedded length	55.0 feet
Elevation of tip	6.90.5

Pile driven Feb 11, 1959 and filled with concrete
Feb 13, 1959, and tested on Feb 25, 1959

DRIVING DATA

Pile driven with Vulcan No 1 with 6,500 Lb ram
(Raymond I-S)

Rated Energy	19,500 Ft Lbs
Weight of driving cap	1,000 Lbs
Approximate weight of pile at final penetration	1,660 Lbs
Strokes per minute	58
Driving time	12 minutes

Figure 10. Intercity viaduct connecting Kansas City, Mo., and Kansas City, Kan. (Te
Pile Program, Location B, Pile No. 7).

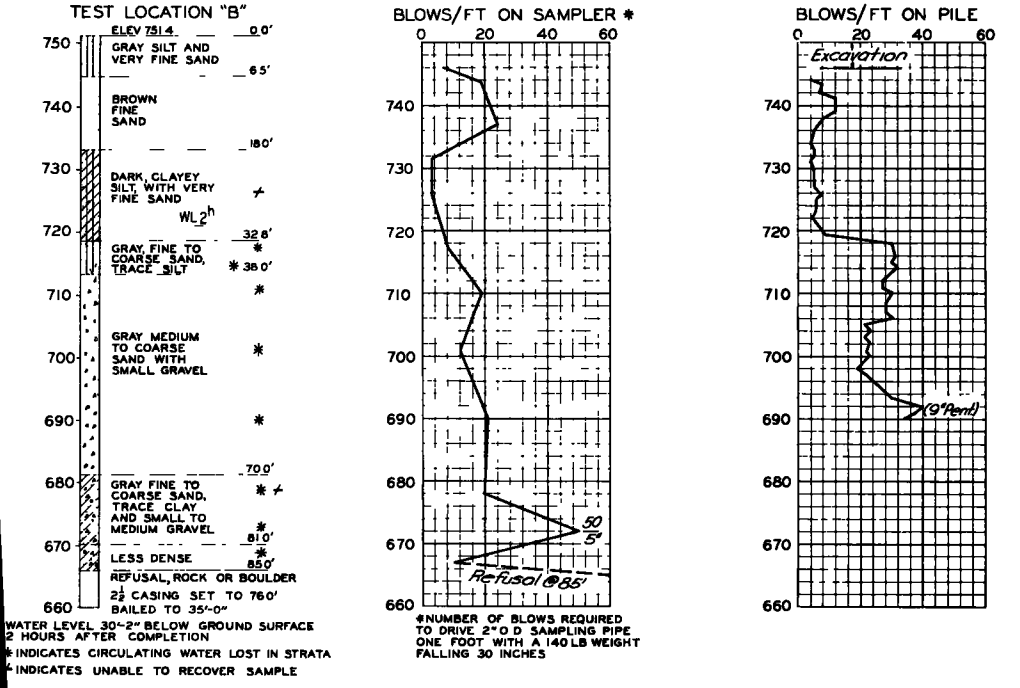

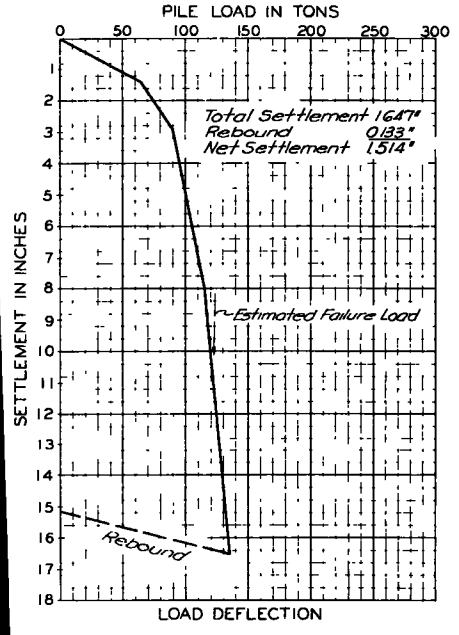

PILE DATA

16" Armco Foundation Pipe Pile - spiral welded
60 foot length 5/16" wall thickness End closed
with a flat steel plate

Driven length	60.0 feet
Loaded length	56.3 feet
Imbedded length	54.8 feet
Elevation of tip	690.7

Pile driven Feb 11, 1959 and filled with concrete Feb 13, 1959, and tested Feb 24, and 25, 1959

DRIVING DATA

Pile driven with Vulcan No 1 with 6,500 Lb. ram (Raymond I-S)

Rated Energy	19,500 Ft Lbs
Weight of driving cap	1,000 Lbs
Approximate weight of pile at final penetration	1,900 Lbs
Strokes per minute	58
Driving time	17 minutes

gure 11. Intercity viaduct connecting Kansas City, Mo., and Kansas City, Kan. (Test Pile Program, Location B, Pile No. 7A).

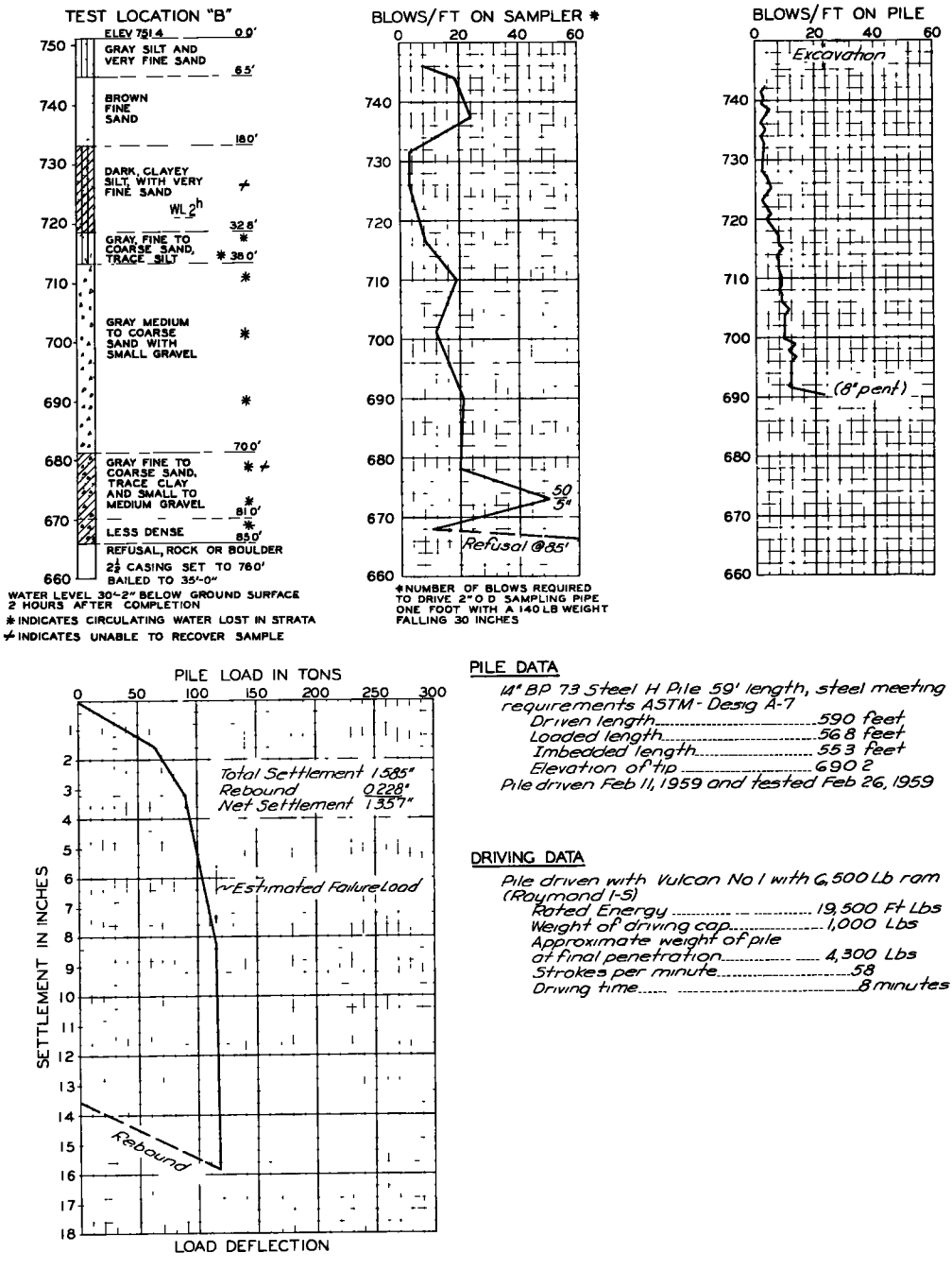

PILE DATA

14" BP 73 Steel H Pile 59' length, steel meeting requirements ASTM - Desig A-7

Driven length	59.0 feet
Loaded length	56.8 feet
Imbedded length	55.3 feet
Elevation of tip	690.2

Pile driven Feb 11, 1959 and tested Feb 26, 1959

DRIVING DATA

Pile driven with Vulcan No 1 with 6,500 Lb ram (Raymond I-S)

Rated Energy	19,500 Ft Lbs
Weight of driving cap	1,000 Lbs
Approximate weight of pile at final penetration	4,300 Lbs
Strokes per minute	58
Driving time	8 minutes

Figure 12. Intercity viaduct connecting Kansas City, Mo., and Kansas City, Kan. (Tes
Pile Program, Location B, Pile No. 8).

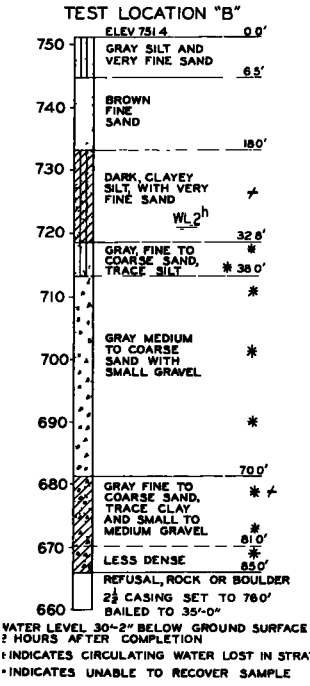

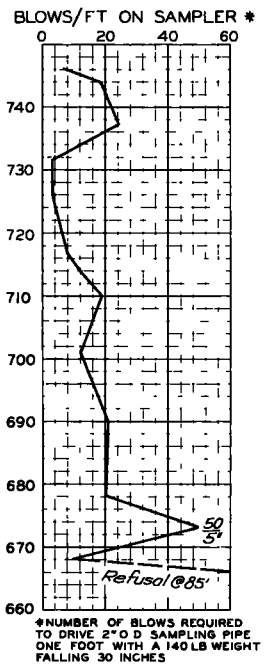

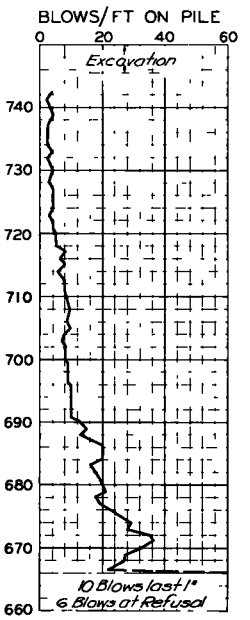

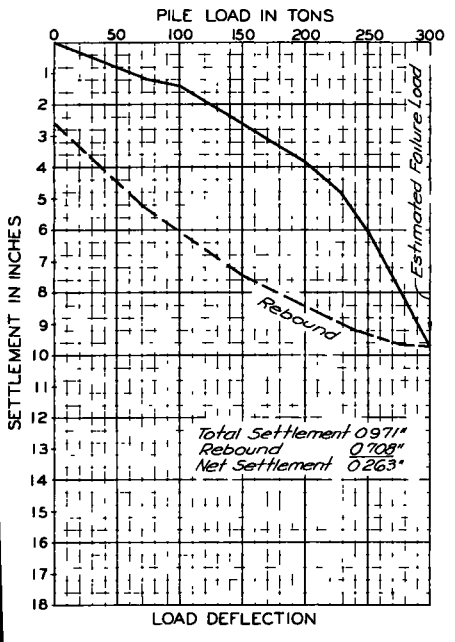

PILE DATA

14" BP-73 Steel H Pile 85' length, steel meeting requirements ASTM Desig A-7

Driven length	85.0 feet
Loaded length	79.9 feet
Imbedded length	78.5 feet
Elevation of tip	667.1

Pile driven Feb 11, 1959

DRIVING DATA

Pile driven with Vulcan No 1 with 6500 Lb ram (Raymond I-S)

Rated Energy	19,500 Ft Lbs
Weight of driving cap.	1,000 Lbs
Approximate weight of pile of final penetration	6,200 Lbs
Strokes per minute	58
Driving time	19 minutes

gure 13. Intercity viaduct connecting Kansas City, Mo., and Kansas City, Kan. (Test Pile Program, Location B, Pile No. 8A).

in which

a = coefficient of energy loss in driving system (1.0 for drop hammer and 0.8 for all others);
W = weight of hammer;
H = height of fall of hammer;
Q = bearing capacity of pile (ton);
So = dynamic compression of pile with a fixed point; and
S = total plastic set per blow.

Any consistent set of units may be used in the formula.

This formula can be expanded as follows:

$$aWH = \tfrac{1}{2} QSo + QS = Q\left(\frac{So}{2} + S\right)$$

If the dynamic compression of the pile is taken as

$$\left(2aWH\ \frac{L}{AE}\right)^{1/2}$$

Then

$$Q = \frac{aWH}{\frac{S0}{2} + S} = \frac{aWH}{\left(\frac{aWHL}{2AE}\right)^{1/2} + S}$$

Let

$$K = \left(\frac{aWHL}{2AE}\right)^{1/2}$$

Then

$$Q = \frac{aWH}{K+S}$$

For a test pile

$$Q\ (\text{actual}) = \frac{aWH}{K\ (\text{actual}) + S\ (\text{actual})}$$

The actual K value for each pile, using the ultimate test loads and sets previously recorded, is obtained by direct computation.

$$K\ (\text{actual}) = \frac{aWH - Q(\text{actual}) \times S(\text{actual})}{Q(\text{actual})}$$

Although this value of K would be reduced for a length of pile shorter than the test pile, it is conservative to assume it constant. Using this value of K, the plastic set required to obtain bearing capacities of twice the design loads of 30, 40, 50, 60, and 70 tons per pile is determined from the formula

$$Q = \frac{aWH}{K+S}$$

The set value thus determined for design loads of 30, 40, 50, 60, and 70 tons per pile was converted to blows per foot and from an inspection of the driving records of the driven test piles, the length of pile was determined. For estimating purposes, the average lengths of cast-in-place friction pile for the design loads were

Location	30-Ton (ft)	40-Ton (ft)	50-Ton (ft)	60-Ton (ft)	70-To (ft)
A	33	40	47	51	55
B	28	30	43	55	55

Comparative cost studies were made for the various design loadings of both friction piles and point bearing piles. For purposes of this comparison, preliminary designs were made for all 136 footings included in the central portion of the Intercity Viaduct

and quantities determined for all foundation items. The items for which quantities were determined and the unit prices applied in the comparison are

Structural excavation at $5.00 per cubic yard.
Footing concrete at $60.00 per cubic yard.
Reinforcing steel at $0.15 per pound.
Cast-in-place concrete piles and 12 BP 53 steel piles at $6.00 per linear foot.
14 BP 73 steel piles at $7.50 per linear foot.

As previously mentioned, various design loadings were assumed. For friction-type pile footings, design loadings of 30, 40, 50, 60, and 70 tons per pile were investigated, using pile lengths that were previously discussed. For the point bearing pile-type footings, design loadings of 6, 9, and 12 kips per square inch of cross-sectional area were used, with both 12 BP 53 and 14 BP 73 steel piles.

It is recognized that cost comparisons are always subject to criticism from the standpoint of the unit prices assumed. In this particular case, however, the cost of piles represents 70 to 80 percent of the total cost of the foundation. For this reason, the unit prices used for excavation, concrete and reinforcing steel would have no significant effect on the comparisons. Likewise, any variations in the cost per foot for piles would not materially change the comparisons.

As a result of the test pile program, the relative driving effort and pile lengths required was determined and the bearing capacities of four types of bearing pile in friction were obtained. It was found that the comparative results obtained by using the four types of piles in friction could be quite different in types of soil different from those which were encountered at this location. As previously mentioned in this report, the top 10 or 15 ft consisted of fine sand, the next 25 ft consisted of silty sand and sandy silt, and the balance consisted of fine to coarse sand and gravel.

Applying the unit prices which were tabulated previously, this test program shows that for the central portion of the Intercity Viaduct, consisting of 136 footings, the most economical plan was to use cast-in-place friction piles with a design load of 70 tons per pile. In second place with an increased cost of a little more than ½ of 1 percent was a footing designed for 4 steel pilings either 12 BP 53 or 14 BP 73 and using a maximum bearing value of 12,000 psi.

Discussion

F. M. FULLER, Raymond Concrete Pile Company—In conjunction with the test program reported by the author the pile contractor at his own expense and under the supervision of an outside firm of consulting engineers drove and load tested additional Raymond Step Taper piles.

Four of these were driven as friction piles approximately 56 ft in length using nominal point diameters ranging from 9 to 12 in. Two of these piles were driven at each test site in close proximity to the contract test piles reported by the author. The results of these tests are summarized in Table 1 and it will be noted that ultimate loads ranged from 160 to 175 tons.

In the supervising engineer's report based on the results of these tests it was concluded that the allowable load on the Step Taper friction piles is not affected materially by varying the tip diameter. Also it was their conclusion that a minimum design load of 70 to 80 tons for a 56-ft long Step Taper pile is justified.

As the author points out, the original purpose of this test program was to make an economic comparison between friction and end-bearing piles. When it became evident that end-bearing steel H piles would be used regardless of the test results and furthermore that only one type of pile would be tested in end-bearing, the contractor proceeded with a 300-ton test on an end-bearing Step Taper pile at test site A (Pile No. A5A). This pile had a nominal 8-in. diameter and was driven approximately 72 ft to a final resistance of 10 blows per inch. Under 300-ton test (maximum capacity of testing equip-

TABLE 1

INTERCITY VIADUCT—CENTRAL PORTION—KANSAS CITY TEST PILE PROGRAM
(Additional Tests on Raymond Piles)

Location	Pile No.	Pile Type	Point Dia. (in.)	Length (ft)	Final Blows per in.	Ultimate Load (tons)
A	2A	Step taper	10 3/8	56	3	165
	2B	Step taper	9 3/8	56	2	165
	5A	Step taper	8 3/8	72	10	over 300
B	5A	Step taper	11 3/8	56	4	160
	5B	Step taper	12 3/8	56	5	175

ment) the gross settlement was 0.83 in. and the net settlement after rebound was 0.36 in. Compared to this the 14 BP 73 steel H-pile driven to refusal had a gross settlement of 0.97 in. and a net of 0.26 in. under 300-ton test.

It was concluded by the supervising engineers that for the Step Taper end-bearing pile a minimum design load of 100 tons could certainly be used.

The complete data on all additional Step Taper piles tested were immediately reporte to all parties concerned.

Table 2 gives the estimated lengths for the different type piles under various design loads as prepared by the highway departments' consulting engineers. Also given in Table 2 is the table of average lengths at each of the two test sites which was included by the author. An examination of these tabulated data will reveal the following:

1. The Step Taper piles were the only piles considered by the engineers to have a design capacity of 70 tons.
2. In all cases where other piles are in the same load group with Step Taper piles, the estimated length for the Step Taper piles is equal to or less than the average length established for that load group.

With reference to (1) this means that the cost comparison between end-bearing and 70-ton friction piles was actually based on steel H-piles versus Raymond Step Taper piles. The cost analysis for cast-in-place piles was based on a unit pile price of $6. per lineal foot. This resulted in the 70-ton Step Taper piles costing about $18,000 les than the steel H-piles. The actual unit cost for the Step Taper piles, as guaranteed to the owners, was considerably less than the estimated unit cost. This difference in unit prices could conservatively be set at $1.00 per lineal foot. Therefore, using

TABLE 2

INTERCITY VIADUCT—CENTRAL PORTION—KANSAS CITY TEST PILE PROGRAM
(Data from Engineer's Report)

Location	Pile No.	Pile Type	Estimated Length (ft) for Design Loads of				
			30 Tons	40 Tons	50 Tons	60 Tons	70 Tons
A	1	14 1/8" Monotube	32	39	46	55	-
	1A	12 1/4" Monotube	33	42	49	-	-
	2	14 3/8" Raymond step taper	32	34	42	46	51
	3	12 3/4" Armco pipe	32	34	-	-	-
	3A	14" Armco pipe	32	33	34	-	-
	4	12 BP 53	37	50	55	-	-
B	5	16 3/8" Raymond step taper	28	29	37	54	56
	6	16 1/4" Monotube	28	32	51	57	-
	7	14" Armco pipe	26	37	53	-	-
	7A	16" Armco pipe	26	27	28	54	-
	8	14 BP 73	46	54	55	-	-
A		Cast-in-place friction[1]	33	40	47	51	55
B		Cast-in-place friction[1]	28	30	43	55	55

[1]For estimating purposes, average length of cast-in-place friction pile (H-piles excluded as friction piles) for the design loads.

$5.00 per lineal foot as the cost of the 70-ton cast-in-place piles the savings over the end-bearing H-piles would actually be about $54,000.

With reference to (2) the estimated lengths for the Step Taper piles were, in some cases, 5 to 6 ft shorter than the average length for that load group. It should be noted that this difference would never show up in any comparison of pile cost based on the same average length for both tapered and constant section piles.

Also it should be noted that in every case, except the 70-ton group, the average length used was equal to or less than the longest pile in the group (excluding H-piles which were not considered as friction piles). In other words, in every case there would be some pile type driving considerably longer than the "average." This also would not show up in any comparison of pile costs based on "average lengths."

In Table 3 are assembled data from the engineer's report to compare the estimated pile lengths based on the Danish formula; the length for each pile at which the various capacities were theoretically attained as determined by the modified Eytelwein formula; and the required pile length on a proportionate basis using the actual capacity at the 56-ft length. Also shown are the final Eytelwein formula capacities based on the driving resistance for each pile together with the actual capacities based on the ultimate test loads after applying a factor of safety of 2.

Obviously, there is little agreement between the Danish formula, the Eytelwein formula, and the actual results. For example:

1. Pile No. 2 (Step Taper) according to the Eytelwein formula developed a theoretical capacity of only 27.8 tons which was the lowest formula capacity of all friction piles (excluding the H-pile). Yet, the Step Taper piles actually developed the highest capacity as determined by load test.
2. In spite of the final test results pile No. 2 (Step Taper) and No. 3 ($12\frac{3}{4}$-in. pipe) were given equal estimated lengths for both 30- and 40-ton loads.
3. Pile No. 3A (14-in. pipe) and Pile No. 7A (16-in. pipe) were each given basically the same estimated lengths for 30-, 40- and 50-ton design capacities. For a friction pile of this type this is not reasonable.
4. All piles (except steel H) in each test group (1 to 3A and 5 to 7A) were assigned basically the same estimated lengths for a 30-ton design capacity. However, the test results definitely indicate a difference in load-carrying ability between the various type piles of the same length.

TABLE 3

INTERCITY VIADUCT—CENTRAL PORTION—KANSAS CITY TEST PILE PROGRAM
Comparison of Estimated Lengths by Danish Formula (D) vs Length by Eytelwein Formula (D)[1] vs Estimated Length by Proportionate Method (P)[2]
For Various Design Loads[3]

e	Type	30 Tons D E P (ft)	40 Tons D E P (ft)	50 Tons D E P (ft)	60 Tons D E P (ft)	70 Tons D E P (ft)	Final Eytel. Formula Capacity (tons)	Actual Capacity by Test FS = 2 (tons)
	Monotube 14 in.	32 41 29	39 47 39	46 - 49	55 - 58	- - 68	48.5	57.5
	Monotube 12 in.	33 43 33	42 44 44	49 53 55	- - 65	- - 76	48.9	51.5
	Step taper 14 in.	32 - 23	34 - 31	42 - 39	46 - 46	51 - 54	26.0	72.5
	Pipe 12 in.	32 34 40	34 - 53	- - 66	- - 79	- - 92	33.6	42.5
	Pipe 14 in.	32 33 32	33 34 43	34 - 53	- - 64	- - 75	40.1	52.5
	H 12 in.	37 - 31	50 - 41	55 - 51	- - 61	- - 71	26.7	55.0
	Step taper 16 in.	28 54 20	29 - 27	37 - 34	54 - 41	56 - 48	39.8	82.5
	Monotube 16 in.	28 32 27	32 48 36	51 54 45	57 55 54	- 55 63	78.0	62.0
	Pipe 14 in.	26 36 31	27 53 41	53 55 51	- - 61	- - 71	52.2	55.0
	Pipe 16 in.	26 27 27	27 27 36	28 53 46	54 55 55	- - 64	63.2	61.5
	H 14 in.	46 55 29	54 55 39	55 - 48	- - 58	- - 68	43.7	58.0

gth by Eytelwein formula based on driving log of test pile.
gth by Proportionate Method based on actual capacity for 56-ft pile.
entry indicates capacity not attainable under method used to determine required length.

An examination of Table 3 and the author's explication of the Danish formula reveal that some very important factors which influence pile driving are disregarded and some very broad assumptions are made. Although the K factor in the Danish formula is related to elastic energy losses, its value in each case was determined by the actual ultimate capacity and final set of the pile. A comparison of final resistance versus actual capacity by load test indicates no correlation. Yet the determination of pile lengths by this formula is based on the results of the driving log for each test pile. Thus, the beneficial effect of the weight and rigidity of certain piles in efficiently transmitting the hammer energy (for example, piles 2 and 5) is entirely disregarded. The high energy losses due to elastic deformations in the light-weight piles is demonstrated by the substantial increase in the driving resistance when the pile tip enters a denser soil. However, according to the Danish formula this would indicate greater capacity which is just the reverse of that proved by the test program.

With reference to Tables 3 and 4 this is indicated for pile 7A which can be classified as a light pile (34 lb per foot as compared to the weight of pile No. 5—180 lb per foot). When this pile encountered the dense stratum 27 ft below ground surface the blow count jumped from 9 blows per foot to 30 blows per foot. Therefore, any capacity which required up to 30 blows per foot according to the Danish formula would be satisfied with this 27-ft pile. In comparison, for the heavy step tapered pile No. 5 the blow count went from 9 to 15 when the pile point encountered the same stratum.

It should be evident, therefore, that predicting pile lengths by some formula where the effects of various pile characteristics are not considered can be very misleading.

Table 4 summarized data from the engineer's report together with supplemental information. Here the safe load as determined by the modified Eytelwein formula (used by the engineers) is compared to the safe load as determined by the Engineering News formula. It will be noted that for all of the light piles (Nos. 1, 1-A, 3, 3-A, 4, 6, 7, and 7-A) the allowable load by the Eytelwein formula is higher than that by the Engineering News formula. Conversely, for the heavy piles (Nos. 2, 5 and 8) the safe load by Eytelwein formula is less than that by Engineering News. In the modified Eytelwein formula the factor 0.1 is multiplied by the ratio of weight of pile to weight of hammer ram. Obviously, this formula favors a light pile and penalizes a heavy pile. Also, it should be obvious from the test results that this formula is basically wrong. The results of this formula are actually contrary to the experience on this test program in which the heavy Step Taper piles carried the highest ultimate load. It is evident therefore, that the elastic energy loss in the light piles is much more serious than inertia

TABLE 4

INTERCITY VIADUCT—CENTRAL PORTION—KANSAS CITY TEST PILE PROGRAM
(Data from Engineer's Report)

Pile No.	Pile Type[1]	Diameter - Inches Butt	Tip	Pile Wgt. (lb)[2]	Avg. Wgt. (per ft-lb)	Final Res. (blows/ft)	Safe Load by Formula[3] (-tons) EYT	EN	Actual Yield Load by Test (-to
1	Monotube	14⅛	8	1,487	27	33	48.5	42	115
1A	Monotube	12¼	8	1,383	25	33	48.9	42	103
2	Step taper	14⅛	8	8,564	153	20	26.0	27	145
3	Pipe	12¾	12¾	1,510	27	22	33.6	30	85
3A	Pipe	14	14	1,660	30	27	40.1	36	105
4	Steel H	12	12	2,968	53	18	26.7	25	110
5	Steel taper	16⅜	10	10,048	180	37	39.8	46	165
6	Monotube	16¼	8	1,670	30	58	78.0	63	124
7	Pipe	14	14	1,660	30	36	52.2	45	110
7A	Pipe	16	16	1,900	34	44	63.2	53	123
8	Steel H	14	14	4,300	73	33	43.7	50	116

[1]Monotube furnished by Union Metal Mfg. Co.; step taper furnished by Raymond Concrete Pile Co., pipe furnished by Armco Drainage & Metal Products, Inc.; all pipes 56 ft long and driven with 19,500 ft-lb hammer.

[2]Add 1,000 lb for weight of driving cap.

[3]EYT = Modified Eytelwein formula used by engineers.
EN = Engineering News formula.

in heavy piles. The superior driving characteristics of a heavy rigid pile (using an adequate size hammer) has been clearly demonstrated on very many pile tests under a variety of sub-soil conditions throughout the country.

The sub-soil at the Intercity Viaduct test sites could generally be classified as granular or cohesionless. This soil type is very commonly found and therefore the results of these tests are not only applicable to the Viaduct site but could be applied elsewhere. Inasmuch as the soil profile is quite common to all parts of the country these tests represent a valuable contribution with wide application. Comparable results could be expected elsewhere.

It is interesting to note that the test load reaction was obtained by jacking against anchor piles. These were Raymond Step Taper piles approximately 70 ft in length. In some cases uplift loads of over 100 tons per pile were resisted.

THE NATIONAL ACADEMY OF SCIENCES—NATIONAL RESEARCH COUNCIL is a private, nonprofit organization of scientists, dedicated to the furtherance of science and to its use for the general welfare. The ACADEMY itself was established in 1863 under a congressional charter signed by President Lincoln. Empowered to provide for all activities appropriate to academies of science, it was also required by its charter to act as an adviser to the federal government in scientific matters. This provision accounts for the close ties that have always existed between the ACADEMY and the government, although the ACADEMY is not a governmental agency.

The NATIONAL RESEARCH COUNCIL was established by the ACADEMY in 1916, at the request of President Wilson, to enable scientists generally to associate their efforts with those of the limited membership of the ACADEMY in service to the nation, to society, and to science at home and abroad. Members of the NATIONAL RESEARCH COUNCIL receive their appointments from the president of the ACADEMY. They include representatives nominated by the major scientific and technical societies, representatives of the federal government, and a number of members at large. In addition, several thousand scientists and engineers take part in the activities of the research council through membership on its various boards and committees.

Receiving funds from both public and private sources, by contribution, grant, or contract, the ACADEMY and its RESEARCH COUNCIL thus work to stimulate research and its applications, to survey the broad possibilities of science, to promote effective utilization of the scientific and technical resources of the country, to serve the government, and to further the general interests of science.

The HIGHWAY RESEARCH BOARD was organized November 11, 1920, as an agency of the Division of Engineering and Industrial Research, one of the eight functional divisions of the NATIONAL RESEARCH COUNCIL. The BOARD is a cooperative organization of the highway technologists of America operating under the auspices of the ACADEMY–COUNCIL and with the support of the several highway departments, the Bureau of Public Roads, and many other organizations interested in the development of highway transportation. The purposes of the BOARD are to encourage research and to provide a national clearinghouse and correlation service for research activities and information on highway administration and technology.